FAN-IN TAILCONE VEHICLE DEFINITION RESULTING FROM ENGINE/TRANSMISSION/AIRFRAME INTEGRATION ANALYSIS

M. L. Potash

United Technologies Corporation

Prepared for:

Army Air Mobility Research and Development Laboratory

July 1975

USAAMRDL-TR-75-28

FAN-IN-TAILCONE VEHICLE DEFINITION RESULTING FROM ENGINE/TRANSMISSION/AIRFRAME INTEGRATION ANALYSIS

Sikorsky Aircraft
Division of United Technologies Corporation
N. Main Street
Stratford, Conn. 06602

July 1975

Final Report for Period 28 May 1974 - 28 May 1975

Approved for public release;
distribution unlimited.

Prepared for

EUSTIS DIRECTORATE
U. S. ARMY AIR MOBILITY RESEARCH AND DEVELOPMENT LABORATORY
Fort Eustis, Va. 23604

EUSTIS DIRECTORATE POSITION STATEMENT

This report describes a fan-in-tailcone vehicle design approach that integrates and manages internal and external airflows so as to minimize vehicle performance penalty. In this case, stringent IR plume and hot part suppression requirements greatly increased external airflows, adding to the complexity of the integration approach and dictating innovative design techniques. Also, techniques were devised to minimize rotor pylon parasite drag. The resulting fan-in-tailcone concept has a payload deficiency when compared to a conventional design approach to IR suppression, but it was judged to be superior in life-cycle costs, primarily due to the elimination of the tail rotor. It also had a slight advantage in mission fuel requirements. The results of this contract should be integrated in future vehicle studies and in the formulation of IR suppression criteria.

LeRoy T. Burrows of the Technology Applications Division served as Project Engineer for this effort.

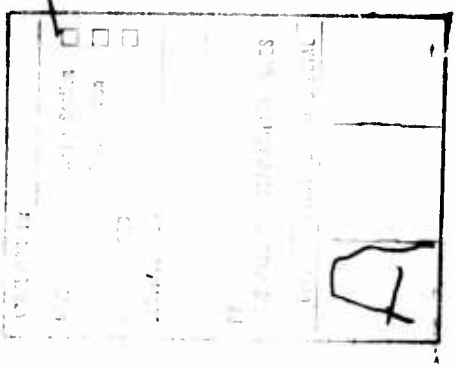

UNCLASSIFIED

SECURITY CLASSIFICATION OF THIS PAGE (When Data Entered)

REPORT DOCUMENTATION PAGE		READ INSTRUCTIONS BEFORE COMPLETING FORM
1. REPORT NUMBER USAAMRDL-TR-75-28	2. GOVT ACCESSION NO.	3. RECIPIENT'S CATALOG NUMBER
4. TITLE (and Subtitle) FAN-IN-TAILCONE VEHICLE DEFINITION RESULTING FROM ENGINE/TRANSMISSION/ AIRFRAME INTEGRATION ANALYSIS		5. TYPE OF REPORT & PERIOD COVERED Final Report 28 May 74 - 28 May 75 6. PERFORMING ORG. REPORT NUMBER SER-50911
7. AUTHOR(s) M. L. Potash		8. CONTRACT OR GRANT NUMBER(s) DAAJ02-74-C-0042
9. PERFORMING ORGANIZATION NAME AND ADDRESS Sikorsky Aircraft, Division of United Technologies Corporation, N. Main Street, Stratford, Connecticut 06602		10. PROGRAM ELEMENT, PROJECT, TASK AREA & WORK UNIT NUMBERS 62207A 1G262207AH89 02 007 EK
11. CONTROLLING OFFICE NAME AND ADDRESS Eustis Directorate, U. S. Army Air Mobility Research and Development Laboratory, Fort Eustis, Virginia 23604		12. REPORT DATE July 1975 13. NUMBER OF PAGES ~~256~~ 188
14. MONITORING AGENCY NAME & ADDRESS(if different from Controlling Office)		15. SECURITY CLASS. (of this report) Unclassified 15a. DECLASSIFICATION/DOWNGRADING SCHEDULE

16. DISTRIBUTION STATEMENT (of this Report)

Approved for public release; distribution unlimited.

17. DISTRIBUTION STATEMENT (of the abstract entered in Block 20, if different from Report)

18. SUPPLEMENTARY NOTES

19. KEY WORDS (Continue on reverse side if necessary and identify by block number)

Fan-in-Fuselage
Transmission Concepts
IR Suppression
Helicopter

20. ABSTRACT (Continue on reverse side if necessary and identify by block number)

The objective of the study conducted under this contract was the identification of innovative engine/transmission/airframe concepts that provide total airflow and power management to meet the projected requirements of future Army helicopters with minimum effect on vehicle performance.

To accomplish this objective, a study system specification for a reconnaissance helicopter was developed, and a current-technology

DD FORM 1 JAN 73 1473 EDITION OF 1 NOV 65 IS OBSOLETE

UNCLASSIFIED

1. SECURITY CLASSIFICATION OF THIS PAGE (When Data Entered)

Block 20. Abstract - continued

baseline air vehicle was synthesized. Advanced subsystem concepts were developed including integration of the IR suppression/ directional control subsystem, dynamic components, airframe components, and airflow subsystems.

An advanced vehicle containing a fan-in-tailcone IR suppressor/ directional control subsystem, a split power (engine input power split into two parallel load paths) transmission to which the engines are directly mounted (close-coupled), and total airflow management (including transmission cooling by the IR fan) was conceived, refined, and compared with current-technology vehicles.

At constant gross weight, the advanced vehicle suffers a 5-percent payload penalty. The 6-percent calculated reduction in fleet life-cycle cost results from decreased vulnerable area to small-arms fire and to elimination of attrition attributable to tail rotor accidents.

2

TABLE OF CONTENTS

	Page
LIST OF ILLUSTRATIONS	4
LIST OF TABLES	7
INTRODUCTION	8
STUDY SPECIFICATION AND BASELINE VEHICLE	9
IR SUPPRESSION/DIRECTIONAL CONTROL SYSTEM STUDY	14
INTRODUCTION	14
EFFECTS OF DILUTION RATIO	14
TAILCONE LENGTH	19
FAN INLET CONFIGURATION	20
EXHAUST NOZZLE CONFIGURATION	20
VANE DESIGN	23
DIRECTIONAL CONTROL SYSTEM	30
IR FAN PITCH CONTROL	30
FAN CONFIGURATION STUDY	33
FEASIBILITY STUDY	34
PRELIMINARY DESIGN	44
ALTERNATE CONFIGURATION	56
AIRFRAME SUBSYSTEMS	59
MECHANICAL SUBSYSTEMS	69
INTRODUCTION	69
GEARBOX DESIGN	70
FAN DRIVE	94
TRANSMISSION COOLING REQUIREMENTS	97
GREASE VS OIL LUBRICATION	99
ENGINE/GEARBOX MOUNTING ARRANGEMENTS	102
ENGINE LOCATION	106
HIGH-SPEED INPUTS	107
AIRFLOW SUBSYSTEMS	110
PRELIMINARY DESIGN AND EVALUATION	118
REFINED DESIGN AND COMPARISONS	129
CONCLUSIONS	145
RECOMMENDATIONS	146
REFERENCES	147
APPENDIX A - SYSTEM STUDY SPECIFICATION	148
APPENDIX B - APPENDIX TO CONTRACT SOW	153
LIST OF SYMBOLS	157

LIST OF ILLUSTRATIONS

Figure		Page
1	General Arrangement, Baseline Aircraft	11
2	Effect of Dilution Ratio on Exhaust Temperature, Exhaust Area and Fan Power	16
3	Exhaust Nozzle Configuration	21
4	Alternate Diverter Door and View Blockage Systems	25
5	Exhaust Vane Configuration	27
6	Effect of Air Passage Height on Flow Rate and Average Radiation Temperature	29
7	Directional Control System Schematic With Individual and Collective Pedal Movement	31
8	Directional Control System Schematic With No Collective Pedal Movement	32
9	Postmixing and Premixing Fan Concepts	35
10	Postmixing Fan Preliminary Layout	36
11	Effect of Total Activity Factor and Dilution Ratio on Fan Efficiency	40
12	Fan Maps for 1250, 2083 and 2916 Total Activity Factors	42
13	Hub/Tip Ratio Study	45
14	Fan Efficiency and Pressure Rise vs Tip Speed and TAF	47
15	Efficiency Map for Fan Selected for Preliminary Design	48
16	Fan Assembly for Premixing Concept	49
17	Spar-Shell Fan Blade	50
18	Computed Blade Shank Excitations	55
19	Critical Speed Diagram	57
20	Tailcone Construction Methods	61

LIST OF ILLUSTRATIONS (continued)

Figure		Page
21	Longitudinal Module Fasteners	68
22	Mechanical Subsystem Study	71
23	Planetary Drive Schematic	73
24	Planetary Drive Layout	75
25	Spur Drive Schematic	77
26	Spur Drive Layout	79
27	Split Power Transmission Schematic	81
28	Split Power Transmission Layout	83
29	Free Planet Transmission Schematic	85
30	Free Planet Transmission Layout	86
31	Roller Gear Drive Schematic	88
32	Roller Gear Drive Layout	89
33	Maroth Transmission Schematic	92
34	Maroth Transmission Layout	93
35	Fan Drive Shaft Diameter vs Weight	95
36	Fan Shaft Diameter vs Critical Speed	96
37	Effect of Fan Inlet on Rotor Pylon Drag	116
38	Advanced Integrated Airflow Schematic	117
39	Preliminary Advanced Vehicle	119
40	Advanced Aircraft Modular Construction	121
41	Advanced Vehicle Three-View Drawing	123
42	Advanced Vehicle Isometric	125
43	Refined Advanced Vehicle - Three-View Drawing	131
44	Refined Advanced Vehicle - Inboard Profile	133

LIST OF ILLUSTRATIONS (continued)

Figure		Page
45	Three-View and Inboard Profile - Conventional Vehicle - No IR Suppression	135
46	Three-View and Inboard Profile - Conventional Vehicle - Plume IR Suppression.	137
47	Life-Cycle Cost Comparison	143
B1	Advanced Technology Engine Weight	154
B2	Typical Performance of Three Advanced Technology Engines	154
B3	Hot Parts Suppression Criteria	156

LIST OF TABLES

Table		Page
1	Baseline Aircraft Design Attributes	10
2	Baseline Aircraft Weight Breakdown	13
3	Heat Loads Contributed to Fan Airflow	18
4	Preliminary Hover Design Points	39
5	Fan Aerodynamic Design Points	43
6	Fan Design Characteristics	46
7	Weight Breakdown, System e	60
8	Weight Breakdown, System k	63
9	Weight Breakdown, System m	63
10	Weight Breakdown, System n	64
11	Weight Breakdown, Polyimide System	64
12	Loss Sources and Efficiency of Transmission . .	97
13	Lubricants Considered	98
14	Sikorsky Operating Experience With Grease Lubrication	100
15	Heat/Vent Systems Considered	110
16	Fan Performance	118
17	Propulsion System Vulnerable Area Comparisons .	128
18	Fan Performance in Refined Aircraft	129
19	Comparative Weight Breakdown	130
20	Mission Profile - Advanced Aircraft	140
21	Mission Profile - Conventional Aircraft With Plume Suppression	141
22	Mission Profile - Conventional Aircraft With No IR Suppression	142

INTRODUCTION

Future Army rotary-wing aircraft will be powered by advanced engines characterized by higher compressor pressure ratios and higher turbine temperatures, resulting in the need for increased compartment cooling. Also, the trend toward multi-engine installations will result in the use of relatively small engines which provide increased engine installation flexibility but result in increased compartmentalization requirements. Survivability requirements that dictate large reductions in IR radiation from aircraft systems (hot part and plume temperature suppression) and reduction in ballistic vulnerability will necessitate new approaches to propulsion system integration. Operational reliability will require an efficient inlet foreign particle protection system to include scavenge.

In summary, future helicopter propulsion system installations will be more complex with respect to handling the variety of external air requirements, especially when hot parts and plume suppression is dictated. Efficient airflow and power management is needed to reduce installation complexity, cooling drag, and engine and transmission installation losses. The work performed under this contract identifies innovative engine/transmission/airframe concepts which provide total airflow and power management to meet projected requirements of future Army aircraft, with minimum effect on vehicle performance.

STUDY SPECIFICATION AND BASELINE VEHICLE

STUDY SPECIFICATION

The study specification to which the baseline and advance vehicle are designed is presented in Appendix A. This specification applies to a reconnaissance type helicopter with a payload of 1000 pounds and capability to accommodate two passengers. Contractual constraints on the engines and airframe used to develop this specification are given in Appendix B.

BASELINE VEHICLE

The baseline vehicle is designed to meet the requirements of the study specification and is shown in Figure 1. The design attributes obtained after alignment of the helicopter design model computer program (HDM) with the design shown in Figure 1 are given in Table 1. Table 2 presents the weight breakdown for this design.

This baseline vehicle's design attributes are used as a starting point for advanced subsystem designs which are described in the next section. Because the baseline vehicle has the same payload as a vehicle designed with the advanced subsystems, the baseline vehicle is also used as the basis for a life-cycle cost evaluation of the advanced vehicle.

TABLE 1. BASELINE AIRCRAFT DESIGN ATTRIBUTES

General		Main Rotor		Tail Rotor/Fan	
Design GW (lb)	8141	Radius (ft)	20.00	Radius (ft)	4.00
Payload (lb)	999	Chord (ft)	1.193	Chord (ft)	.460
Weight Empty (lb)	5522	No. of Blades	4.0	No. of Blades	4.0
Fuel (lb)	1086	Rotor Solidity	.0758	Rotor Solidity	.1464
Hover Power (shp)	1050	Tip Speed (fps)	730.0	Tip Speed (fps)	700.0
Hover - Climb (hp)	1129	Aspect Ratio	16.759	Aspect Ratio	8.696
Main Rotor Design (hp)	903	CT/Sigma	.0850	CT/Sigma	.1233
Tail Rotor Cant (deg)	.00	Main Rotor Lift	8141.3	Tail Rotor Lift	.0
MR Disc Loading (psf)	6.48	Figure of Merit	.7457	Figure of Merit	.7133
Main GB Design (hp)	1258	Blade Area (sq ft)	95.5	Blade Area (sq ft)	7.3

NOTES: IR Suppressor Power = 90 shp
EAPS Installation Loss = 3%

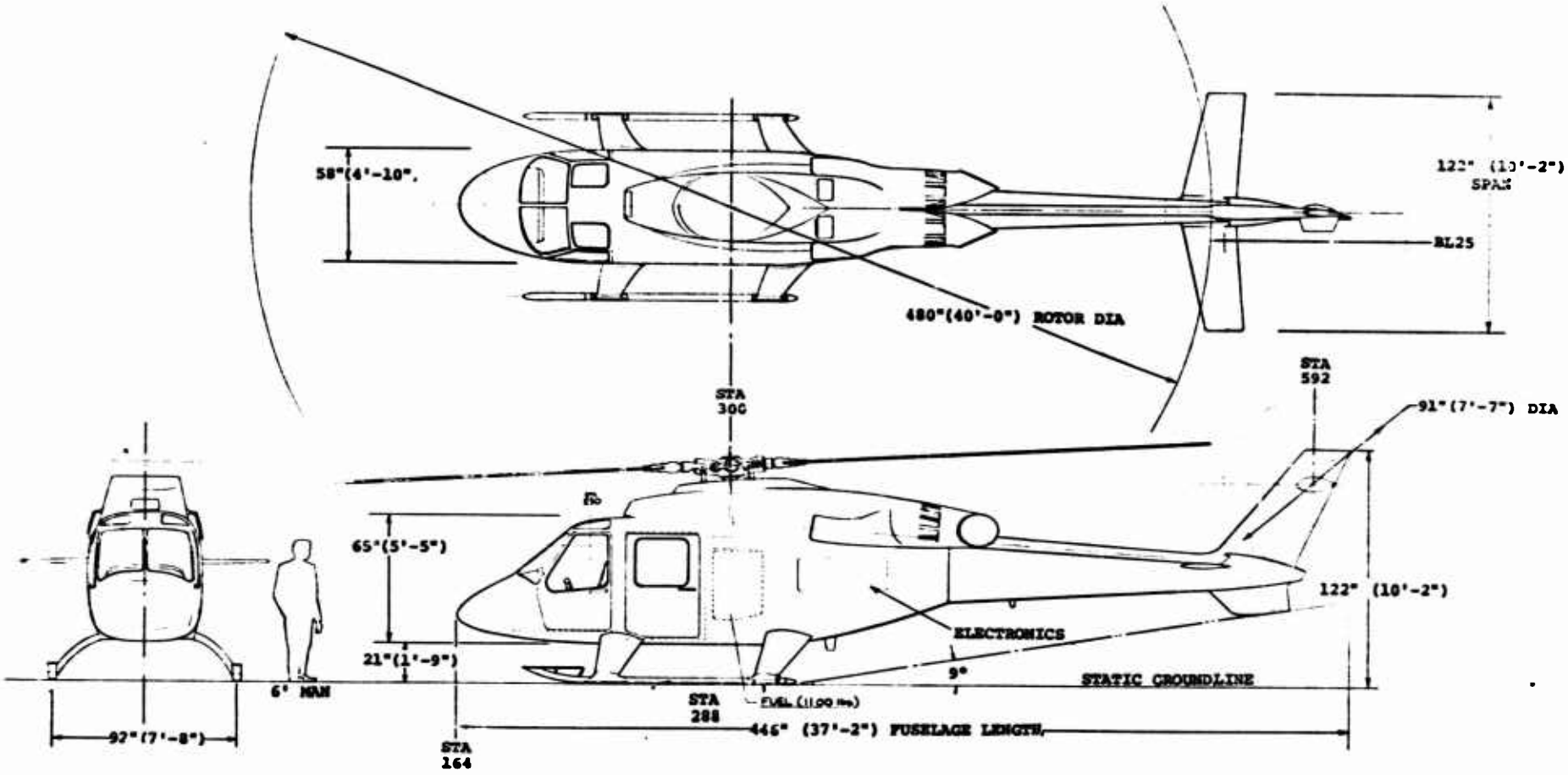

Figure 1. General Arrangement, Baseline Aircraft.

TABLE 2. BASELINE AIRCRAFT WEIGHT BREAKDOWN

Group	Weight (lb)
Main Rotor Group	(643)
Tail Group	(133)
Tail Rotor	34
Horizontal Tail	40
Vertical Tail	59
Body Group	(753)
Alighting Gear	(223)
Engine Section	(140)
Propulsion Group	(1763)
Engine Install	394
Exhaust System	284
Engine Controls	25
Starting System	17
Fuel System	220
Drive System	823
Flight Controls	(515)
Instruments	(135)
Hydraulics	(44)
Electrical	(247)
Avionics	(306)
Armament	(53)
Furnishings	(453)
Airconditioning	(30)
Anti-Ice	(18)
Load & Handling	(10)
Contingency	(55)
Weight Empty	(5521)
Useful Load	(2617)
Crew (2)	500
Fuel Trapped	14
Fuel Internal	1083
Oil Trapped	6
Oil Engine	14
Payload	1000
Design Gross Weight	(8138)

IR SUPPRESSION/DIRECTIONAL CONTROL SYSTEM STUDY

INTRODUCTION

The fan-in-tailcone concept was developed to reduce the impact of IR plume suppression by integrating the plume suppressor with the directional and antitorque system. The analysis includes trending studies, which quantitatively assess the effects of the ratio of fan-to-engine airflows (dilution ratio), qualitative discussions of the effects of variable tailcone length, determination of fan inlet and exhaust nozzle configurations, and a fan configuration study which includes discussion of different fan/engine air mixing configurations. A qualitative analysis compares this concept with an alternate (fan-in-tailcone plus tail rotor) configuration.

The system studied contains a fan mounted at the juncture of the fuselage and tailcone. It is shaft-driven by the main transmission and pumps both engine exhaust gas and ambient air. The ambient air dilutes the exhaust, thereby lowering its temperature and IR signature. The ratio of ambient air to exhaust flow is referred to as dilution ratio. The mixed gas is directed to the rear of the tailcone and diverted laterally or aft to produce the desired thrust.

EFFECTS OF DILUTION RATIO

General

Based on the total installed power of 1682 SHP calculated for the baseline aircraft and the engine performance data in Appendix B, a total engine airflow of 10 pounds per second at an exhaust temperature of 1100°F is assumed for these studies. Since the most severe suppression requirement and the most demanding aircraft power requirement coincide in hover at 4000 ft, 95°F, this condition is selected for use in the dilution ratio study.

Nozzle Area Required

The nozzle area required to produce a constant thrust with any given mass flow is obtained as follows. In terms of dilution ratio $DR = W_a/W_e$, the equation of continuity is

$$W_e\ (1 + DR) = \rho VA \qquad (1)$$

The relationship between thrust, velocity and area is given by

$$V = Fg/[W_e(1 + DR)] \quad (2)$$

Substitution of Equation (2) for the velocity, V, in Equation (1), and solving for the area, we obtain

$$A = W_e^2 (1 + DR)^2/\rho gF \quad (3)$$

Assuming that the thrust required is the same as the 787 pounds required for the baseline aircraft, Equation (3) is solved and shown in Figure 2.

Fan Power Required

The fan power required can be divided into three categories: thrusting power, duct losses, and fan inefficiency. The duct losses are made up of inlet losses, duct friction losses, and turning losses at the thrusting nozzle. The inlet configuration is designed to maintain a fan inlet total pressure loss of -2"H_2O (-10.4 psf). Other duct losses are calculated for the design dilution ratio of 11 which was ultimately selected. These losses are then flow rate scaled to apply to other dilution ratios. The tailcone frictional pressure loss at the design point is calculated as follows for 120 lb/sec flow at 185°F mixed temperature in a duct 15 feet long and 3.75 feet in diameter:

$$\Delta p = 4f(L/D)q \quad (4)$$

where the friction factor 4f is a function of the duct Reynolds number

$$R_e = WD/\mu A$$

$$= (120)(3.75)/[(1.417 \times 10^{-5})(3.75^2 \times \pi/4)]$$

$$= 2,875,000 \quad (5)$$

The friction for this Reynolds number is 4f = 0.01.

Substituting for 4f, L, D and $q = W^2/2\rho gA^2$ in Equation (4), we obtain

$$\Delta p = .01(15/3.75)[120^2/(2)\ (.0533)\ (32.2)\ (11.04^2)] \quad (6)$$

$$= 1.4 \text{ psf}$$

Proper vane design (discussed later) can restrict the turning loss to approximately 0.1 velocity heads where the velocity head is based on the vane exit area of 10.66 ft^2. Substituting into the equation

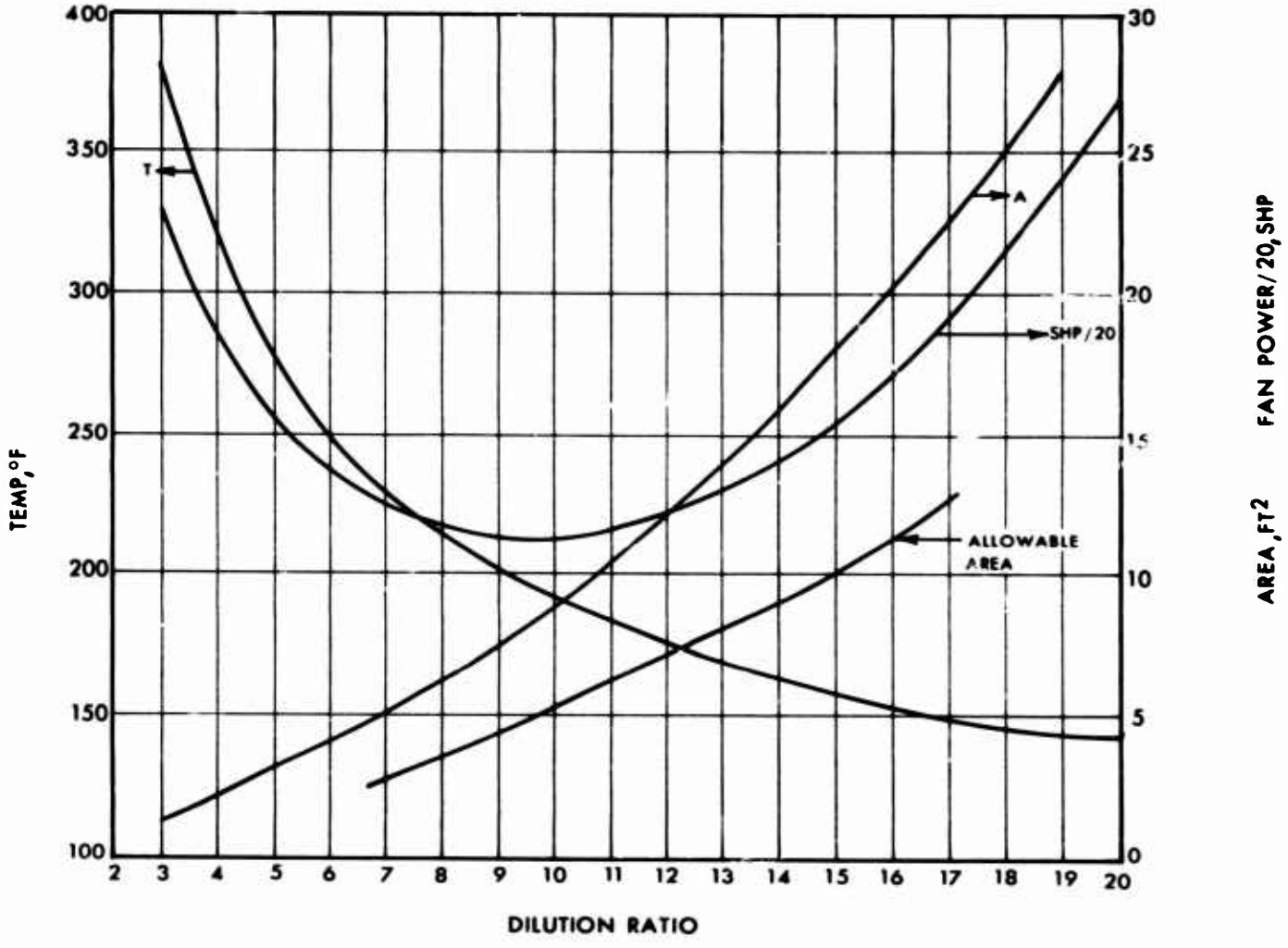

Figure 2. Effect of Dilution Ratio on Exhaust Temperature, Exhaust Area and Fan Power.

$$\Delta p = k_t\, q$$

$$= 0.1\, W^2/2\rho g A^2 \qquad (7)$$

we obtain a turning loss of 3.7 psf.

The total calculated downstream loss of 5.1 psf is increased to 10.4 psf to provide allowance for any foreseeable installation contingencies. The fan power associated with the inlet (10.4 psf) and downstream (10.4 psf) losses is

$$HP = W\Delta p/550\,\rho$$
$$= (120)(20.8)/(550)(.0533)$$

$$= 85 \qquad (8)$$

For other dilutions, the power associated with duct losses will vary as the cube of the total flow rate so that

$$HP = 85[(DR+1)1/12]^3 \qquad (9)$$

The propulsive power (the power required to produce the exhaust velocity given in equation (2)) is given by

$$HP = W_e(1+DR)V^2/[(2)(550)g] \qquad (10)$$

or in terms of thrust,

$$HP = F^2 g/[2W_e(1+DR)(550)] \qquad (11)$$

The propulsive power from Equation (11) is added to the duct loss power obtained in Equation (9) to obtain the total fan power (exclusive of fan efficiency effects). The total power is plotted versus dilution ratio in Figure 2.

Mixed Gas Temperature

The temperature of the mixture of engine exhaust gas and ambient airflow is given by

$$T_M = [(T_e\, W_e + T_a\, W_a)/(W_e + W_a)] + Q/[(W_e + W_a)C_p] \qquad (12)$$

After substitution of the dilution ratio for W_a, equation (12) becomes

$$T_M = [(T_e + T_a\, DR)/(1 + DR)] + Q/[W_e\, C_p\, (1 + DR)] \qquad (13)$$

For the purposes of this study, the quantity of heat added to the fan airflow is estimated to be 27.6 BTU/sec, as shown in Table 3.

TABLE 3. HEAT LOADS CONTRIBUTED TO FAN AIRFLOW

Type	Quantity (BTU/sec)
Cockpit	4.4
Transmission	19.0
Electronics	1.4
Avionics	2.8
Total	27.6

Substitution of 95°F for T_a, 1100°F for T_e, 10 lb/sec for W_e, 27.6 BTU/sec for Q and .24 BTU/lb-°F for C_p in Equation (13) results in the following expression:

$$T_M = (1111.5 + 95\ DR)/(1 + DR) \tag{14}$$

In addition to the heat loads shown in Table 3, the work done on the air by the fan must be accounted for.

The fan power is given by the sum of equations (9) and (11).

$$HP = [F^2g/2W_e(1+DR)(550)] + 85\ [(DR+1)/12]^3 \tag{15}$$

The thermal equivalent of this power is

$$Q + 550\ HP/J \tag{16}$$

and its effect on the total temperature of the mixed air is

$$\begin{aligned} \Delta T &= Q/[\ W_e(1+DR)C_p] \\ &= F^2g/\ [2W_e^2(1+DR)^2JC_p] \\ &+ (550)(85)\ [(1+DR)/12]^3/[W_e(1+DR)JC_p] \end{aligned} \tag{17}$$

Since we have assumed that the thrust required is the same as the 787 pounds required for the baseline aircraft during a critical yaw maneuver, Equation (17) can be solved for the total temperature rise of the fan airflow as a function of dilution ratio.

This temperature rise is added to the mixed temperature calculated in Equation (14) and the result plotted in Figure 2.

IR Suppression Criteria

The allowable hot metal area and associated temperatures below the lower temperature limit as defined in Appendix B were correlated to a radiation level provided by the Eustis Directorate in a portion of the 3 to 5 micron bandwith. Since the nozzle temperature (if uncooled) is a function of dilution ratio, the allowable area is also a function of dilution ratio. This functional relationship is shown on Figure 2, where it can be seen that in all cases, the area required for thrust generation exceeds the area allowed for hot metal IR signature. This discrepancy, which is resolved by cooling the vanes, is discussed in the section on turning vanes.

As shown in Figure 2, the maximum allowable plume temperature of 400°F fixes the minimum dilution ratio at approximately 2.5:1.

Selected Dilution Ratio

Based on a desire to operate near the bucket of the power required curve, a dilution ratio of 11 to 1 is selected as the primary design point. This dilution ratio also represents the maximum exhaust nozzle area compatible with a fan and duct diameter of 3.5 to 4 feet. It should be noted that the maximum yaw thrust level was used in the calculations of this section. This thrust requirement sizes the fan. However, if a variable pitch fan is provided, the power required for steady-state antitorque can be reduced by diverting some of the fan flow aft, thereby reducing the backpressure on the fan.

TAILCONE LENGTH

The calculations in the previous section were based on the assumption that the tailcone length and directional control thrust were the same as required for the baseline aircraft. If we examine the effects of changing the tailcone length (at a given dilution ratio), the following trends are developed:

With an increased tailcone length, the thrust required is reduced. In order to obtain this reduced thrust at a constant dilution ratio (constant total mass flow), the nozzle area must increase inversely proportional to the thrust. This is undesirable for several reasons: (1) the area to be cooled (nozzle area) increases; (2) the nozzle area at the baseline

length is already as large as is practical for the fan and tailcone under consideration; (3) the advanced configuration balances and any additional aft CG movement will necessitate growth in the nose area. Further, increased overall length, in general, is not advantageous.

Decreased tailcone length increases the total thrust required, which causes an increase in required nozzle velocity for a given mass flow. The associated propulsive and turning loss power increases proportional to the square of the thrust and increases both gearbox power and weight and engine power and fuel flow, which override the decreased weight of the tailcone. While a detailed design study might show some advantage to a small decrease in tailcone length, a length similar to that on the baseline aircraft is close to optimal.

FAN INLET CONFIGURATION

The fan inlet configuration chosen consists of independent supply ducts for the engine exhaust, fan inlet, and transmission cooling air duct. All inlets are tuned to achieve the desired flow balance.

Separate inlets are provided for the transmission cooling air and fan inlet because of the increased pressure loss that would be required to duct all of the fan air around the transmission and because of the drag reduction available through judicious location of an air inlet aft of the main rotor pylon.

The use of an upstream plenum for the fan inlet was rejected primarily because of a desire to duct the engine exhaust flow into the fan in a manner which will promote mixing with the ambient air and decrease the likelihood of obtaining locations of excessive temperature on the tailcone duct walls or the hub or blades of the fan. Such a plenum would also decrease ram pressure recovery and ease of maintainability.

EXHAUST NOZZLE CONFIGURATION

General

The exhaust nozzle configuration chosen consists of two moveable deflector doors which open and close an aft-facing nozzle and two sets of side-facing turning vanes as shown in Figure 3. Because the hot exhaust gas is ducted through the tailcone, the fan must always provide cooling airflow and the rear nozzles can never be closed in all directions.

The aft nozzle provisions require masking the hot engine exhaust from direct view through the aft end of the tailcone (centerbody plugs were considered and found to add considerable

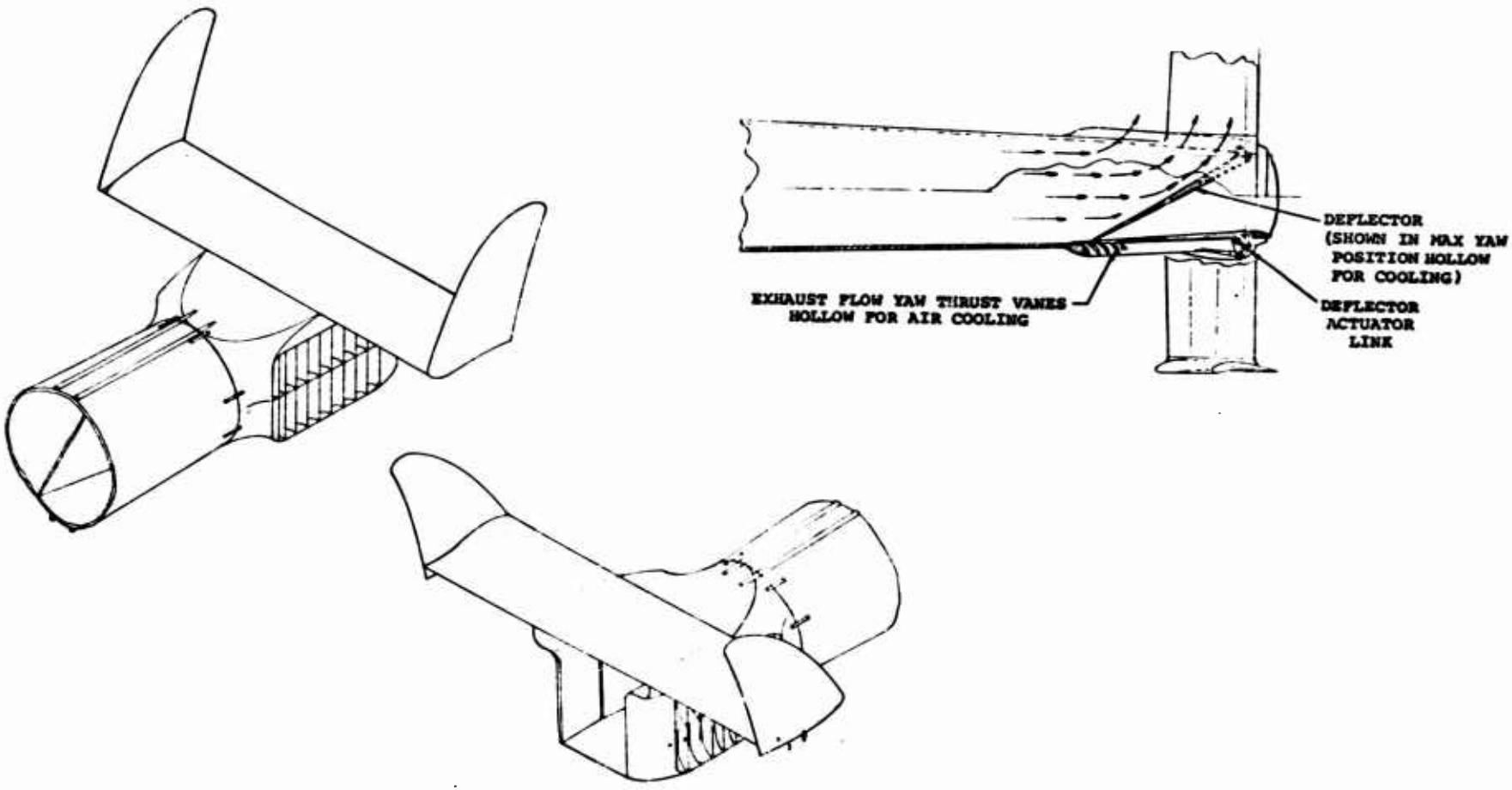

Figure 3. Exhaust Nozzle Configuration.

vehicle length as shown in Figure 4). A more desirable masking system is obtained by a planar strip of material having a length equal to the tailcone length and a height equal to the tailcone diameter. This strip is given one 180° twist and installed within the tailcone to mask the fan and engine exhaust.

An attempt was made to pivot the doors from their midpoint instead of the aft end. If successful, this attempt to aerodynamically balance the doors might have eliminated the requirement for power assist for the door control system. As shown in Figure 4, this configuration requires excessive constriction of the flow passage in plan view which entails either an expansion loss at the exit plane or excessive duct and nozzle height to compensate for the decreased width.

VANE DESIGN

The turning vanes are of circular arc profile. Figure 5 shows a plan view of the mean camber line of the vanes. These vanes are hollow to permit air cooling to acceptable IR levels. As shown in Figure 5, the deflection doors turn the air somewhat prior to its passage through the turning vanes, so that the vanes accomplish only a portion of the turning.

Assuming the presence of one horizontal splitter, the aspect ratio of the air passages varies from 3.3 to 11.2. Each passage has a mean bend radius to thickness ratio of 4:1. The individual passage pressure loss coefficients are calculated with the assumption that the entire 90° turn is accomplished by the turning vanes and vary from 0.092 to 0.100.

Vane Cooling

The turning vanes are cooled by passing 2.1 lb/sec (1.05 lb/sec on each side) of cooling air through vertical passages .12 inch thick, which run from an inlet manifold at the top of the vanes to an outlet manifold at the bottom. Air is provided to the inlet from the pressure side of the fan through a duct located on the top side of the tailcone. As shown in Figure 44, the design of the daisy exhaust precludes the introduction of exhaust gas into the cooling air duct. An additional 0.4 lb/sec of cooling air is used to cool the two deflection doors which are visible through the vanes, with the door hinges serving as distribution manifolds. A trade-off study verified that it is more efficient to cool these doors than to enlarge the turning vanes to block the doors from view.

Cooling Air Pressure Loss Analysis

The hover design point fan pressure of 48 psf includes 11 psf inlet loss. This leaves 37 psf for downstream losses.

Since W/s is a function of t, h_c is also a function of t.

The coolant temperature at any point on the heat exchanger is given by the relationship

$$(T_c - T_{ci}) / (T_g - T_{ci}) = 1 - e^{-UA/WC_p} \qquad (24)$$

where $U = 1/(1/h_c + 1/h_g)$
$A = sx$

The heat balances on the vanes are given by

$$Q = h_c (T_w - T_c) \qquad (25)$$

$$Q = U (T_g - T_c) \qquad (26)$$

Substitution of Equations (25) and (26) into Equation (24) yields the following solution for the local wall temperature

$$T_w = T_g h_g/(h_c+h_g) + h_c [T_{ci}+(T_g-T_{ci}) (1-e^{-Usx/WC_p})] / (h_c+h_g) \qquad (27)$$

or

$$T_w = T_g - \beta e^{-\gamma x}$$

where

$\beta = h_c(T_g - T_{ci})/(h_c + h_g)$
$\gamma = Us/WC_p$

For radiation purposes, the average temperature is given by

$$Tw = \sqrt[4]{\int_{x=0}^{L} (T_w+459)^4 sdx / \int_{x=0}^{L} sdx} - 460 \qquad (28)$$

Equation (27) can be substituted into Equation (28), after which the fourth power binomial can be expanded and integrated term by term, with the result that

$$(T_w + 460)^4 = [a^4 L + 4a^3\beta(e^{-\gamma L}-1)/\gamma - 3a^2\beta^2(e^{-2\gamma L}-1)/\gamma + 4a\beta^3(e^{-3\gamma L}-1)/3\gamma - \beta^4(e^{-4\gamma L}-1)/4\gamma]/L \qquad (29)$$

where $a = T_g + 460$

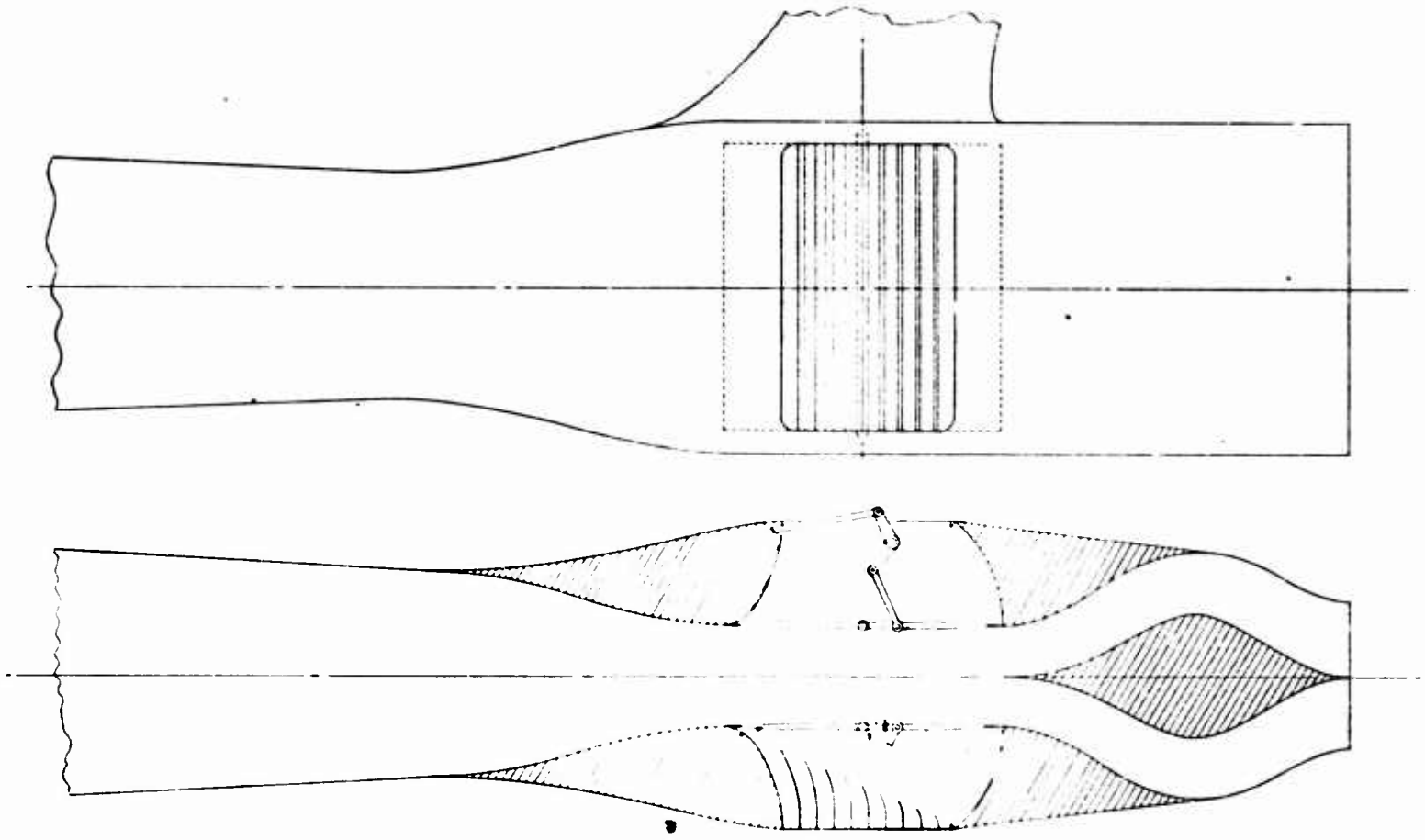

Figure 4. Alternate Diverter Door and View Blockage Systems.

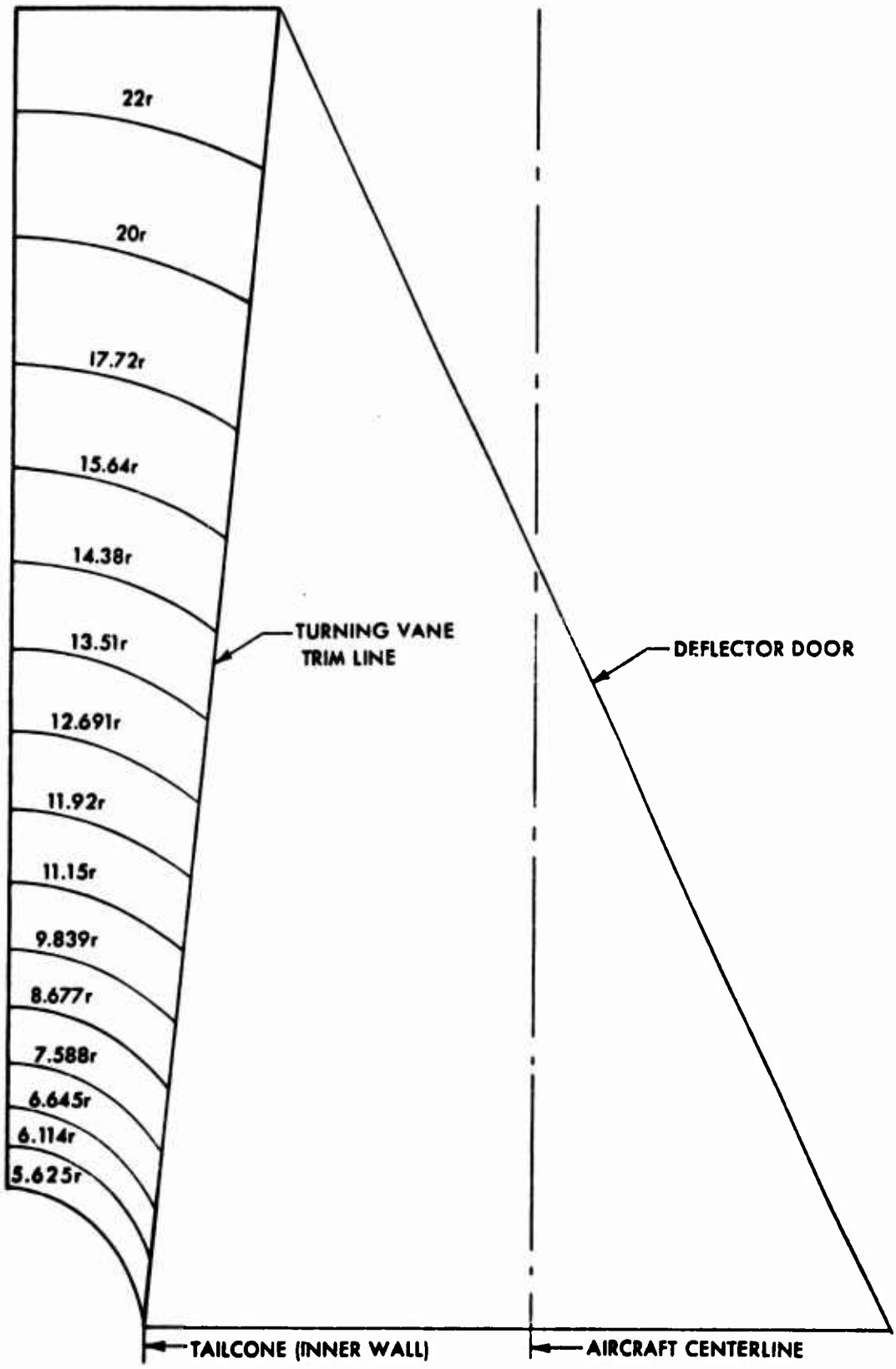

Figure 5. Exhaust Vane Configuration.

The external heat transfer coefficient is given by

$$h_g = .023\ R_e^{.8}\ P_r^{.4}\ k/D_H \qquad (30)$$

All of the vanes have different geometry, but a Reynolds number and hydraulic diameter of 300,000 and 0.5 ft are typical. The resulting heat transfer coefficient is h_g = 16.8 BTU/ft/hr/°F.

Substitution of

T_g = 185°F
L = 2.75 ft
h_c = f(t)
T_{ci} = 100°F (allows 5°F for fan work and upstream heat sources)
h_g = 22 BTU/ft^2-hr-°F (allows 30% increase for entrance effects)
(W/s) = f(t)

permits calculation of $\bar{T}$ as a function of cooling air passage height, t. The results of these calculations are shown in Figure 6.

The selected design point of t = .01 ft, W/s = .0488 lb/sec-ft and $\bar{T}$ = 153.8°F provides a radiation margin to accommodate local warm areas on the tailcone. Since both surfaces of the vanes are cooled, the average vane thickness is .02 ft. A vertical member is installed at the mean camber line to provide additional stiffness and to maintain a physical correspondence with the analytical model.

Tailcone Temperature and Radiation

The tailcone is constructed from 1-inch thick Nomex honeycomb with Kevlar prepreg skins .03 inch thick on the outer surface and .02 inch thick on the inner surface. The design of the engine daisy exhaust maintains a film of ambient air in contact with the inner skin of the tailcone until mixing is complete at the aft end.

Assuming a worst case condition of completely mixed air (185°F) in contact with the tailcone inner surface and an average rotor downwash velocity of 60 ft/sec over the tailcone outer surface, an average tailcone outer surface heat transfer coefficient of h_a = 8.15 BTU/ft^2/hr/°F is calculated. The internal heat transfer coefficient and the thermal conductance of the honeycomb are 14.44 and .452 BTU/ft^2/hr/°F, respectively. The resulting tailcone outer surface temperature is 99.6°F on a 95°F day.

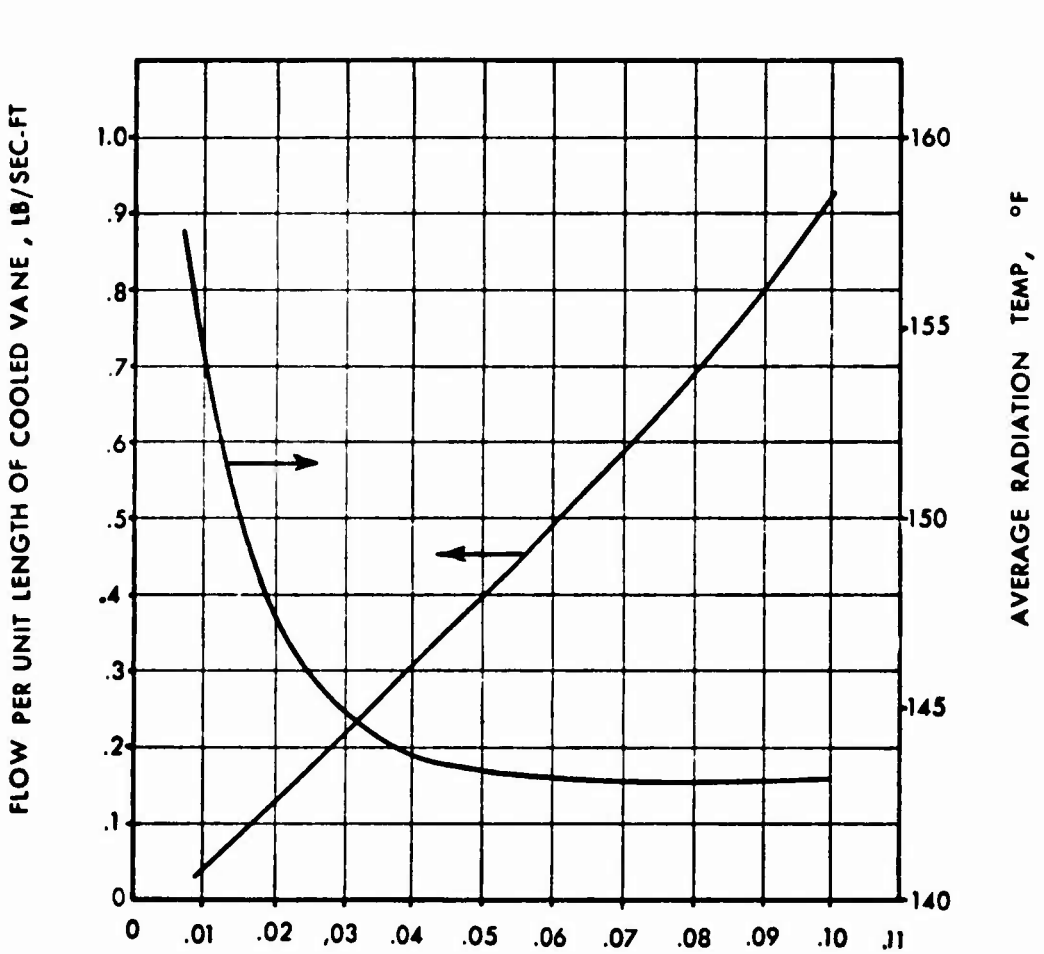

Figure 6. Effect of Air Passage Height on Flow Rate and Average Radiation Temperature.

The infrared signature of the 33 ft^2 side projected area of the tailcone is 0.12 watt per steradian which, when added to the signature of the exit vanes, does not exceed permissible levels.

DIRECTIONAL CONTROL SYSTEM

The directional control system is designed to provide the required antitorque and directional control thrust in hover and directional control thrust in cruise. Antitorque reaction in cruise is provided by the vertical stabilizer. The directional control system actuates the deflector doors, which varies the airflow split between the two side nozzles and the aft nozzle.

The control system as originally conceived, operated the two doors by a combination of individual and collective pedal movements as shown schematically in Figure 7. The collective pedal motion controlled the aft nozzle opening (forward thrust), while the individual pedals controlled the yaw thrust. As a result of a preliminary design evaluation, the collective pedal motion was eliminated and replaced with an input from the aircraft forward cyclic stick as shown schematically in Figure 8. The separation of the two doors (forward thrust level) is, therefore, almost completely a function of flight speed; as a result, the coupling between forward and side thrust is reduced in magnitude. For simplicity, the system is shown schematically in Figure 8 as a control rod operated system for one pilot. In practice, the same schematic operation is attainable with closed-loop cables and inputs from two sets of pedals. Such a system could easily provide two sets of control cables and dual servos to decrease control system vulnerability to small-arms fire.

IR FAN PITCH CONTROL

Control of the IR fan pitch is based on the following premises:

1. In order to maintain IR suppression, the total fan flow should remain nearly constant despite variable requirements for antitorque and directional control thrust. Thrust variation should be attained through the use of variable aft-end geometry. This approach eliminates any potential control lag problems associated with changing the fan airflow to change thrust level.

2. When IR suppression is not required, or ambient temperatures are low, it is desirable to decrease the fan flow to reduce its power consumption.

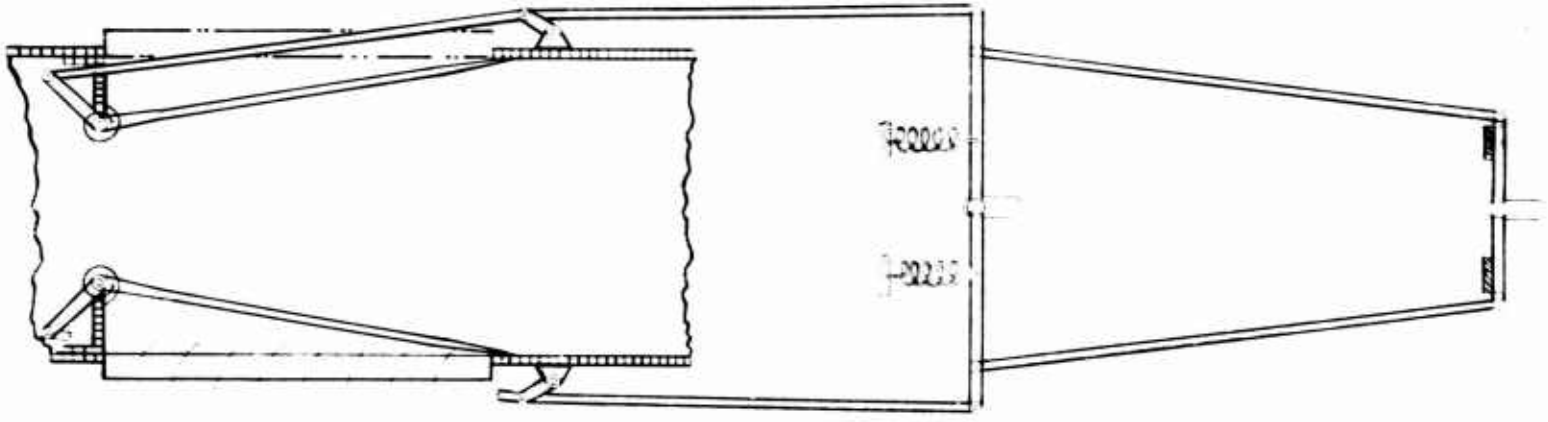

Figure 7. Directional Control System Schematic With Individual and Collective Pedal Movement.

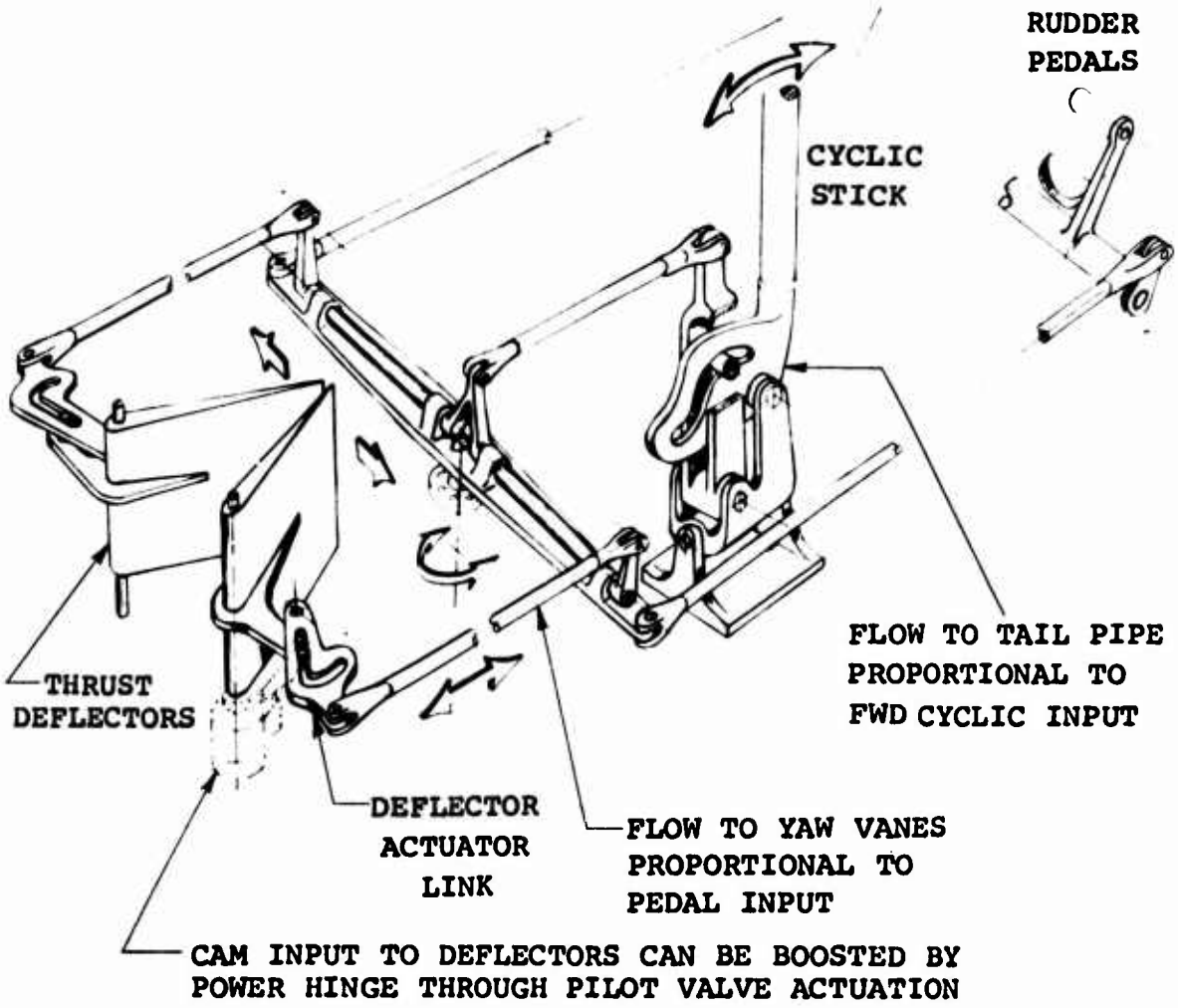

YAW CONTROL SYSTEM SCHEMATIC
(NO SCALE)

NOTE: OVERRIDE SLOT IN THE DEFLECTOR ACTUATOR LINK ALLOWS YAW CONTROL DURING FWD THRUST FLIGHT. PUSHROD ARRANGEMENT IS SHOWN FOR CLARITY; HOWEVER, SYSTEM MAY BE IMPLEMENTED WITH A CLOSED-LOOP CABLE OR FLY-BY-WIRE CONFIGURATION.

Figure 8. Directional Control System Schematic With No Collective Pedal Movement.

3. In order to reduce momentum drag in cruise, the fan flow should not increase beyond IR requirements. Further, since the main rotor is a more efficient thruster than the fan, it is not desirable to generate net forward thrust in cruise, and the fan should merely overcome the inlet and ducting losses.

The first consideration is met by controlling the fan pitch to maintain a constant dynamic pressure in the tailcone duct downstream of the fan. Constant maximum thrust is available regardless of ambient temperature as shown below:

$$\begin{aligned} q &= \rho V^2/2g \\ &= \rho V(W/\rho A)/2g \\ &= VW/2gA \\ &= F/2A \end{aligned} \qquad (31)$$

The second consideration is met by providing an alternate reduced setting for the dynamic pressure control point for the fan. The setting selected provides a dilution ratio of 10.1 to 1 at sea level standard day conditions. This reduced setting is selected so that (a) sufficient thrust for steady-state hover is available and (b) the exhaust temperature of 157.2°F at sea level standard day conditions is less than the 183.5°F temperature attained at 4000 ft, 95°F with the higher fan control point. It is necessary that the control system design provide automatic return to the higher control point whenever the deflector doors in the aft end reach the maximum antitorque thrust position.

The third condition is met by sizing the aft-facing nozzle so that the exhaust velocity is equal to the cruise speed at sea level standard day conditions with the fan pressure control at the lower setting as discussed in the previous paragraph. During a design refinement stage, the nozzle size was reduced from 7.32 ft^2 to 6.30 ft^2. As a result, 131 pounds of thrust are produced in cruise. However, the change in design point raises the fan efficiency from 57 percent to 83 percent, and the cruise fan power increase from 40.7 hp to 60.7 hp provides the thrust at an efficiency comparable to that of the main rotor.

FAN CONFIGURATION STUDY

Hamilton Standard, under subcontract, conducted a fan design study for an advanced fan-in-fuselage helicopter concept. The study was conducted in three phases: (1) a feasibility study, (2) a preliminary design, and (3) a blade and temperature stress investigation.

FEASIBILITY STUDY

A design feasibility study was conducted by Hamilton Standard to identify a fan concept which could supply and modulate airflow for antitorque control while at the same time provide IR suppression for the advanced helicopter. Upon identification of a viable concept, weight and aerodynamic performance parametric data were developed to support aircraft studies.

Concept Selection

The two basic approaches which were considered are illustrated in Figure 9. Each has its particular design considerations, benefits and technical challenges. The first approach, referred to as the postmixing concept, isolates the two gas streams in separate ducts as they pass through the fan disk. Dilution of the engine exhaust is accomplished in the tailcone. The second approach, referred to as the premixing concept, involves injecting the engine exhaust into the fan duct ahead of the fan, resulting in dilution upstream of the fan disk. Each approach is discussed below.

1. Postmixing

   Several variations of the postmixing concept were explored. Each employed separate flow paths for the ambient air and 1100°F engine exhaust and required two sets of blades. The blades in the engine exhaust stream prevent back-pressuring the engine power turbine with the dilution air and the associated power loss. A second set of blades provides the dilution air. As the range of operating conditions for the engine exhaust is judged to be small, variable pitch for the first set of blades is not considered necessary. Based upon Hamilton Standard's earlier involvement in fan-in-fuselage helicopter studies, under subcontract in Army Contract DAAJ02-73-C-0033, it was judged that adequate antitorque thrust modulation would require a variable-pitch outer fan. This was subsequently confirmed during the performance studies described herein.

   Postmixing is typified by Figure 10. The fan is mounted on a bearing set within the center body; the fan's coaxial disks are front driven from the main transmission. The variable-pitch mechanism is located at the fan center where it is protected from the high temperature of the engine exhaust. The integration of the fan components in this manner provides a significant reduction in system complexity.

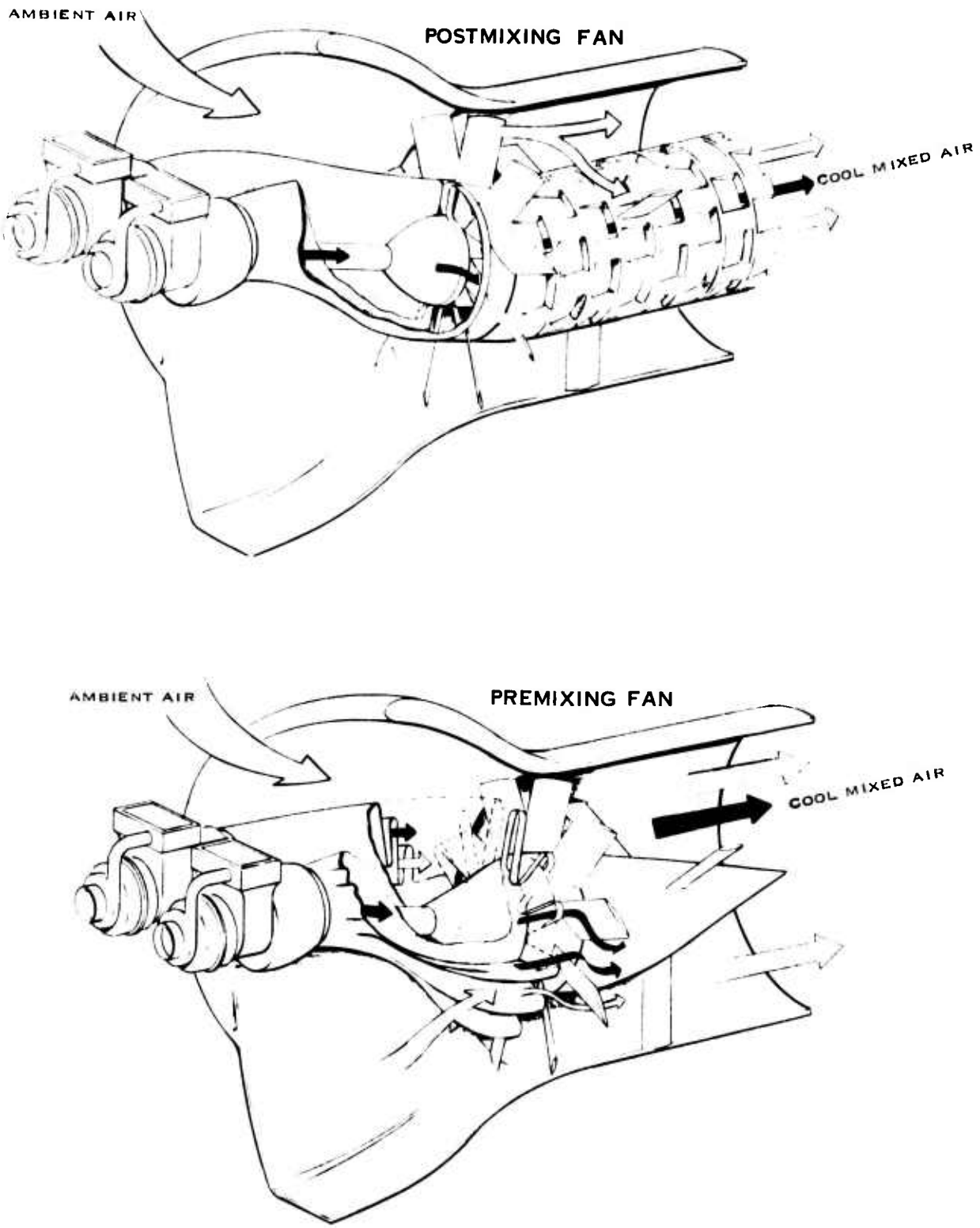

Figure 9. Postmixing and Premixing Fan Concepts.

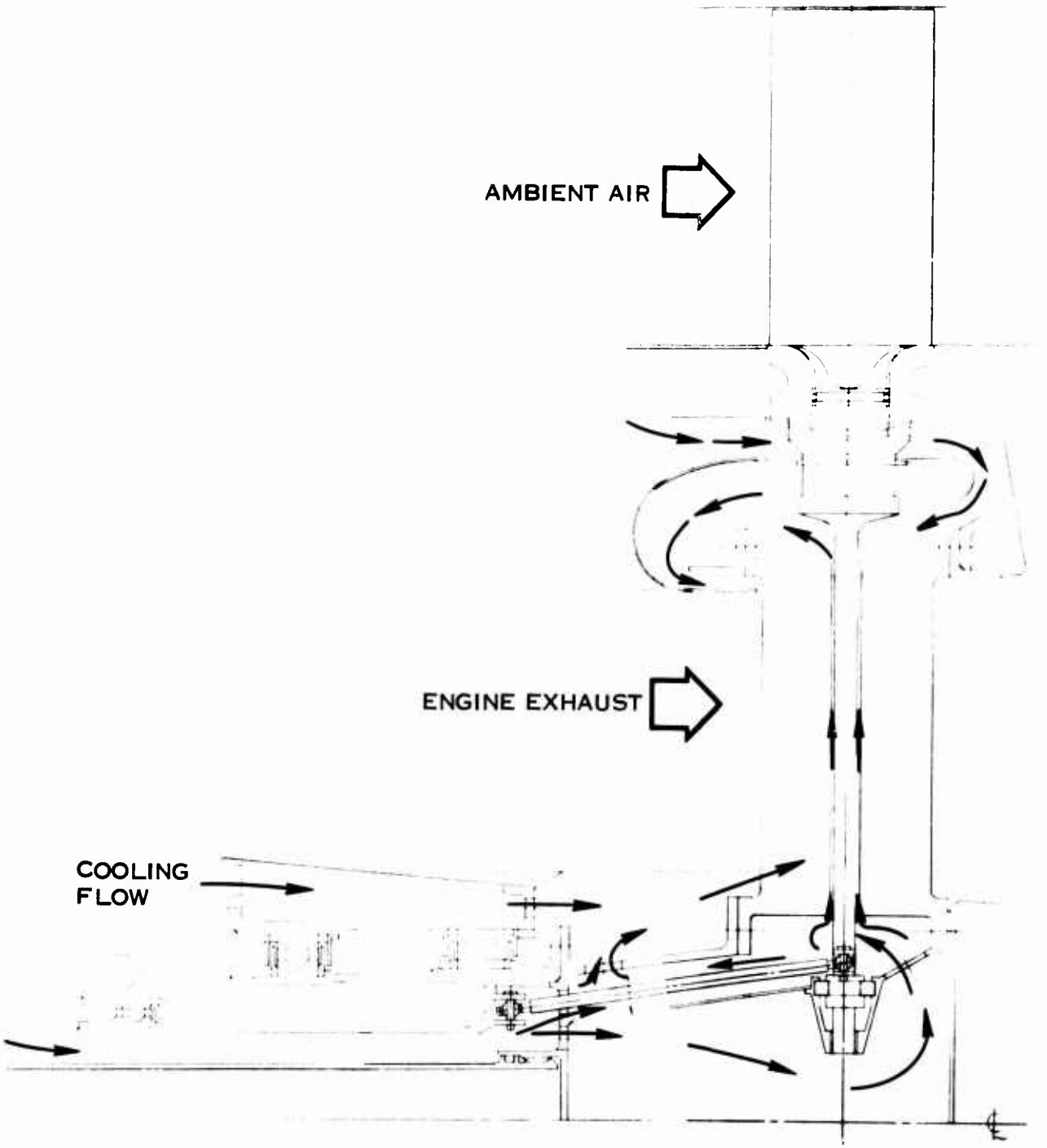

Figure 10. Postmixing Fan Preliminary Layout.

In the postmixing design concept, the hot engine exhaust is located within the cool annulus provided by the dilution air. This keeps the engine exhaust remote from the composite honeycomb aircraft skin which would otherwise require substantial additional insulation or cooling to maintain a surface temperature low enough to obtain the desired signature level. Locating the hot engine exhaust within the dilution airflow path, however, places it in close proximity to the pitch change mechanism and support bearings. These areas are lubricated and, therefore, require special attention to achieve the required thermal isolation. This isolation could be accomplished by a layer of cool air channeled through an intricate series of baffled passages to both cool and insulate the critical areas. The low pressure at the inner radius of the low-temperature blading, however, makes it doubtful that the fan would be an adequate source of cooling air; a higher pressure ratio auxiliary cooling fan would be needed. This is contrary to the objective of obtaining improved maintainability and reliability through pneumatic system integration.

In the consideration of the fan for use in the hot engine exhaust, it was obvious that special materials are required. The fan blades, disk and flow path surfaces were identified as those areas which require unique materials. The temperature and exhaust products at this location are similar to conditions routinely encountered in engine hot sections and, therefore, appropriate materials are available. However, the ferrous alloys suitable for this environment are considerably heavier than conventional fan blade materials. In addition, the lightweight composite structure normally selected for the postmixing approach is compounded by the duplication of structure and components required to provide the coaxial gas flow paths.

The structural path between the engine exhaust fan and dilution air fan requires both thermal isolation, to minimize heat conduction into the critical bearing and actuator areas, and flexibility between the hot and cool structure, to minimize thermal distortion and growth effects. Thermal isolation is obtained by providing a structural path for the dilution air fan disk which is longer than required by geometrical considerations to minimize thermal conduction. In addition, materials of low thermal conductivity, such as titanium, are used to minimize heat conduction.

2. Premixing

The second approach investigated in the feasibility study is premixing of the engine exhaust ahead of a single variable pitch fan which pumps both engine exhaust gas and dilution air. Conceptually, it is similar to the postmixing concept, but without the complexity of the separate high-temperature fan blading.

The engine exhaust manifold distributes the engine exhaust in a series of hot gas streams spaced around the disk. This provides some mixing of the gas streams ahead of the disk and maintains a cool boundary layer on both the inner and outer surfaces of the fan duct. While this approach does not require the separate high-temperature fan of the postmixing concept, two factors related to premixing must be considered in the concept evaluations.

a. Although it is not necessary to use high-temperature ferrous alloys for the fan blades in the postmixing concept, they must be capable of withstanding elevated temperatures. Design point temperatures of up to 330°F associated with a 3/1 dilution ratio are predicted. Higher dilution ratios produce lower temperatures. The effective temperature is obtained by the combined effect of mixing that occurs ahead of and within the fan disk and the temperature averaging which takes place as the blades pass through the alternating hot and cool gas streams. These temperature levels are well within the capability of available composite materials which would be used for the blades.

b. The fan blades passing through the density and velocity variations produced by the alternating streams of engine exhaust gas from the closely coupled manifold will create a high-frequency noise signature unique to this configuration. Close coupling of the exhaust manifold and fan is dictated by other aircraft system considerations, such as transmission weight and vehicle center of gravity. It is not within today's state of the art to analytically predict the noise levels or audio-detectability distance of this concept. However, the necessary technology can be obtained by proper emphasis on experimental investigation.

It was judged, on the basis of this effort, that relative simplicity and lighter weight of the premixing approach provides the more practical fan for this aircraft concept. Preparation of the weight and aerodynamic performance parametric studies was based on the premixing approach.

Parametric Data

Generalized aerodynamic performance and weight trends were established for the selected premixing fan concept to facilitate vehicle trade-off studies and selection of a specific fan size for the preliminary design effort. These data are discussed below.

The most powerful parameter in fan aerodynamic design is solidity, i.e., total activity factor (TAF) where $\sigma = .0657$ (TAF)(R)/100π; therefore, an initial sizing study was conducted to establish the solidities that were needed to cover the pressure/weight requirements for dilution ratios of 6:1, 11:1 and 15:1, which are the regions of greatest interest. These solidities form the basis for an aerodynamic design and computation of fan maps for several fans. Efficiency was computed as a function of total activity factor and fan pressure rise for 3.5-foot-diameter, 0.5-hub/tip-diameter ratio, 600-foot/second-tip-speed optimum aerodynamic design fans operating at each of the design points shown in Table 4. The results of the study are presented in Figure 11.

From these curves, it was concluded that a very wide range of total activity factors, from approximately 1000 to 4000, is required to cover dilution ratios of 6:1 to 15:1. It was clear that this range of solidities could not be covered by the three fan designs planned without involving large and questionably accurate interpolation for intermediate solidities. It was decided to concentrate on four solidities which cover the 11:1 to 15:1 dilution ratio without necessitating inordinately large interpolations. Solidities of 1250, 2083, 2916 and 3750 were selected as the basis for aerodynamic design.

TABLE 4. PRELIMINARY HOVER DESIGN POINTS

Dilution Ratio		6/1	11/1	15/1
Total Weight Flow	(lb/sec)	70	120	160
Pressure Rise (for fixed thrust)	(lb/ft^2)	119	57.8	42.1
Altitude	(ft)	4000	4000	4000
Ambient Temperature	(°F)	95	95	95
T_M	(°F)	238.6	178.8	157.8

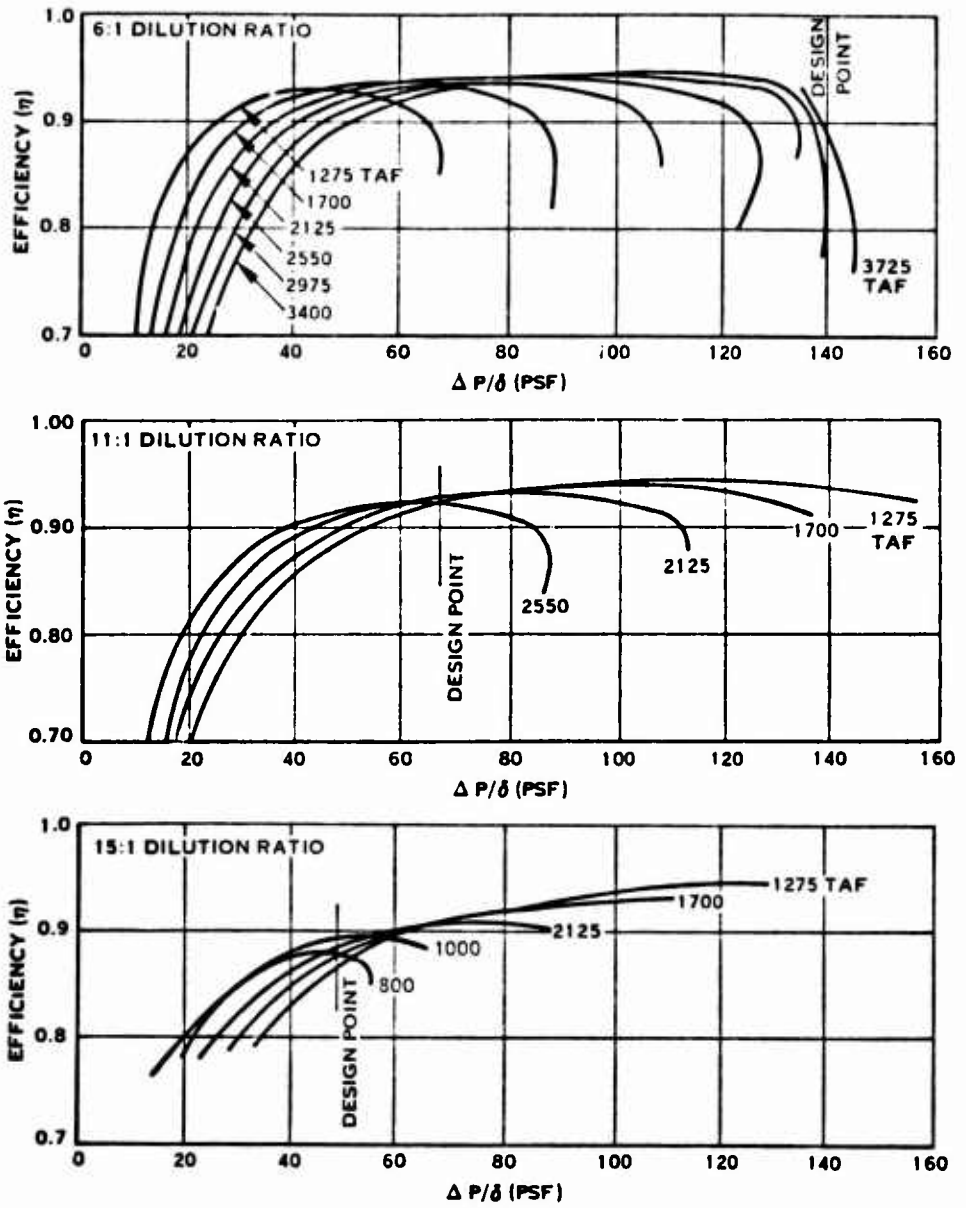

Figure 11. Effect of Total Activity Factor and Dilution Ratio on Fan Efficiency.

Fan designs consisting of width, thickness, twist and camber distributions were established for each solidity, and aerodynamic performance maps were computed. Efficiency was determined as a function of corrected weight flow, pressure rise and blade angle. In this generalized form, variations of mixed gas temperature and diameter and limited variations in tip speed (±10%) could be investigated. These data were plotted sequentially as they were computed starting with 1250 TAF. The initial data showed that the use of the higher solidities is of little interest because they could not provide reasonable cruise efficiency. Therefore, the computed fan map for 3750 TAF was not plotted, and emphasis was shifted to the determination of a fan design which provides improved cruise efficiency. Figure 12 presents the computed fan maps for 1250, 2083 and 2916 TAF fans.

A vehicle having an 11:1 dilution ratio was selected as the basis for the off-design performance improvement study. The off-design conditions and performance requirements for this vehicle are shown in Table 5. The critical yaw maneuver and 140-knot cruise condition were identified as the key design points, as they represent the extremes of the required fan pressure rise. Of the four fans for which performance maps had been computed, i.e., 1250, 2083, 2916 and 3750 TAF, the 1250 TAF fan provided the highest cruise efficiency, 32%, indicating that a solidity reduction would be needed to obtain improved cruise performance.

Further studies were conducted to examine both tip speed and solidity for potential cruise performance improvements. Reductions of both parameters were shown to be beneficial, and a 565-ft/sec tip speed, 1000 total activity factor fan resulted in a cruise efficiency of 57% while providing 93% efficiency in hover. This aerodynamic design was selected as a basis of the preliminary design study.

Weight

An analytical expression for fan weight was developed so that trends for the major influencing variables could be established for vehicle studies. The fan components which are included in the expression are blades, disk, pitch change mechanism, support housing and spinner. Aside from configuration, fan diameter, solidity and tip speed, in that order, have the most powerful influence on weight. Previous weight trend studies have established the sensitivity of fan weight to these factors.

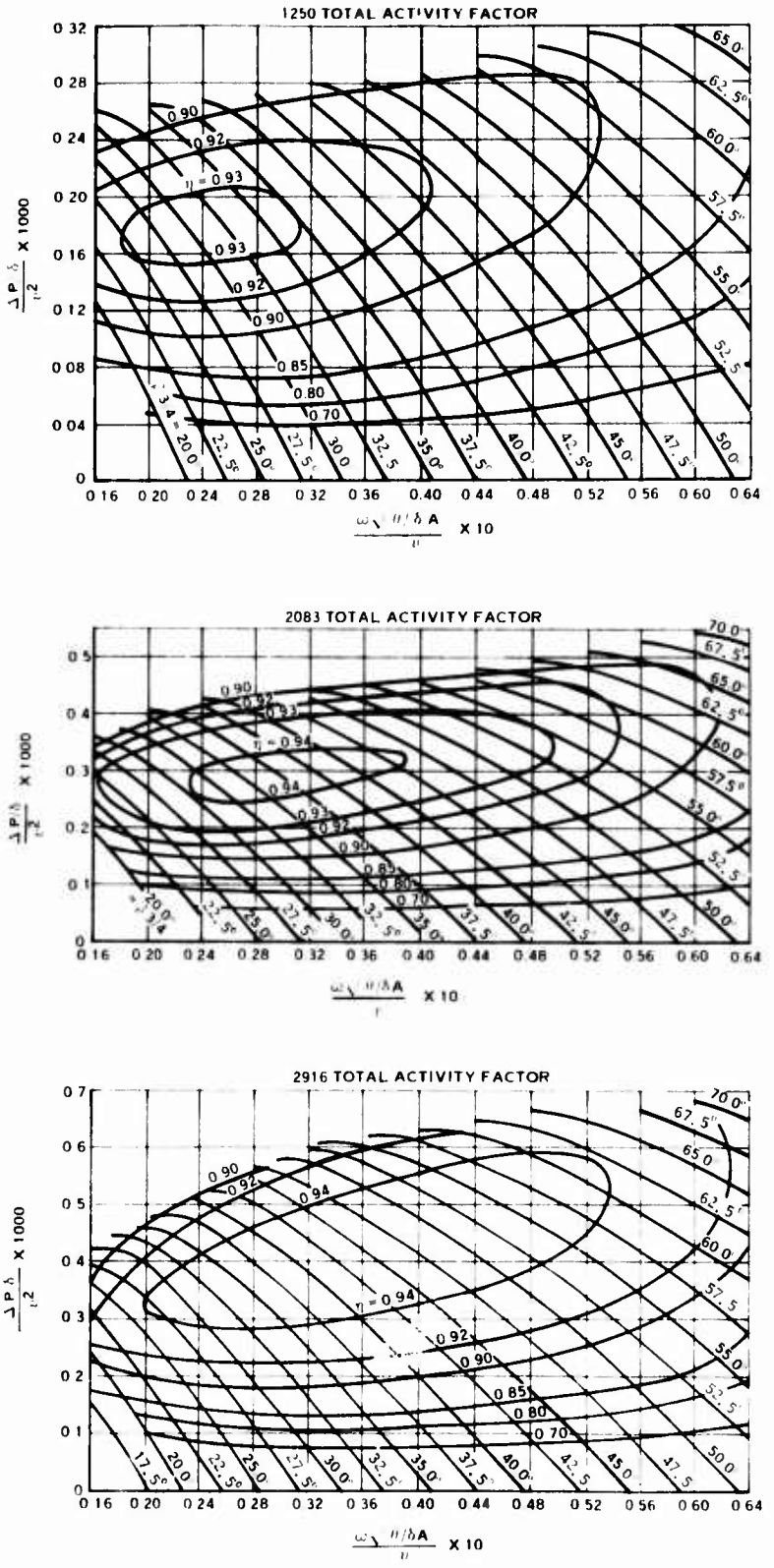

Figure 12. Fan Maps for 1250, 2083 and 2916 Total Activity Factors.

TABLE 5. FAN AERODYNAMIC DESIGN POINTS

		Hover	Cruise 140kt	Hover	Hover	Critical Yaw	Cruise 140kt
IR Suppression		No	Yes	Yes	Yes	Yes	Yes
Weight Flow**	(lb/sec)	100	111	111	120	120	120
Pressure Rise	(lb/ft^2)	41.2	7.4*	40.9	47.1	57.8	42.5
Altitude	(ft)	4000	SL	SL	4000	4000	4000
Ambient Temperature	(°F)	95	59	59	95	95	95

*This design point was later changed to 16.4 psf to reduce the aft nozzle area.

**Flow rates were later increased by 2.5 lb/sec to cool the aft nozzle vanes and deflection doors.

The Blackhawk fan-in-fin production weight estimate, developed by Hamilton Standard during the Army's sponsored program, and recent lift and propulsion fan designs were adjusted to account for component and configuration differences and then used to establish a baseline weight factor which could be scaled for changes in the parameters noted above.

The structures and materials employed in the weight formula are consistent with a production application for the late 1970's and are within today's state of the art. The blades, a major component, are fabricated from a metal matrix composite, boron-aluminum, capable of operation at a temperature level considerably higher than anticipated for this application.

The weight expression

$$Wt = 3.9D^2 \, (TAF/1000) \, (TS/600)^{.5} \qquad (32)$$

has been correlated with recent Q-Fan design weight estimates, as well as production weight estimates for the fan-in-fin.

PRELIMINARY DESIGN

Aerodynamic

The 1000 TAF, 565-foot/second tip speed, 4-foot-diameter fan design tentatively selected for the 11:1 dilution ratio aircraft during the feasibility study was examined to determine whether a hub/tip ratio reduction from 0.5 to 0.4, to accommodate a smaller engine exhaust manifold diameter, had a significant effect on fan performance. Fan efficiency was computed as a function of corrected pressure rise for hub/tip ratios of 0.4, 0.5 and 0.6. The results of this study, shown in Figure 13, indicated that the yaw maneuver design point could not be met by the selected fan with a 0.4 hub/tip ratio.

The parameters which significantly affect pressure rise, with the exception of hub/tip ratio, are solidity and tip speed. Increasing either parameter produces a corresponding increase in fan pressure rise capability. A study was conducted in which variations of TAF from 1000 to 1155, tip speeds from 550 to 600, and fan blade geometry were examined. The objective is to increase the maximum fan pressure rise to a value 10% higher than the maximum operating requirement at the critical yaw condition without reducing cruise efficiency. Minimum solidity and tip speed are also objectives because of their direct effect on weight and noise, respectively. Experience has shown that this provides an adequate stall margin for this type of fan, insuring smooth operation under all anticipated steady-state and dynamic operating conditions and inlet distortions. The results of this study, shown in

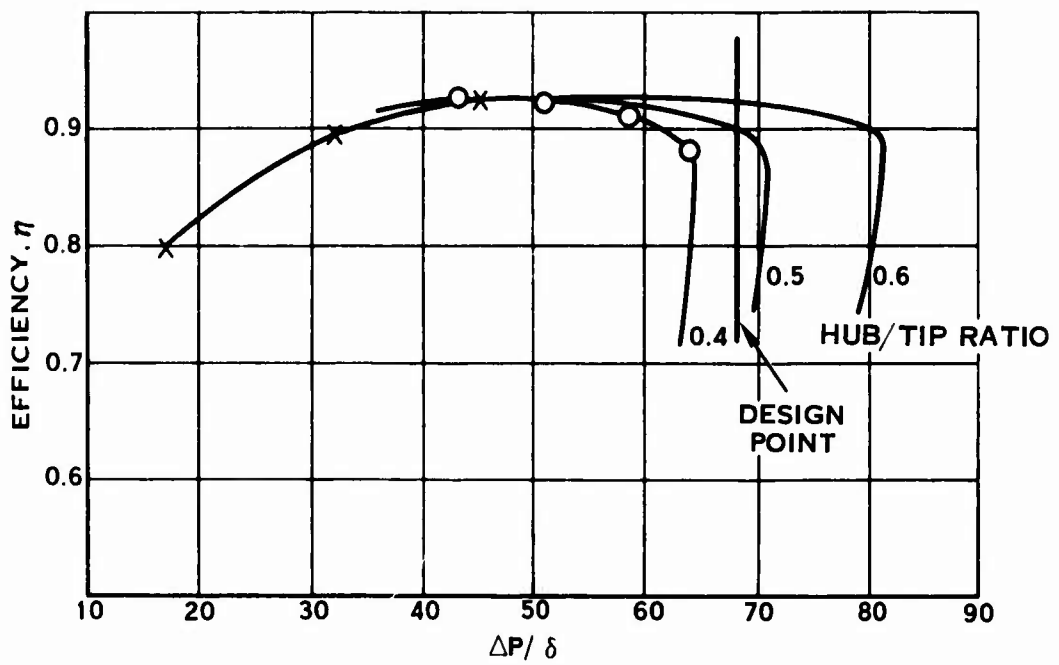

Figure 13. Hub/Tip Ratio Study.

Figure 14, indicate that an increase in solidity to 1050 TAF and tip speed to 592 provides the objective of 10% stall margin, while maintaining a 57% cruise efficiency. Performance at all other aerodynamic design points remained essentially unchanged.

This aerodynamic fan is selected as the basis of the mechanical design concept. A partial efficiency map, covering all design point operating conditions, is shown in Figure 15.

Mechanical

A fan preliminary design concept was developed from the work of the feasibility study and fan-in-fin experience. Major components included in the fan assembly were blades, hub, support bearing and housing, exit guide vanes, pitch change mechanism and center body fairing. The fan assembly is shown in Figure 16.

Fan design characteristics are presented in Table 6.

TABLE 6. FAN DESIGN CHARACTERISTICS

Diameter	4.0 ft
Number of Blades	8
Tip Speed	592 ft/sec
Solidity	1050 TAF
Dilution Ratio	11:1
Pressure Ratio	1.032
Maximum Power	261 hp

A lightweight spar-shell blade concept is selected for use. Materials are selected for their temperature capability and foreign object resistance. The spar-shell blade concept, illustrated in Figure 17, consists of a central structural member; the spar, which incorporates a round retention to facilitate variable pitch; a shell, attached to the spar, which forms the blade airfoil; and a metallic leading-edge sheath to protect against local damage by impact with small objects such as rocks and ice. The spar is solid titanium, which has been employed in a variety of recent applications. The blade shells are constructed of a lightweight, boron-aluminum composite material. This material has been shown to have high strength at design temperatures above 600°F and excellent FOD resistance. Major progress has been made in establishing fabrication processes which have been shown to be competitive with conventional monolithic materials.

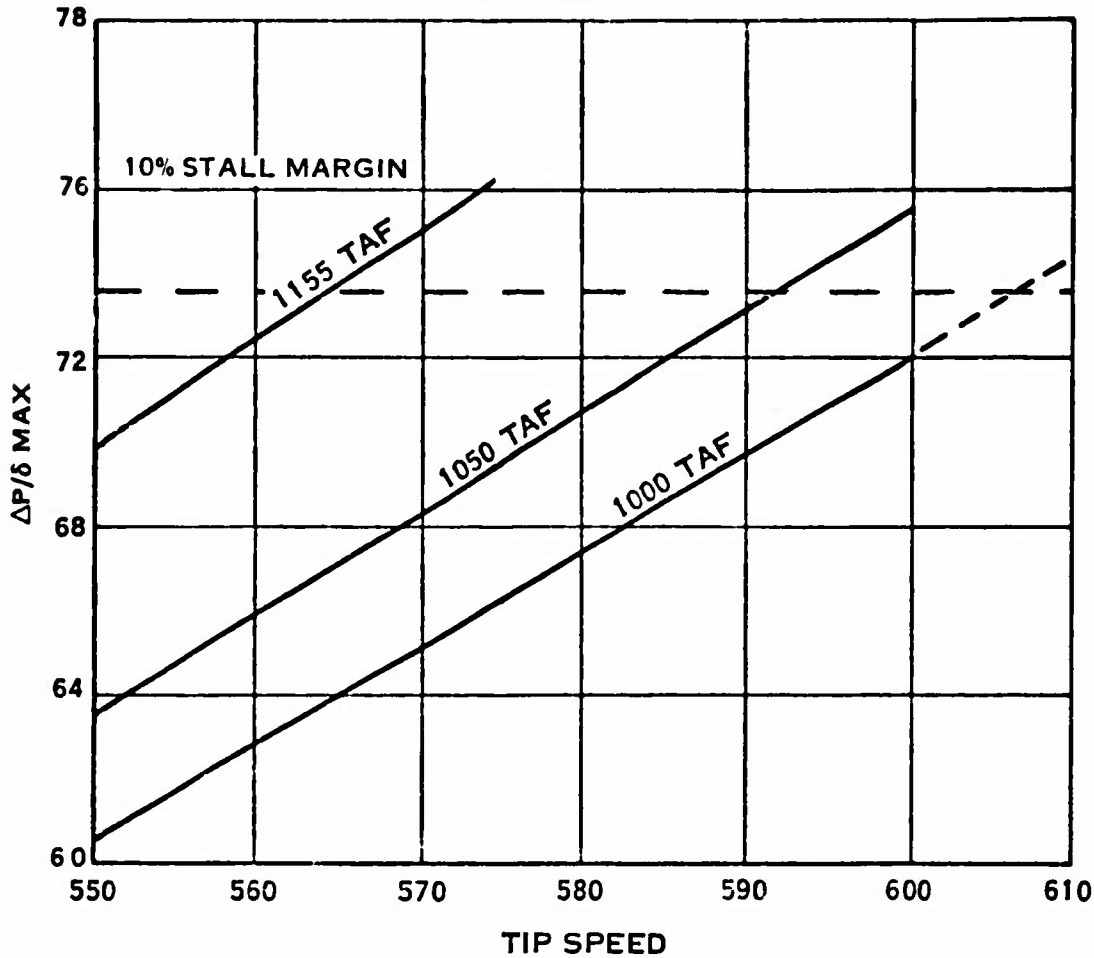

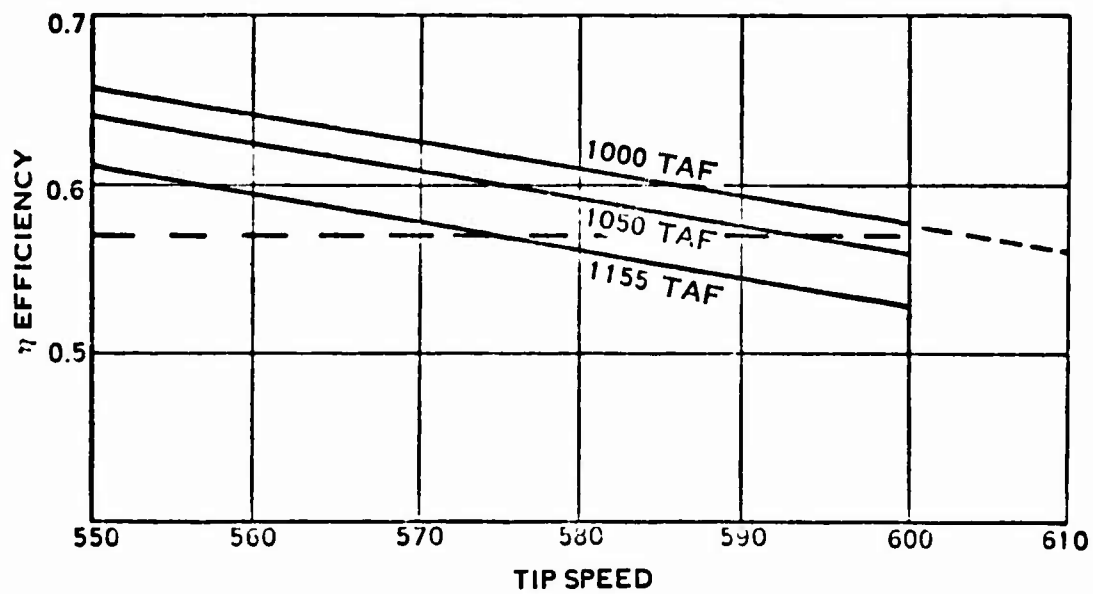

Figure 14. Fan Efficiency and Pressure Rise vs Tip Speed and TAF.

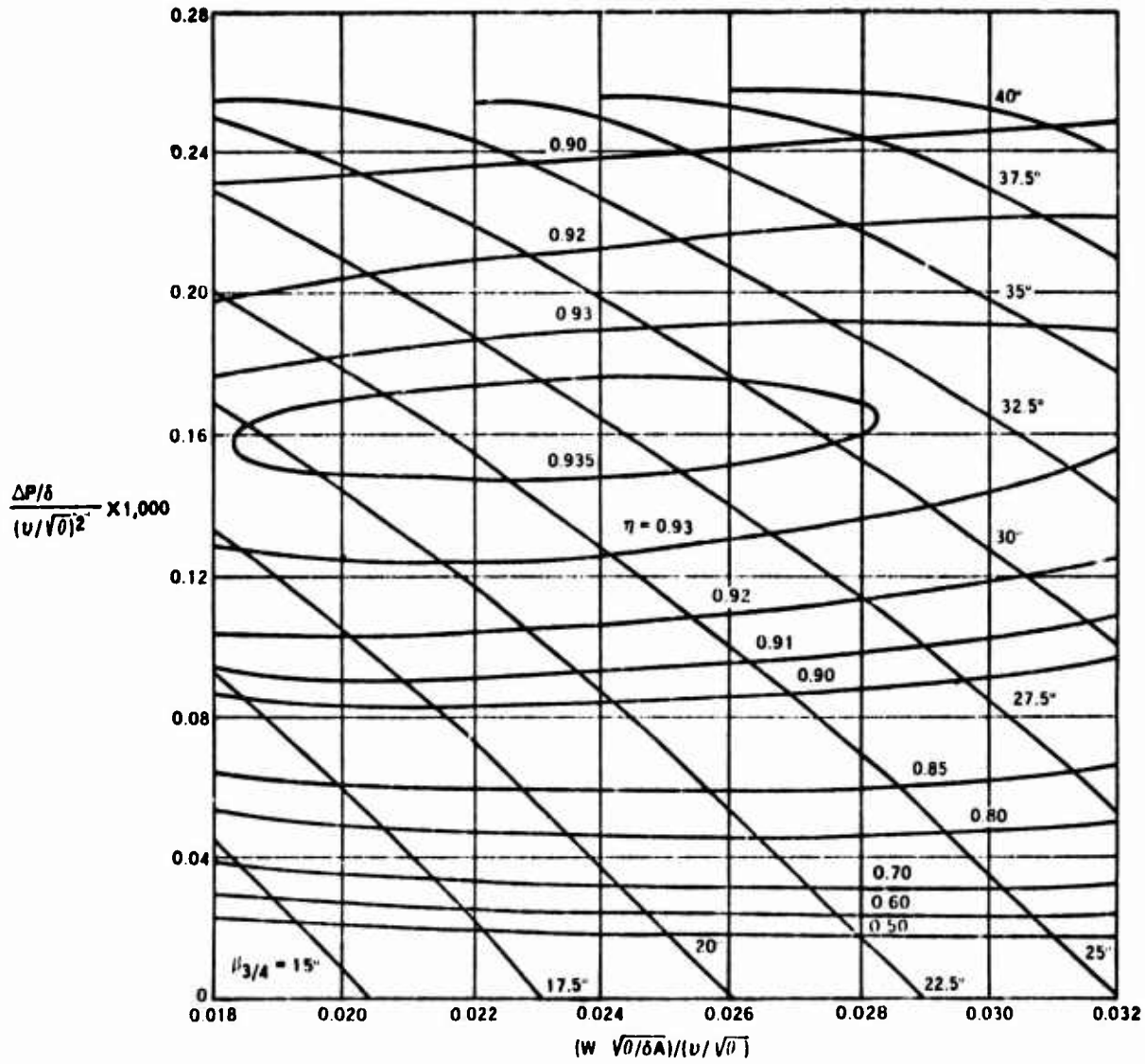

Figure 15. Efficiency Map for Fan Selected for Preliminary Design.

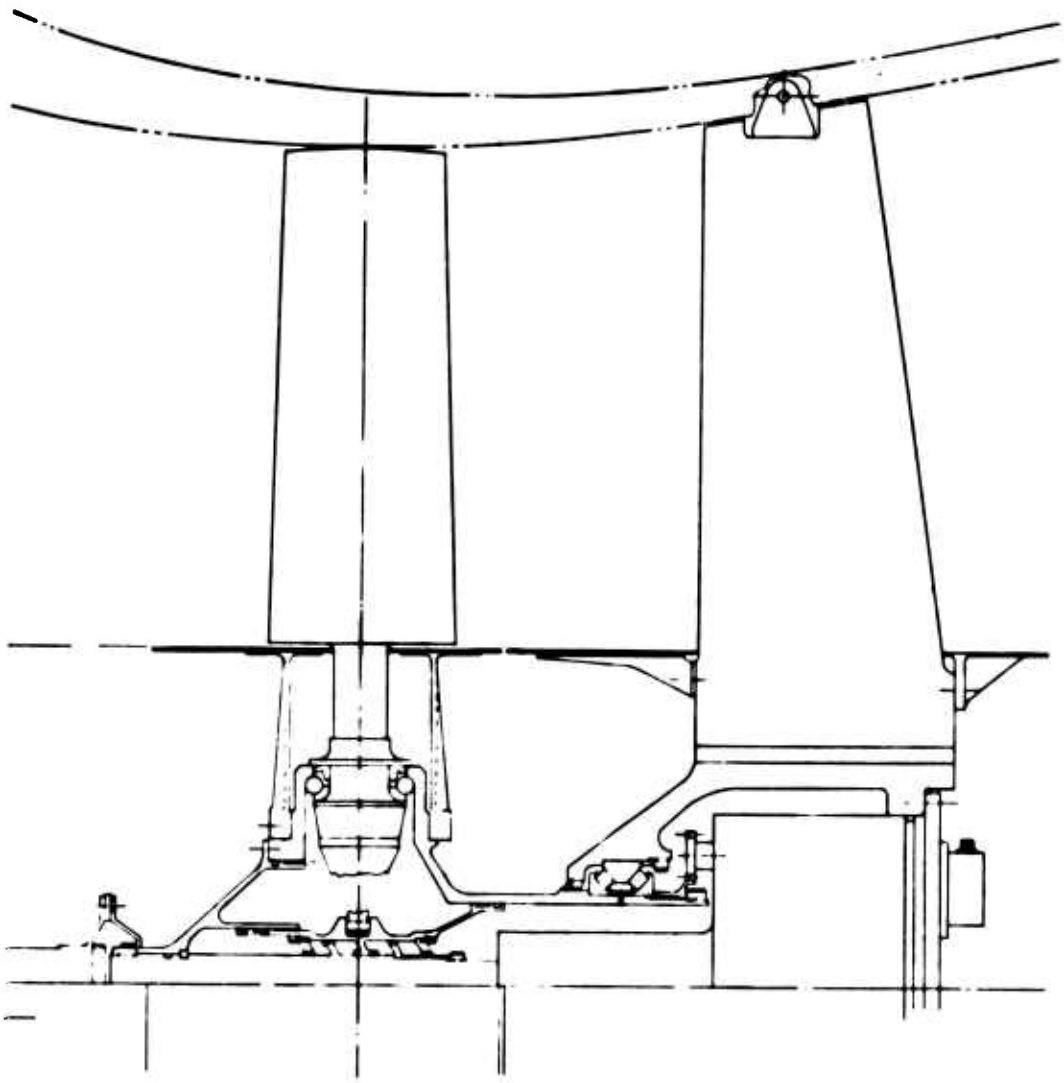

Figure 16. Fan Assembly for Premixing Concept.

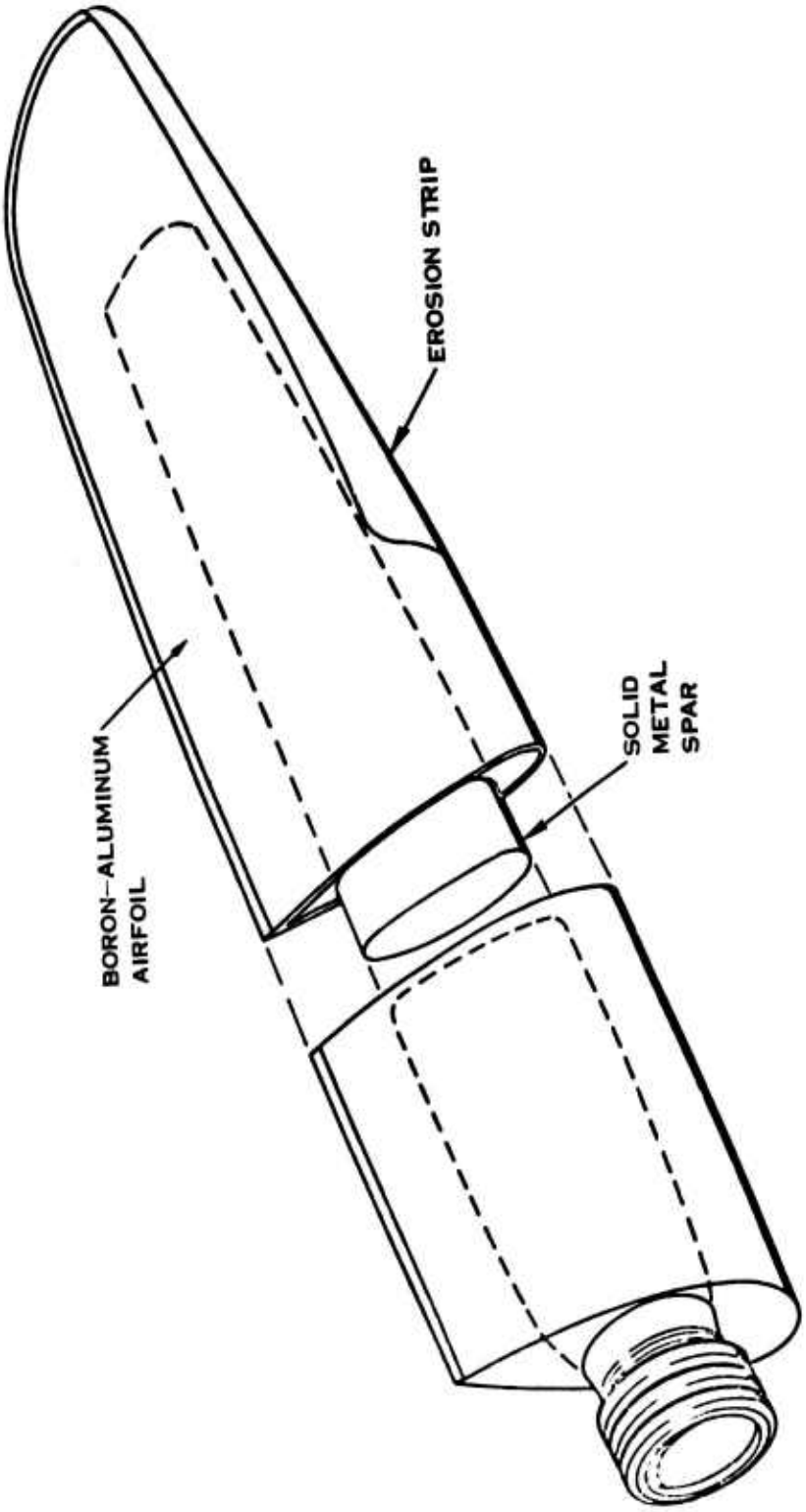

Figure 17. Spar-Shell Fan Blade.

The fan hub is a forged high-strength steel component incorporating integral bearing races. Prior design studies have shown this to provide the lightest weight structure. The blade is supported through a split race ball bearing. The retention bearing is dry film lubricated to obtain a significant improvement in reliability. While this practice is not current state of the art, it is believed to be obtainable through appropriate development effort. A blade seal is provided to prevent dirt from entering the retention area. The seal centrifugal load is supported by a split collar which bolts to the blade shank. This collar also prevents inward radial movement of a static blade.

The fan support is a high-angle duplex taper roller bearing, a lightweight concept developed under Army Contract DAAJ02-72-C-0012. This concept allows use of a short, large-diameter tail shaft, which both lowers the overall weight and provides greater design flexibility by increasing the useable space on the fan centerline.

The three exit guide vanes are designed to provide the high stiffness required to minimize fan vibration. A hollow magnesium structure meets this requirement. The control housing and vane support ring are also magnesium.

A hydraulic actuator provides the pitch change force. The actuator is redundant for improved mission reliability. The actuator cylinders are coupled to the blade with a yoke and trunnion. The lubrication system for the support bearing is integrated with the actuator to minimize the complexity of the required pumps and valving. A redundant fly-by-wire control system is provided.

Weight

A weight was computed for the fan assembly, including the rotor, static structure and control, as described above. The weight correlates favorably with prior estimates for fan-in-fin production weights. The computed weight is 130 lb.

Reliability

A calculation of fan mean time between failures was made. This work was based on the performance of similar hardware in an aircraft environment. Blade foreign object damage has not been included since it could not be identified with any confidence for this unique operating environment. The computed mean time between failures is 12,000 hours.

Effect of Premixing on Blade Temperature and Stress

The premixing approach directs the engine exhaust into the fan duct via a multilobed nozzle upstream of a single variable pitch fan. The fan mixes the hot exhaust gas with dilution air and propels the warm diluted mixture through the tailcone to the control nozzle. This concept eliminates the requirement for separate high-temperature fan blades and complex thermal isolation of fan components, required by the postmixing concept, but raises several questions relative to aerodynamic performance, blade aerodynamic excitations and temperatures, and acoustic signature.

The hot exhaust is directed into the inlet of the fan through eight elliptical lobes 5-in. minor axis by 10-in. major axis between the 45 percent and 87 percent radii of the blade, leaving a cool layer on the duct and hub surfaces. The eight lobes are spaced on a 10-jet configuration (every 36°), but with two lobes 180° apart omitted to provide two exhaust-free locations downstream of the fan. The exit velocity of the exhaust is essentially the same as the inlet velocity of the fan and at a temperature of 1100°F. The effective diameter of the lobes is $5 \times 10 = 7$ in., so that the fan being 4 in. from the exhaust plane is only 0.57 diameter downstream from the lobes.

The flow field at the plane of the fan is a function of the initial configuration and the mixing that can take place in the 4-in. distance between the exhaust plane and fan. The mixing of a jet involves two phenomena: turbulent mixing due to velocity differences between the jet and environment and the temperature (density) diffusion of the jet with the environment. Because the jet velocity is approximately the same as the environment, the only mixing in this case is due to diffusion, which is very slow.

Application of the mixing theory developed from the literature and tests shows that complete mixing for a jet to ambient temperature ratio ($T_e/T_a = 1620/520 \approx 3$) and velocity ratio ($V_e/V_a = 1$) requires at least 20 diameters or 150 in. In 4 inches the spread is only about 1/4 in. and insignificant. Little improvement could be obtained by further separation within the constraints of the aircraft configuration. Thus, for all practical considerations, the configuration and magnitude of the flow density and temperature at the fan plane is the same as at the exhaust plane. As mixing is relatively insensitive to small changes in nozzle geometry and V_e/V_a ratio, no attempt at improvement is made.

The asymmetric flow is found to have only a small impact on performance. A calculation of fan efficiency as a function of pressure rise for a totally mixed flow condition was compared to performance calculated for the asymmetric flow conditions. The difference, less than two percent, is not considered to have a significant effect on the power requirements of the fan considering the benefit provided by this approach.

The fan blades passing through the velocity and density variations produced by the hot exhaust jets will create a high-frequency noise signature unique to this configuration. The noise signature can be improved by acoustic treatment of the inlet and exhaust ducts. It is not within today's state of the art to make an accurate calculation of the noise levels or audio-detectability of this concept. However, the necessary technology can be obtained by proper experimental investigation.

Analysis of the blade temperature for the AH-56 pusher propeller passing through the engine jet exhaust shows that the thermal inertia of the blade is such that the temperature fluctuation with time is only a few degrees from the mean. Therefore, in this cursory analysis only the mean temperature is calculated.

The temperature of a blade passing through a hot jet is affected not only by the mean temperature of the gas, but by the film heat transfer coefficient which affects the heat transfer to the blade and the blade ram temperature rise. The film heat transfer coefficient is given by the equation

$$h = h_a \, (V/V_a)^{.78} \, (T_a/T)^{.68} \tag{33}$$

Based on experimental recovery ratio of 0.75, the ram temperature rise of a blade is given by the equation

$$\Delta T = (V/127)^2 \tag{34}$$

Thus, the total temperature T_a varies with radius and is

$$T_a = 555 + (V_{ax}^2 + \Omega^2 R^2)/16000 \tag{35}$$

For the subject fan with a $V_{ax} = 180$ ft/sec and ΩR tip = 600 ft/sec, T_a is given by the expression

$$T_a = 555 + 25(r/R)^2 + 2.0 \tag{36}$$

Assuming no blade conductive heat loss, the maximum mean temperature of the blade section at 57 percent or 15.8 in. radius, where the jets are 5 in. wide, is given by the expression

$$T_B = [\, T_e(8)(5)h_e/h_a + (2\pi)(15.8-40/2\pi)T_a \,]/$$
$$[\, (8)(5)h_e/h_a + 2\pi\,(15.8-40/2\pi)\,]$$
$$= 807°R \qquad (37)$$

where

$$h_e/h_a = (1/3)^{.68}\,(1)^{.78}$$
$$= .47$$

and

$$T_a = 555+25(15.8/24)^2 + 2.0 = 568°R$$

The actual temperature depends on the conductivity of the specific blade materials and construction. If the blades were made of solid aluminum, then the temperature would be lower, whereas if they were made of solid fiberglass, they would have a hot spot near the maximum mean temperature of 807°R. This analysis assumes no heat is lost by conduction through the hub.

In like manner, the maximum blade temperatures for 6:1 and 15:1 dilution ratio fans were calculated. These values are within the capabilities of existing composite fan blade material, and blade heating was dismissed as a potential impass for the premixing concept.

Because of the density variation created by the eight jets, the blades are subjected to aerodynamic excitations. The blade loading was calculated at 4.5° azimuthal increments and ten radial stations using a multi-azimuth Aerodynamic Strip Analysis Computer Program. The resulting blade shank loadings were then analyzed using a Fourier Analysis Computer Program resulting in the in-plane and out-of-plane blade shank excitations shown in Figure 18. The excitations are a result of two sources of even orders: one of relatively low magnitude at orders of 2iP and one of relatively high magnitude at orders of 10iP, where i is an integer. The former are due to the omission of the two jets, whereas the latter are due to the jets themselves.

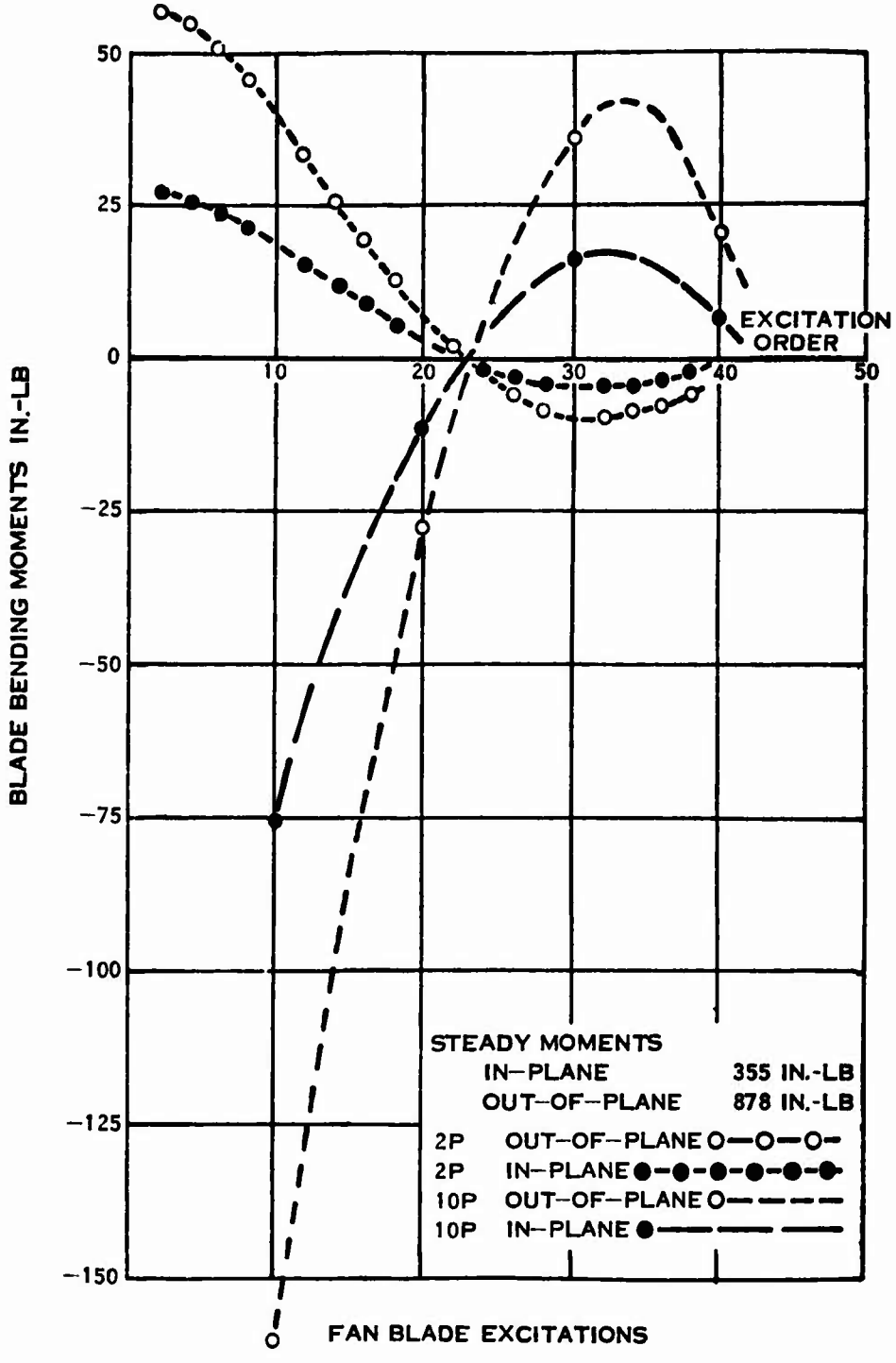

Figure 18. Computed Blade Shank Excitations.

In order to determine the likely structural response and, therefore, significance of the above excitations, it is necessary to estimate the dynamic characteristics of the blades. Because these fan blades are similar to those for the fan-in-fin fan, their critical speeds were scaled from the calculated values of the latter to obtain a critical speed diagram (Figure 19). It is estimated from this diagram and prior experience that this concept might result in a bending critical speed within ten percent of the lower 2P excitation with forcing magnitudes of about 26 in.-lb in-plane and 55 in.-lb out-of-plane, and one within twenty percent of the 10P excitation with forcing magnitudes of 75 in.-lb in-plane and 160 in.-lb out-of-plane. Blade stress for these loadings is estimated as 2200 $\pm$ 2600 psi.

These stress values would be increased by inflow aberrations, which would be primarily 1P and 2P and, based upon earlier work, are estimated to increase the cyclic stressing by approximately 75 percent of the steady stress. These stress levels are well within the capabilities of existing materials operating at the elevated temperatures associated with the premixing fan concept.

Examination of the critical technical issues, i.e., performance, acoustics, blade temperature and stressing, disclosed no situation which might preclude the use of the premixing concept, nor does the development of this approach appear to offer an unreasonable development risk of cost.

ALTERNATE CONFIGURATION

The alternate configuration which consists of a fan-in-fuselage plus a small tail rotor was rejected on the basis of qualitative comparative assessment. The assessment is based on the following design assumptions.

1. IR fan dilution ratio: Same as primary configuration. This results from the fact that a reduction in dilution ratio raises two major problems: (1) keeping the tailcone of essentially ambient temperature and (2) increased steady-state temperature at inner surface of tailcone requires use of polyimide/glass instead of high-temperature epoxy resin/Kevlar tailcone skins.

2. IR fan provides antitorque thrust. Thrust for yaw maneuvers is provided by tail rotor.

Weight Empty

The alternate configuration is anticipated to weigh 235 pounds more than the primary configuration, including 20 inches of cockpit nose extension for balance.

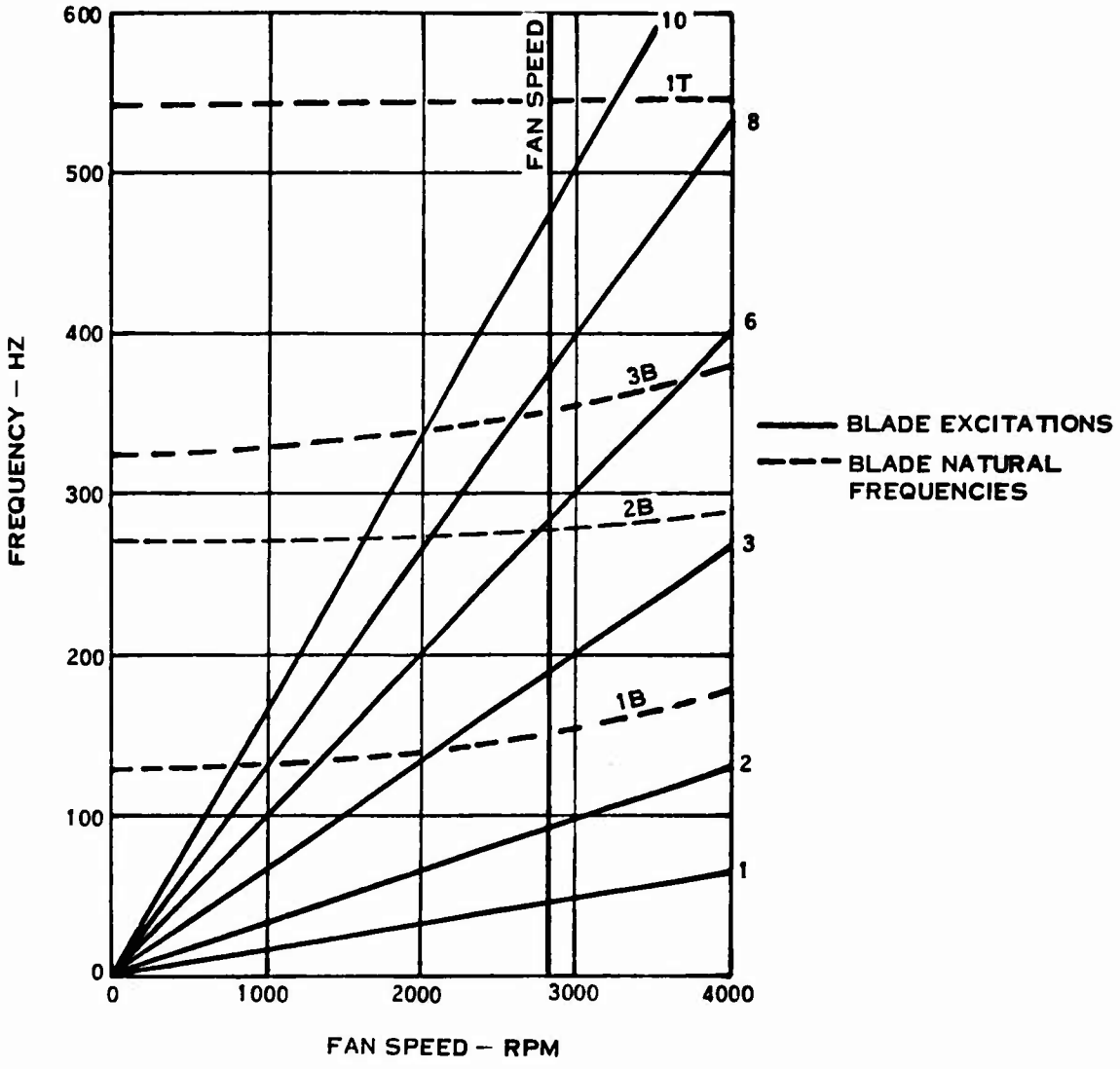

Figure 19. Critical Speed Diagram.

Survivability/Vulnerability

The primary configuration can continue forward flight and perform an autorotation landing following loss of the fan in forward flight, but loss of the fan in hover is considered an attrition. The alternate configuration offers a small survivability advantage provided that the control system is designed so that the tail rotor can maintain hover yaw control after loss of the fan.

Reliability

The alternate configuration offers a small increase in mission reliability.

Maintainability

Alternate configuration requires substantially more maintenance.

Installed Power

Alternate configuration requires 40 SHP additional installed power.

Producibility

Alternate configuration is more expensive due to added tail rotor, tail rotor drive system and control system.

Complexity

The control system of the alternate configuration is more complex, especially since it is desired that the ability to hover with either system be maintained.

AIRFRAME SUBSYSTEMS

DUCTED STRUCTURAL TAILCONE

The tailcone is the duct system for the gas flows pumped by the IR fan. These gases are utilized at the tail for antitorque directional control and forward thrust.

The design parameters are:

- Operation with cooled exhaust plume of 190°F and capability to withstand short periods of time with 400°F exhaust.
- Tailcone fan diameter of 48 inches.
- Tailcone length of 160 inches.
- Minimum diameter of duct 40 inches.

The strength of materials at the temperatures involved rules out the use of aluminum or magnesium alloys for the duct. Materials considered were stainless steel, titanium, S glass with polymide resin, and PRD49 Kevlar with high-temperature resin.

The following methods of construction of the tailcone were considered and are shown in Figure 20. All methods considered are presented here even though IR considerations rule out all metallic skin configurations unless nonstructural insulation is added.

Type a - Sheet metal with closed space forms made as top and bottom halves. This configuration causes an increased duct height at aft end, decreasing blade clearance.

Type b - Similar to 'a' - This is assembled with blind rivets.

Type c - Sheet metal with Z stringers - Outer skin is attached with blind rivets. This configuration may suffer from column instability.

Type d - Similar to 'c' except stringer is formed in the skin panel. Same potential disadvantages as 'c'.

Type e - Sheet metal with top hat stringers. This reduces number of stringers required because double flanges and stringers can be lighter. The stringers are spot bonded to outer skin in the flat.

Type f - Sheet metal with outer stringers, inner frames - This configuration increases diameter of tailcone at the cost of additional weight.

Type g & h - Tubular stringers either round or square - Requires blind riveting.

Type j - Corrugated stiffener between two skins. This is judged to be relatively heavy.

Type k - Kevlar skin and inner duct with Kevlar channel stringers and Nomex honeycomb case. Stringers may be reinforced with graphite flanges to improve compression strength.

Type l - Same as 'k' except structural foam core.

Type m - Similar to 'k' with top hat type stringers.

Type n - Four tubular longerons, may be round or square, with geodetic members between. Very light skins supported with very light structural foam. This system has manufacturing complexity but has excellent tolerance to ballistic damage.

WEIGHT COMPARISONS

Weight breakdowns for four typical systems are presented in Tables 7 through 10.

TABLE 7. WEIGHT BREAKDOWN, SYSTEM e

Item	Weight - lb
Outer skin (.020 aluminum)	48.6
Inner duct (.012 titanium)	43.0
IR Vane (.005 titanium)	32.8
16 stringers (.016 aluminum)	15.0
5 frames (.020 aluminum)	3.9
Fasteners, doublers and bonding	4.0
Latches (8)	3.6
Total	150.9

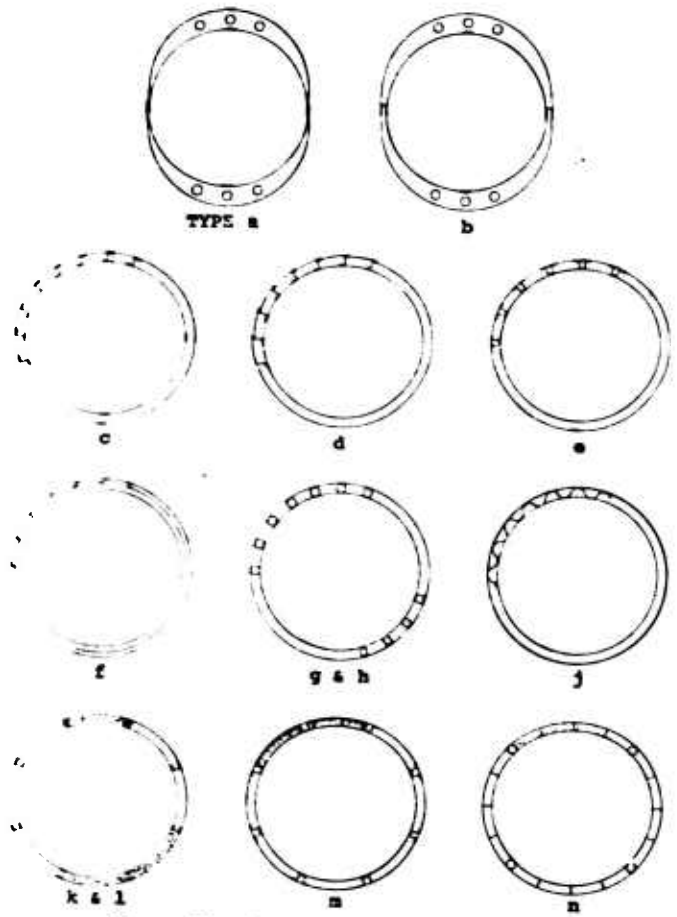

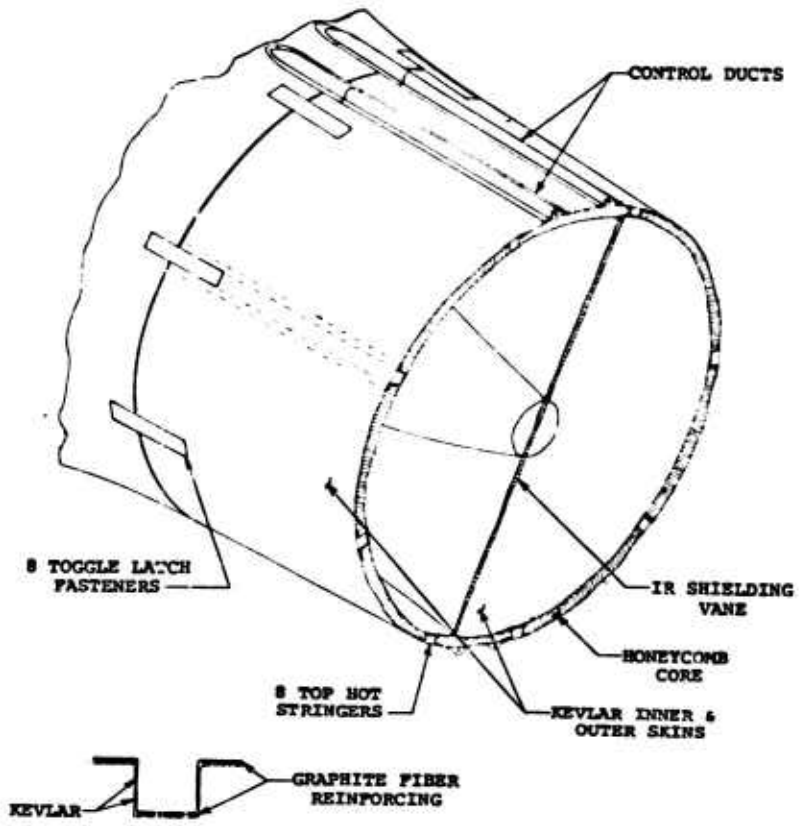

Figure 20. Tailcone Construction Methods.

TABLE 8. WEIGHT BREAKDOWN, SYSTEM k

Item	Weight - lb
Outer skin (.03 Kevlar Prepreg)	34.7
Inner duct (.02 Kevlar Prepreg)	22.1
8 stringers (.03 Kevlar + Graphite)	6.7
IR Vane (.02 Kevlar Nomex)	11.2
Case (1.8 lb/cu ft Nomex)	22.4
End Frames (.03 Kevlar)	1.3
Fasteners, doublers, bonding	3.0
Lightning protection gauge	1.0
Latches (8)	3.6
Total	106.0

Type '1' - Since structural foam is approximately three times the density of Nomex honeycomb for similar compressive shear strength, there would be a weight penalty of approximately 45 lb by comparison to type k. The advantage of structural foam is cost, both of material and of manufacturing.

Structural foam has a greater deterioration of properties at elevated temperatures (250°) than honeycomb.

TABLE 9. WEIGHT BREAKDOWN, SYSTEM m

Item	Weight - lb
Outer skin (.03 Kevlar Prepreg)	34.7
Inner duct (.02 Kevlar Prepreg)	22.1
End frames (.03 Kevlar Prepreg)	1.3
8 Stringers (.02 Kevlar + graphite)	8.6
IR Vane (.02 Kevlar + Nomex)	15.6
Case (1.8 lb/cu ft Nomex)	21.1
Fasteners, doublers, bonding	3.0
Lightning protection gauge	1.0
Latches (8)	3.6
Total	111.0

TABLE 10. WEIGHT BREAKDOWN, SYSTEM n

Item	Weight - lb
Outer skin (.02 Kevlar)	23.1
Inner duct (.02 Kevlar)	22.1
32 geodetics (.03 Kevlar)	27.2
4 Longerons (.05 composite)	6.4
Foam case (2 lb/cu ft)	22.4
Fasteners, doublers, bonding	5.0
Fishplates	2.3
Lightning protection gauge	.3
Latches (8)	3.6
End frames	1.3
IR Vane	11.2
Total	125.1

HIGH-TEMPERATURE SYSTEMS

The use of S glass with polyimide resin and polyimide honeycomb gives a much higher temperature capability than Kevlar skin with Nomex honeycomb. A weight breakdown is given in Table 11.

TABLE 11. WEIGHT BREAKDOWN, POLYIMIDE SYSTEM

Item	Weight - lb
Outer skin (.03 S glass and polyimide)	52.0
Inner duct (.02 S glass and polyimide)	33.2
IR vane (.01 and .3 polyimide honeycomb)	30.2
8 stringers (.020 S glass)	8.6
Case (4 lb/cu ft polyimide)	46.9
End frames (.03 S glass)	2.0
Case adhesive (.1 lb/sq ft/surface)	31.4
Fasteners, doublers, bonding	4.0
Latches	3.6
Total	211.9

This shows that there is considerable weight penalty in obtaining the higher temperature capability of S glass with polyimides, especially since IR considerations prohibit high duct temperatures.

In addition, lay-up labor is many times as much with polyimide resin due to poor tack strength and poor draping qualities of this material.

Consideration was given to using stainless steel or titanium honeycomb for its superior performance under elevated temperatures.

Stresskin SS honeycomb may have a slight temperature advantage over titanium honeycomb. It is usable up to 1000°F, against a maximum range of 800° - 1000°F for titanium.

However, weight consideration (approximately 315 lb) rules out stainless steel. Material cost of stainless steel honeycomb is an order of magnitude greater than PRD 49.

Titanium honeycomb is much lighter, but is expensive and is estimated to make the cost of material alone for the tailcone over $30,000.

Fabrication costs for both of these metallic honeycomb designs are also expected to be significantly greater than for PRD 49.

Cost rules out both stainless steel and titanium honeycomb for use in the tailcone.

LIGHTNING STRIKE HAZARD

Composite construction with graphite fiber stringers and Kevlar or glass cloth skins is vulnerable to disruption of laminates when struck by lightning. One method of reducing this hazard is by covering the stringers with a strip of aluminum gauze on the outside of the tailcone. This gauze is laid up and bonded to the external surface.

The weight penalty would be .7 - 1.7 lb depending on whether additional adhesive is required, and assuming a 4-inch strip covering each stringer.

ATTACHMENTS

Attachment to the tail assembly, which would probably also be of sandwich construction, may be performed by circumferential bolts or screws. As the circumference at this point is approximately 120 inches, 40 fasteners result in a pitch of 3 inches.

Forward attachment to the aft fuselage is by similar means; or as an alternative, 8 'King' type toggle fasteners could be used. This would make the whole tailcone readily removable for maintenance, transportation, concealment or storage. Control cables would be routed in external conduits, where they too would have quick-release couplings. Toggle fasteners could have safety screws to prevent inadvertent release of the toggle.

MODULAR CONSTRUCTION

The helicopter is divided into four major modules:

I Cockpit and cabin
II Propulsion module
III Tailcone
IV Tail duct and stabilizers

Item II, the propulsion module, may be subdivided into four further modules:

a Fuselage section
b Tail fan assembly
c Transmission and engines
d Rotor head

The transmission and engines complete with engine accessories and fireproof bulkheads are mounted as a unit on the fuselage section. This unit is utilized as a load bearing structure to stiffen the top of the fuselage.

Although the transmission/engine module is preassembled, it is possible to replace engines without removal of the complete module.

The transmission and engine fairings are divided into sections which permit easy removal and access to components.

The propulsion module is an independent unit, except for controls, and lends itself to easy maintenance because of its compactness. It is readily transportable to major overhaul facilities.

MODULE ATTACHMENTS

For a module to be readily assembled or dismantled, the following requirements must be met:

a. Minimum number of attachments
b. Easy accessibility to attachments
c. Self lineup (i.e., conical interface)
d. Quick disconnect for controls, hydraulics, electronics
e. Minimum services between modules

The first requirement necessitates concentration of structural load paths to a few major members. This is contrary to vulnerability practices which favor multiple minor structural members.

The easiest accessibility is provided by radial type attachments with the fasteners being in shear. This method, however, has poor lineup characteristics. Tension type fasteners used longitudinally with cone interface to facilitate lineup and to take the shear loads are more practical, but ready access must be maintained. Figure 21 shows typical attachments of this type.

Ancillary services are designed to have the minimum connections across the module interface. Connections that must be made have quick disconnects and are readily accessible. Control rods or cables are preset so that rigging or adjustment is not affected by disconnect.

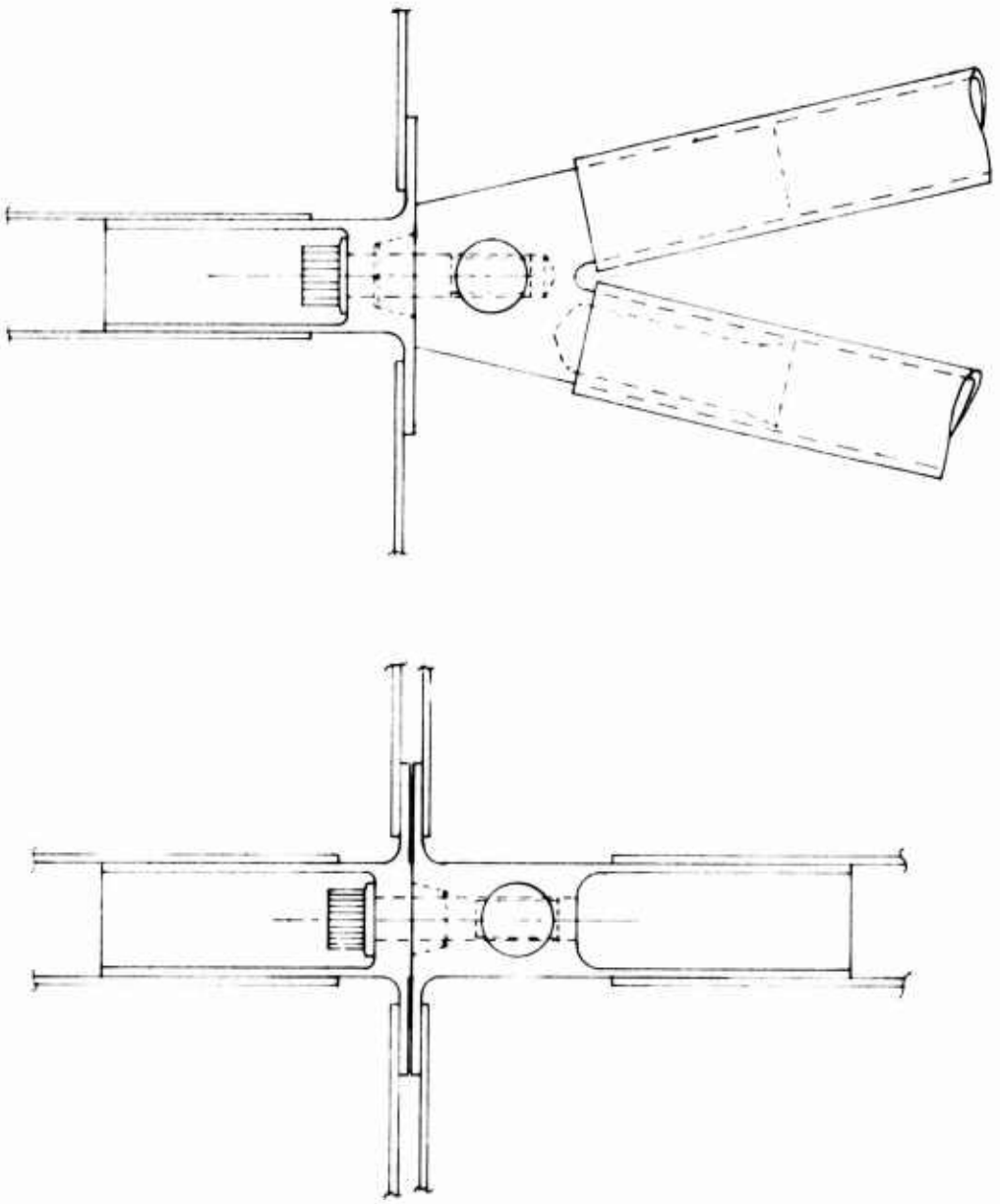

Figure 21. Longitudinal Module Fasteners.

MECHANICAL SUBSYSTEMS

INTRODUCTION

To arrive at a transmission concept for the engine/transmission/airframe advanced integration techniques study, a number of transmission attributes were investigated as outlined in Figure 22. Moving across the chart from left to right, a determination was first made of engine location, with an aft-mounted horizontal engine being deemed most desirable. From an assessment of future engine technology, and based on contractual requirements, engines with an input speed range of 30,000 rpm are included.

An assessment of engine gearbox mounting was made, with the result that a close-coupled engine transmission scheme offers the lightest solution and permits operation with the highest system critical speed. Other engine gearbox mounting arrangements that were considered include a conventionally coupled engine and a remote coupled engine.

High-speed transmission inputs were investigated since they present the largest problem in developing a successful transmission design. As part of high-speed inputs, high-speed bevel and spur gears were investigated as well as various bearing arrangements for supporting the bevel gears. A high-speed spur gear arrangement was concluded to be a simpler, lighter input arrangement than the bevel set. To shift the bearing design problem to a slower speed shaft, a split power transmission scheme was investigated in which a counterrotating planetary on the input functions as a torque splitter. This planetary has a high-speed input or sun gear which is supported by three planetary pinions. The bearings that now present a design problem are the planetary pinions which are subjected to one-third the load and two-thirds the speed of the input shaft.

The transmission for the advanced integration techniques program that was selected consists of a high-speed aft-mounted, close-coupled engine driving a high-ratio split power transmission. The rear engine exhaust is ducted to a daisy mixer. The mounting of the engine transmission package consists of four attachments between the gearbox and airframe, and a fifth attachment between the rear engine mount and airframe.

Other items that were considered in arriving at an advanced transmission concept were an evaluation of various types of drives with vertical engines, fan drives, transmission cooling, and accessories, and integration of the transmission with the hydraulic power system.

The types of drives that were investigated include conventional planetary, Maroth nutating, free planet and split power drives. For transmission cooling, a conventional oil cooler, use of fins on the housing with no oil cooler, electrostatic cooling, and integrated engine and transmission cooling were investigated. Also considered in the design of our advanced transmission concept was integration of the hydraulic power system with transmission system. For the hydraulic power system, servo and hydraulic lines integrated with the transmission housing were investigated.

GEARBOX DESIGN

Conventional Planetary Drive

The conventional planetary drive transmission utilizes a spur gear mesh to three simple planetary units to drive the main rotor. Figure 23 shows the planetary drive for a vertical engine configuration. The conventional planetary is not selected for the final drive configuration due to the high weight, as well as a large number of bearings.

This conventional planetary drive does offer certain advantages including simplicity of manufacture with no parts larger than parts currently in manufacture.

The actual arrangement of the components is shown in Figure 24. The vertically mounted engine output shaft turns at 30,000 rpm and drives through an overrunning cam roller type freewheel unit to a spur mesh. The output gear of this combining spur mesh drives the input sun gear of the first stage planetary. Power is transmitted through two other planetary stages to the main rotor.

High-Ratio Spur Gear Drive

A high-ratio spur gear drive concept is a drive which transmits power to the main rotor through a star epicyclic drive to two spur gear meshes. Figure 25 shows the high-speed spur drive for a vertical engine configuration. The high-ratio spur drive is not selected as the final drive configuration due to high star epicyclic pinion speed and large 28-inch-diameter bull gear size.

The high-ratio spur gear set does, however, offer certain advantages, including:

(1) Simplicity of manufacture with seven spur gears and one simple three-pinion epicyclic drive unit.

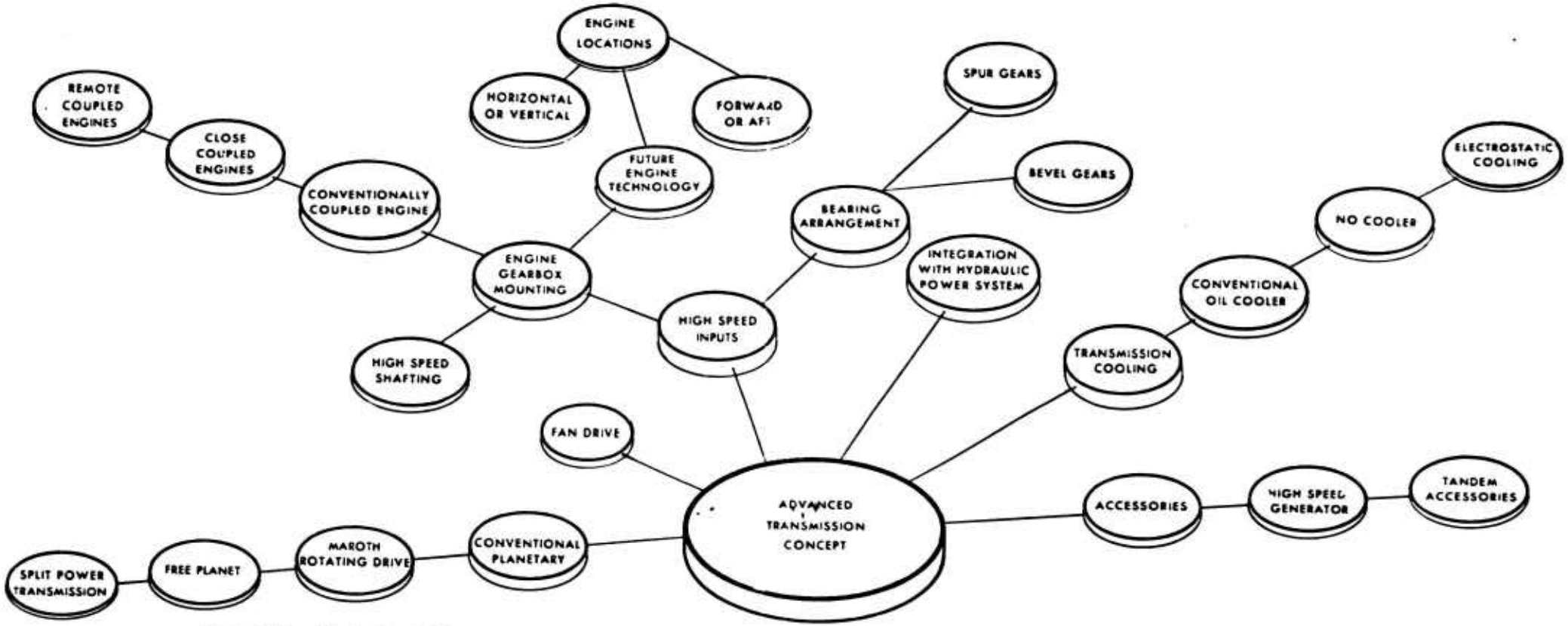

Figure 22. Mechanical Subsystem Study.

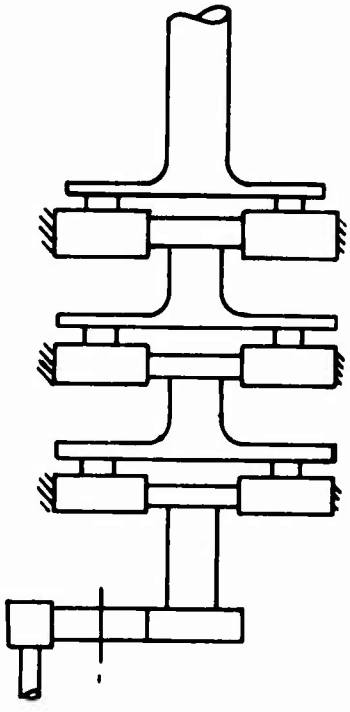

THREE-STAGE PLANETARY

Figure 23. Planetary Drive Schematic.

(2) A reduction in weight over a conventional three planetary drive unit.

(3) A flat, relatively low height transmission.

The actual arrangement of the components is shown in Figure 26. The vertically mounted engine output shaft turning at 30,000 rpm drives the sun gear of a star epicyclic unit. The output ring gear, which is turning 8,000 rpm, drives through an overrunning cam roller type freewheel unit to a spur pinion. This spur pinion drives the main rotor shaft through a jack shaft arrangement.

Split Power Transmission

A comparative review of all the advanced transmission systems indicates that a split power transmission, with the rotor driven by a single combining gear instead of the usual planetary unit, has the greatest overall advantage.

The main features of this transmission system are summarized as follows:

(1) The transmission system which is close-coupled to the aft-mounted front drive engine has the lightest weight of all drives considered. This transmission can be fabricated to a weight of .55 pound per horsepower using stress levels not greater than those achieved in current production helicopters. This weight-to-power ratio is approximately 25 percent smaller than that achieved in current transmission systems.

(2) The use of the close-coupled engine design results in an input shaft design which has the highest shaft natural frequency of any considered.

(3) The transmission utilizes a fabricated housing which is 15 percent lighter in weight than a cast housing and is 10 percent less costly.

(4) High efficiency is obtained (97.4 percent) since the loss sources are equivalent to 1 counterrotating epicyclic unit, 1 spiral bevel mesh, and 1 spur mesh, each carrying installed engine power. The reduction ratio obtained in the counterrotating epicyclic unit has eliminated one mesh when compared with conventional gearing.

(5) The overrunning clutch for each engine can be sized for half power as a result of splitting power from each engine into two paths.

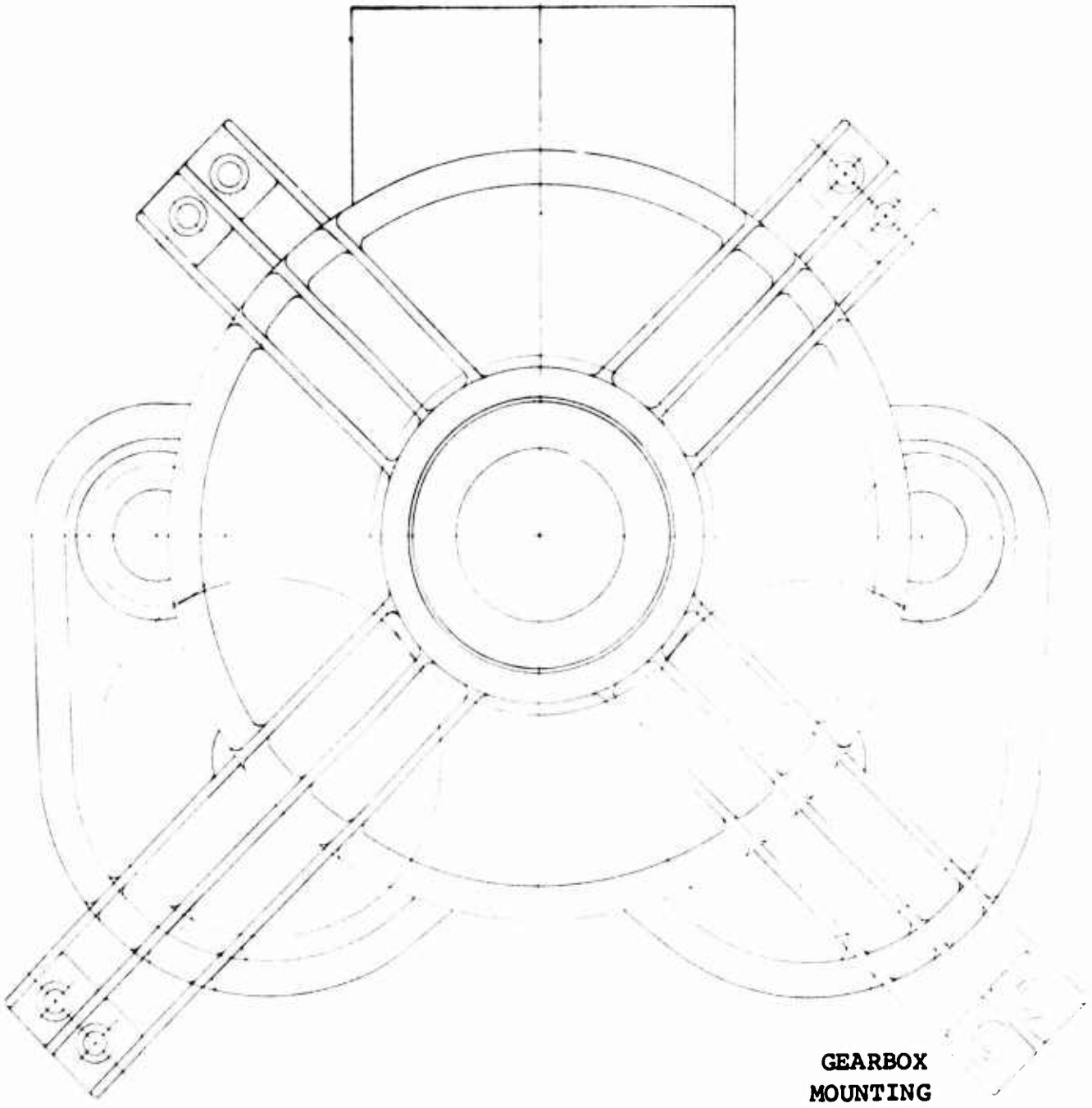

PLAN VIEW

Figure 24. Planetary Drive Layout.

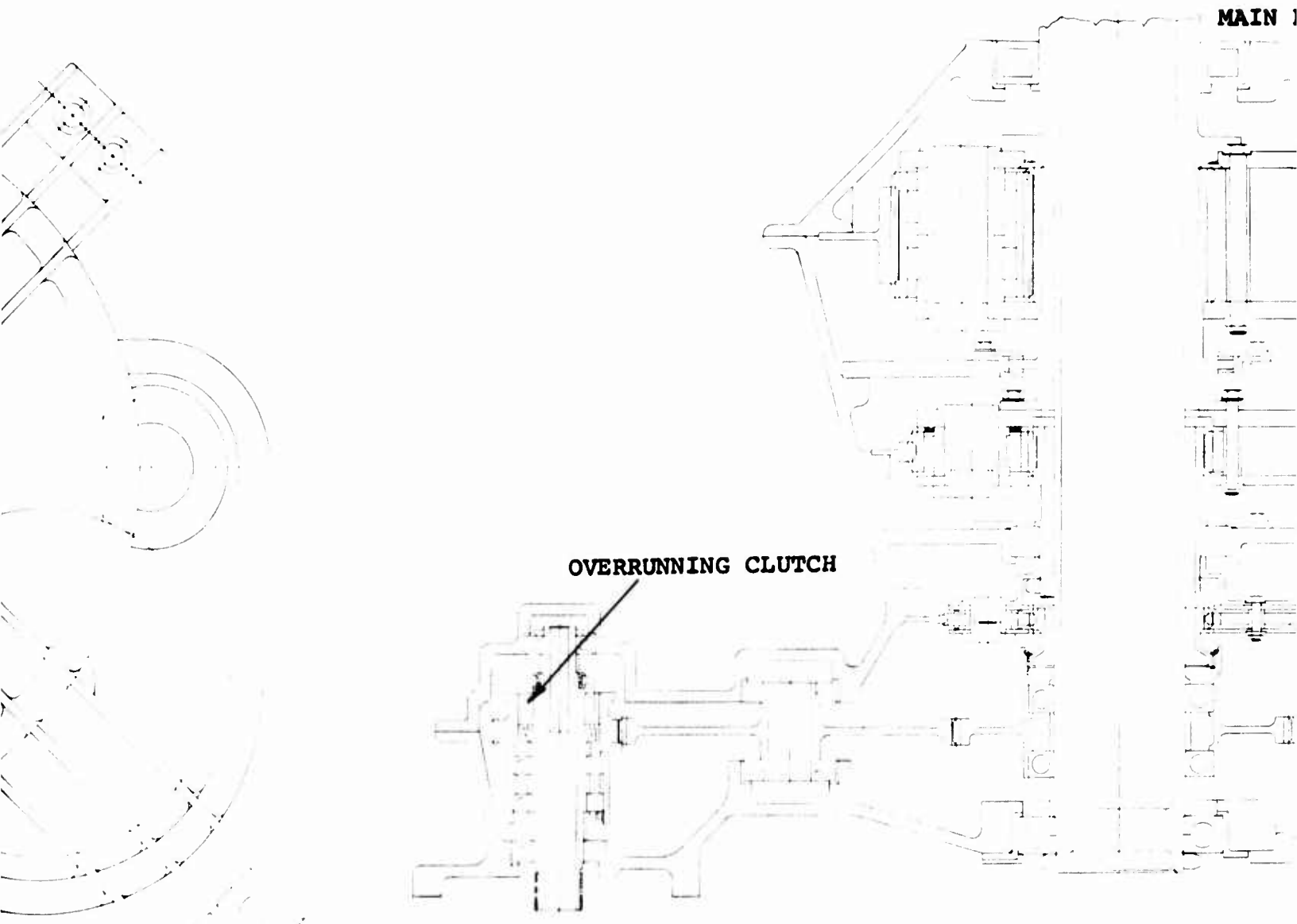
MAIN
OVERRUNNING CLUTCH
GEARBOX
MOUNTING
ENGINE INPUT
30,000 RPM

ve Layout.

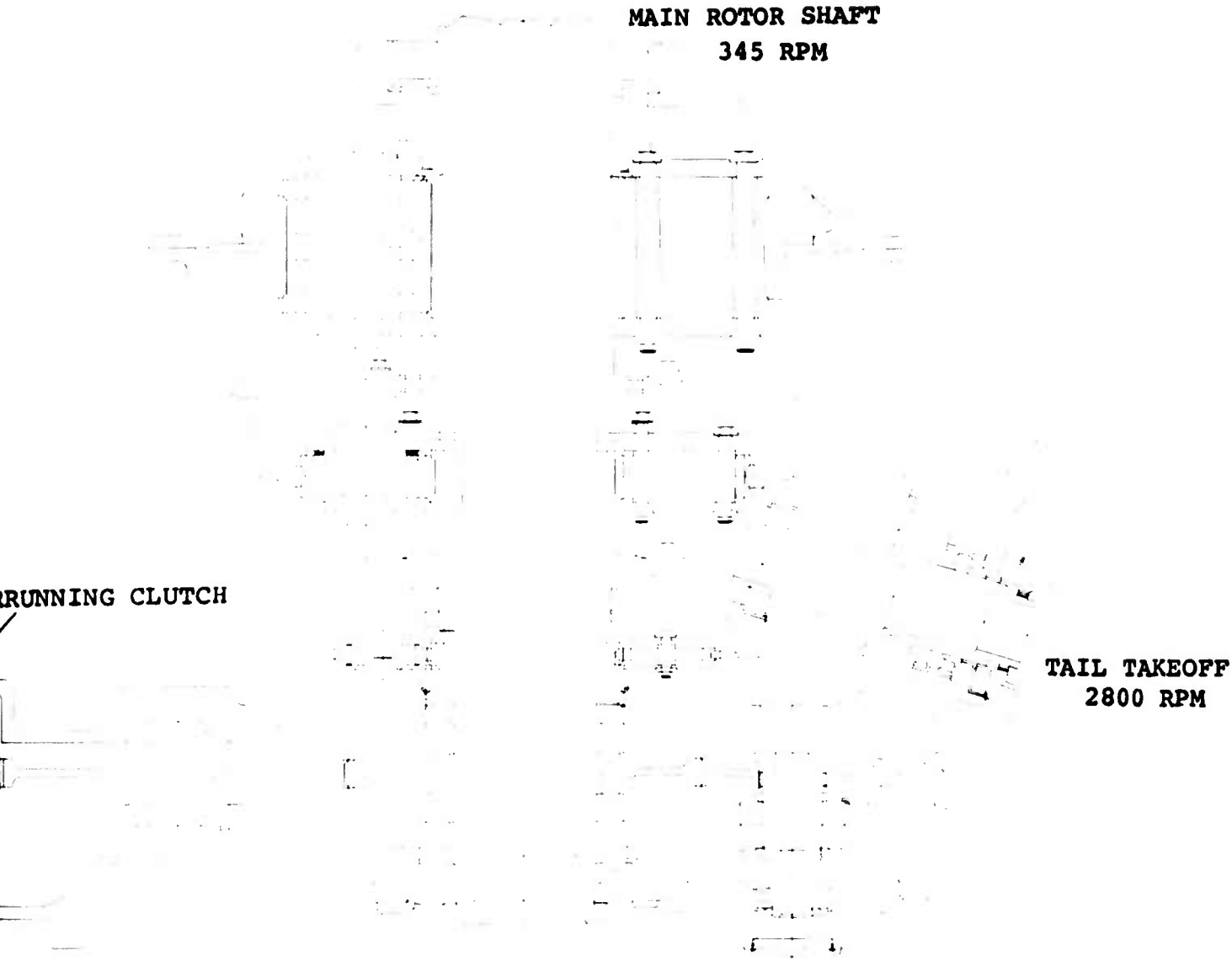
MAIN ROTOR SHAFT
345 RPM
RRUNNING CLUTCH
TAIL TAKEOFF
2800 RPM
ENGINE INPUT
30,000 RPM
SCALE INCHES

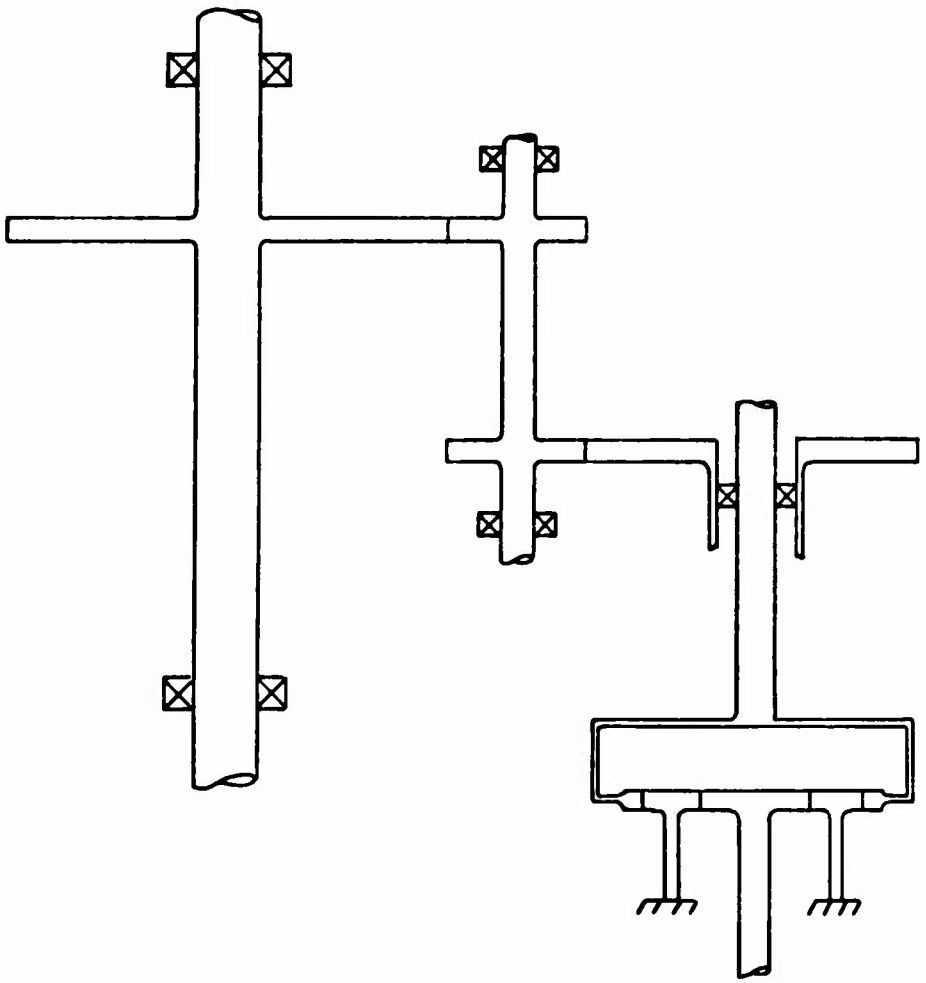

Figure 25. Spur Drive Schematic.

(6) Each engine drive train is independent of the other, or is redundant, as far as the spur mesh where the power is combined to drive the main rotor.

(7) The drive paths from each engine are inherently load balancing so that problems of tooth loading arising from uneven loading are avoided.

(8) A counterrotating epicyclic unit accepts high engine speeds, 30,000 rpm, while keeping gear pitch-line velocities down to less than 15,000 fpm. This eliminates bearing problems associated with high-speed bevel input gears.

(9) Due to counterrotation, the input epicyclic unit splits the engine power into two paths, at the same time achieving reduction ratios of 11.02 and 12.85 to the ring gear and planet carrier, respectively. These speed reductions ensure that the planet pinion bearings are not unduly affected by centrifugal loads.

(10) The input epicyclic units, which are field replaceable, are designed with floating sun gears and only three planet pinions in order to achieve equalization of gear tooth loads.

The final arrangement of this transmission consists of close-coupled aft-mounted engines, cantilevered from the fabricated housing of a split power transmission. Each engine drives the sun gear of a counterrotating epicyclic unit, as shown in Figures 27 and 28. The counterrotating epicyclic unit has two output shafts, one from the planet carrier and one from the rotating ring gear; each carries one-half the engine power and drives the spiral bevel gear mesh. This bevel mesh, which makes the angle change necessitated by a horizontal engine installation and vertical rotor shaft, drives a high-ratio spur gear set, whose bull gear is connected to and supported by the main rotor shaft.

The overrunning clutch is located on one path of each engine split power drive (sized for 1/2 power) between the output spur gear pinion and the bevel gear mesh.

Power to the IR suppression fan is provided by a bull gear driven spur gear through a bevel set to the shaft-connected fan. The drive shaft connecting the IR suppression fan to the transmission is of a single-shaft segment with flexible multiple disc couplings at either end.

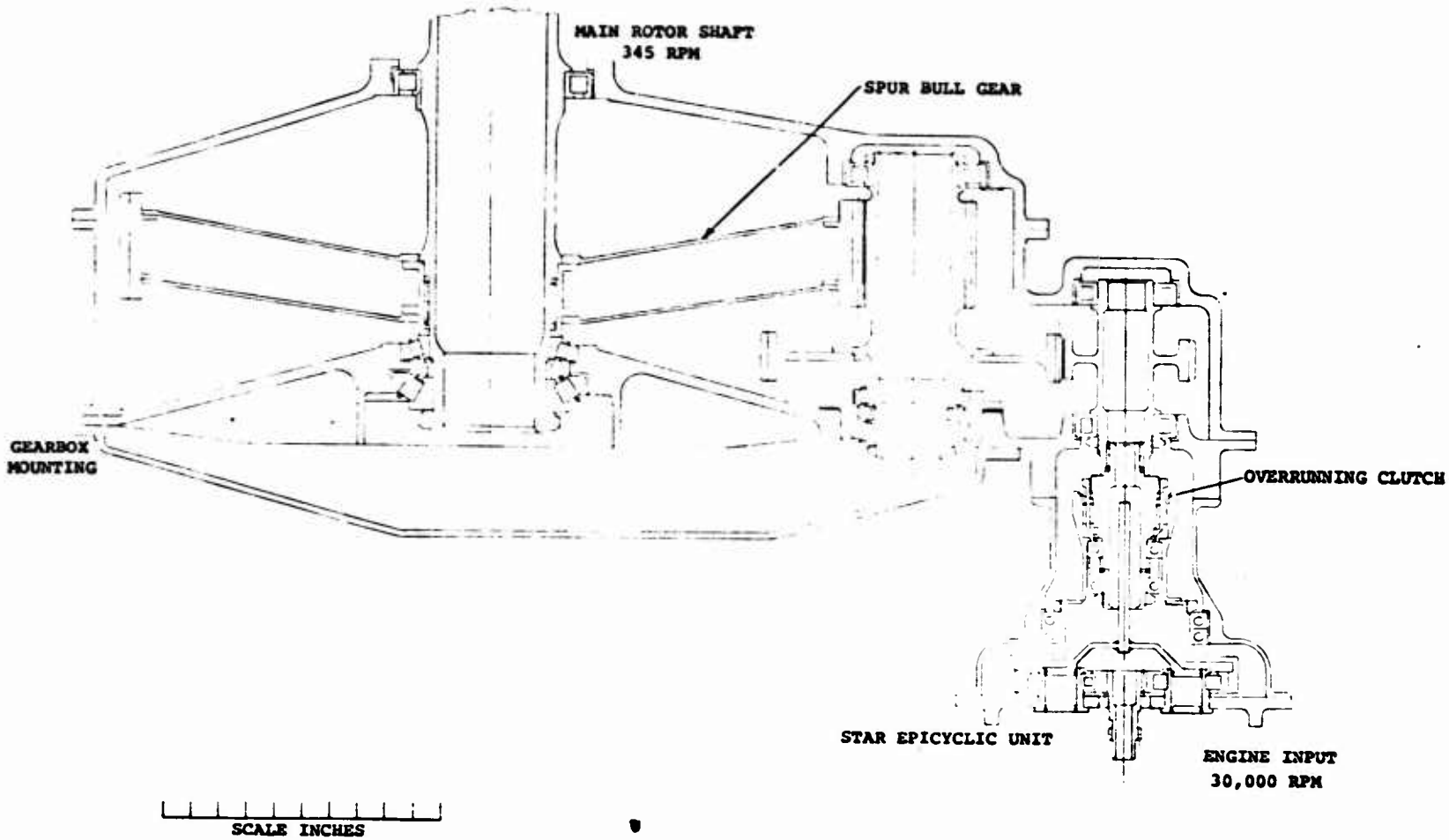

Figure 26. Spur Drive Layout.

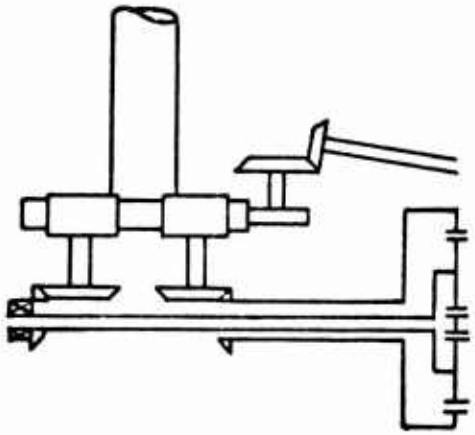

Figure 27. Split Power Transmission Schematic.

Accessory drives are provided for two hydraulic pumps (servo and utility system), two generators, and main rotor tachometer by spur pinions vertically mounted, which mate with the main rotor bull gear. This enables redundant accessory drives with the fewest gears possible and is more reliable due to its proximity to the main rotor drive.

The transmission housing for the primary drive train is located and supported in a welded 2024 aluminum plate housing, input sections are supported in 201.0-T7 aluminum casting, while the main rotor shaft upper roller bearing is supported in a welded truss housing of Custom 455.

Free Planet Transmission

A free planet transmission concept covers broadly those planetary arrangements wherein the planets are not constrained by being mounted on a carrier or spider. The free planet design shown schematically in Figure 29 has not been considered for the selected concept due to the large overall package and difficulty for the design investigated in achieving a reduction ratio greater than 30 to 1.

The free planet design, however, does offer some potential advantages listed below:

(1) Eliminates planet bearing power losses and failures.

(2) Has low planetary weight.

(3) Permits reduction in a single compound stage at high efficiency.

(4) Provides sufficient flexibility and self-centering to give good load distribution between planet pinions.

(5) Construction effectively isolates planetary elements from reflections of housings.

(6) Tends to cause uniform facewise loading of the gear teeth.

(7) Greater operating time after loss of lubricant since planet pinion bearings are eliminated.

The free planet arrangement, shown in Figure 30, is designed such that

- the application defines the forces and the associated geometry in the transverse plane

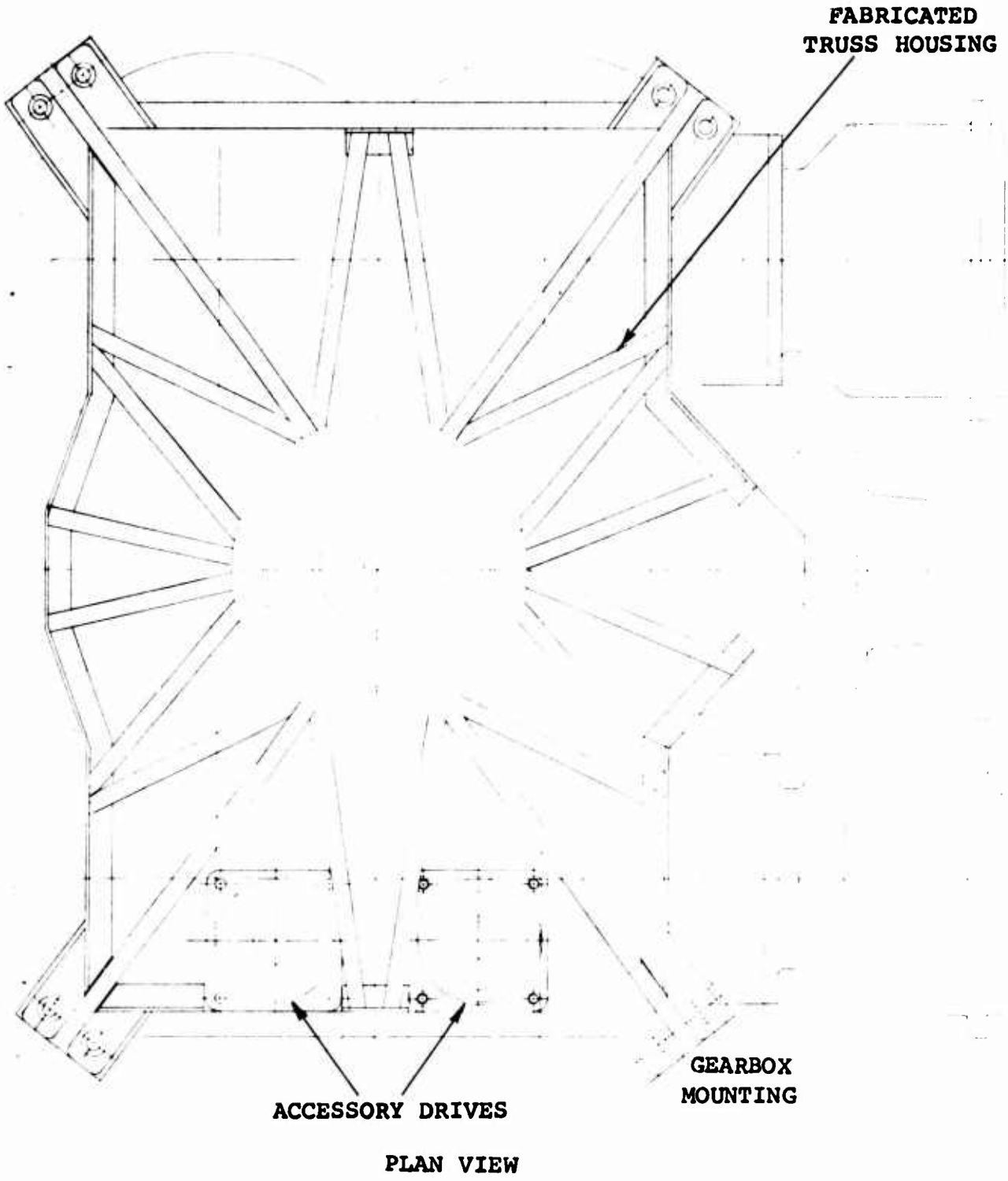

Figure 28. Split Power Transmission Layout.

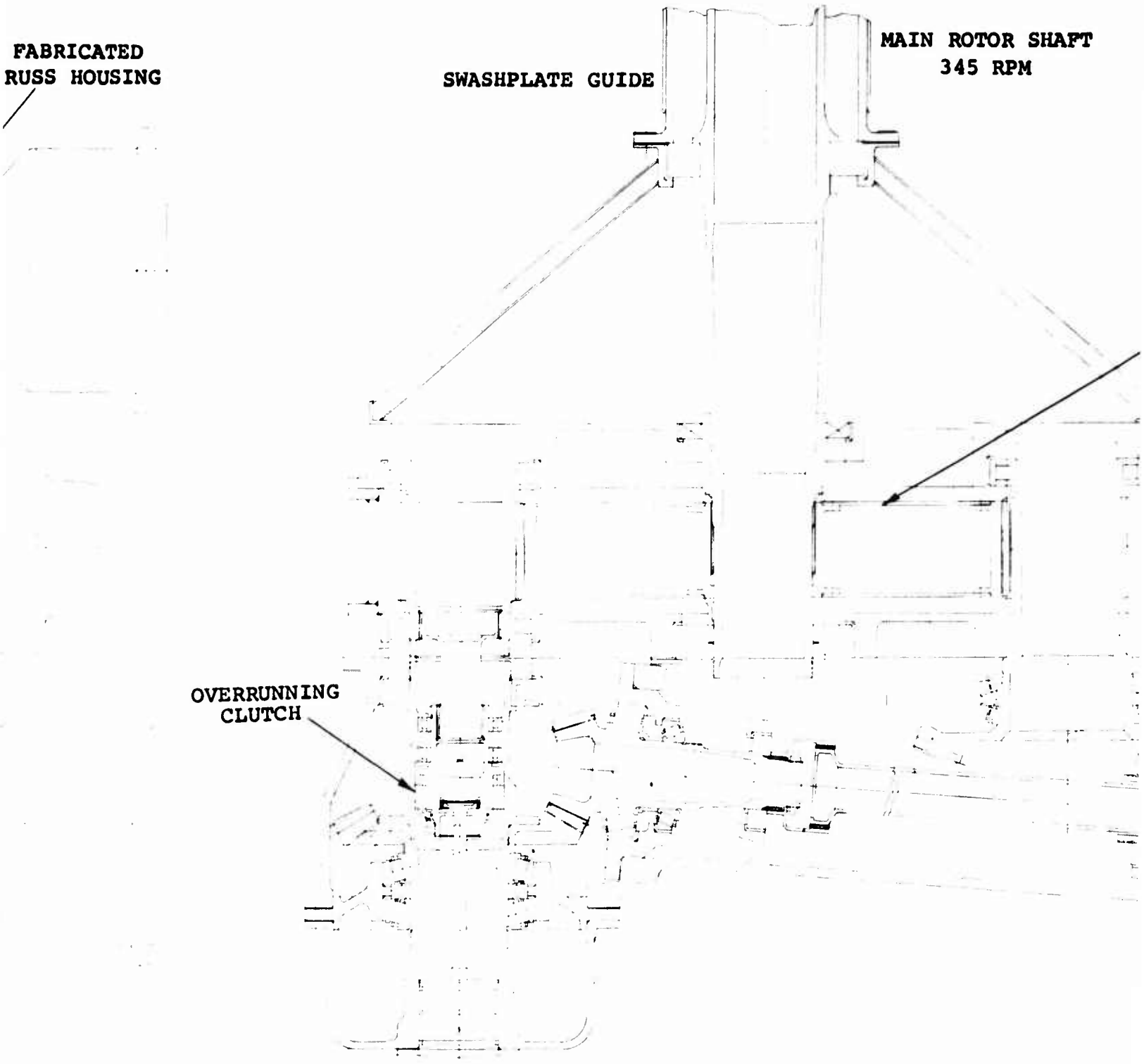
FABRICATED
RUSS HOUSING
SWASHPLATE GUIDE
MAIN ROTOR SHAFT
345 RPM
OVERRUNNING
CLUTCH

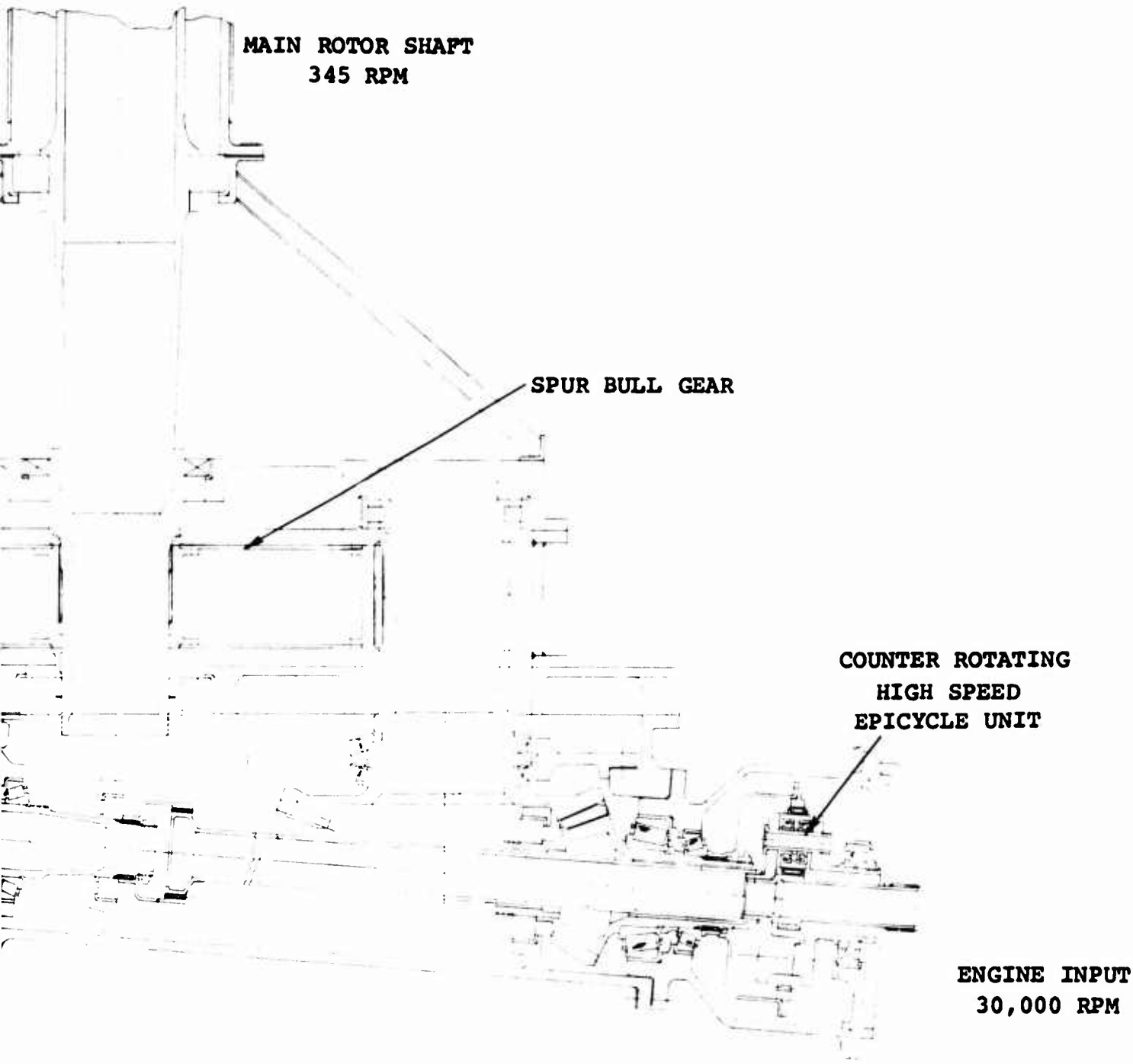
MAIN ROTOR SHAFT
345 RPM
SPUR BULL GEAR
COUNTER ROTATING
HIGH SPEED
EPICYCLE UNIT
ENGINE INPUT
30,000 RPM

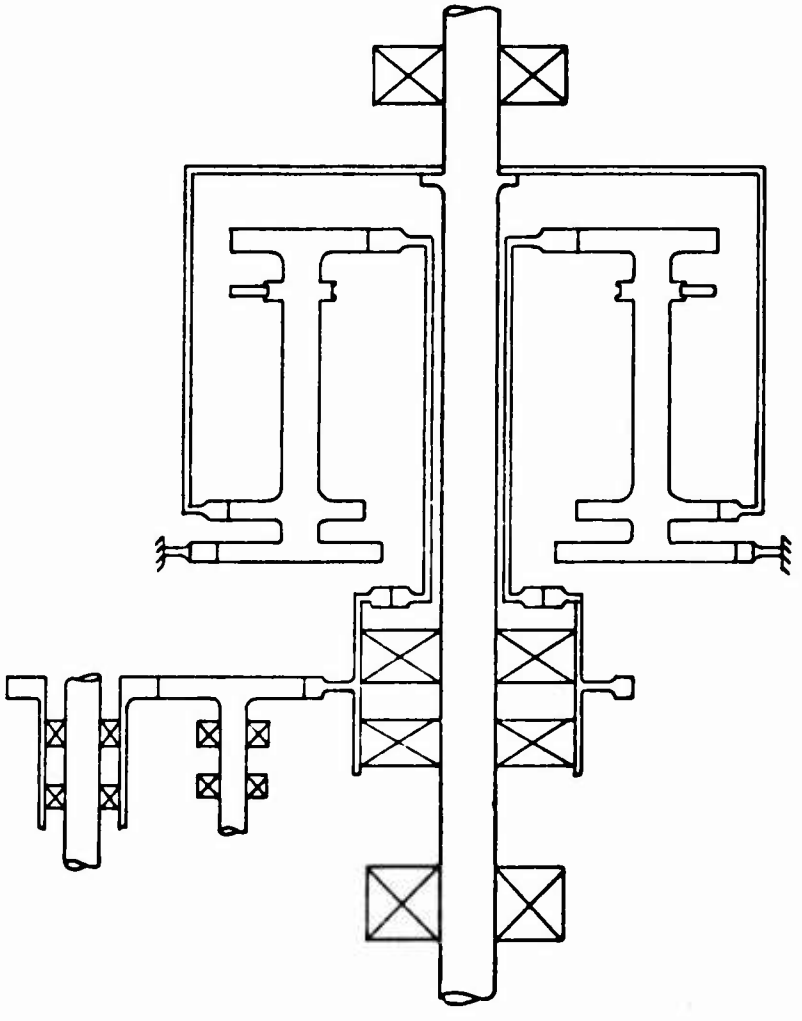

Figure 29. Free Planet Transmission Schematic.

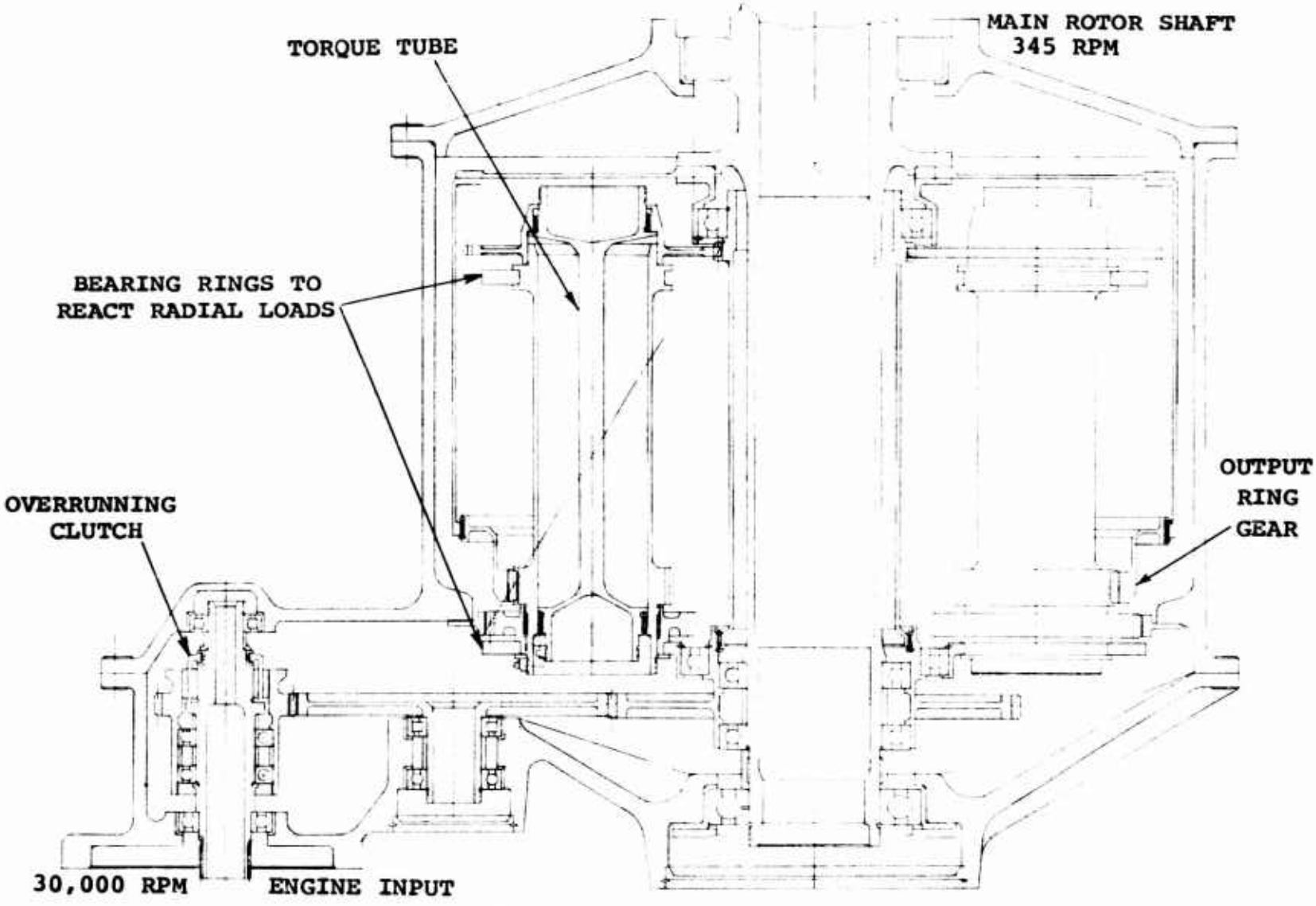

Figure 30. Free Planet Transmission Layout.

- the use of free-floating support or retaining rings reacts the loads in the radial plane

- the axial distances separating the gear face centers in the tangential plane are selected to avoid planet skewing moments. In essence, the sum of the moments about any point is zero.

Roller Gear Drive

The roller gear drive transmission concept is a drive which transmits power through friction in a planetary arrangement of preloaded rollers and a conventional geared planetary or epicyclic gear train in a compound arrangement. Figure 31 shows a 50:1 reduction ratio vertical engine roller gear drive design that was considered for this study. Roller gear drive was not selected for the advanced transmission concept since it presented difficult problems for manufacturing with a resultant high cost.

The roller gear drive design, however, does offer some potential advantages, including:

(1) an improvement in efficiency with the gears operating at the theoretical pitch line

(2) an improvement in reliability with fewer highly stressed parts and fewer bearings

(3) a reduction in weight which is estimated to be five to seven percent of a conventional planetary transmission design

(4) a reduction in height of 3 to 4 inches as a result of the gears operating at the pitch line.

The actual arrangement of the components is shown in Figure 32. The vertically mounted engine output shaft turning at 50,000 rpm drives the input pinion of the spur combining mesh at 12,500 rpm. Within the input pinion is an overrunning cam roller type freewheel unit. The output of the spur combining gear, which is concentric about the main rotor shaft, drives the 50 to 1 roller gear drive reduction unit. The unit consists of a fixed cage with two stationary rows of pinions, ring gear output, and a sun gear input. A split power path at the sun gear and ring gear induces symmetrical loading for each mesh in the roller gear unit. Two rollers per mesh whose diameter equals the gear's pitch diameters straddle the gears of the sun, first-row pinion, and second-row pinion. The first-row pinion is positioned by the sun and second-row pinion rollers and is thus accurately located by three contact points. The second-

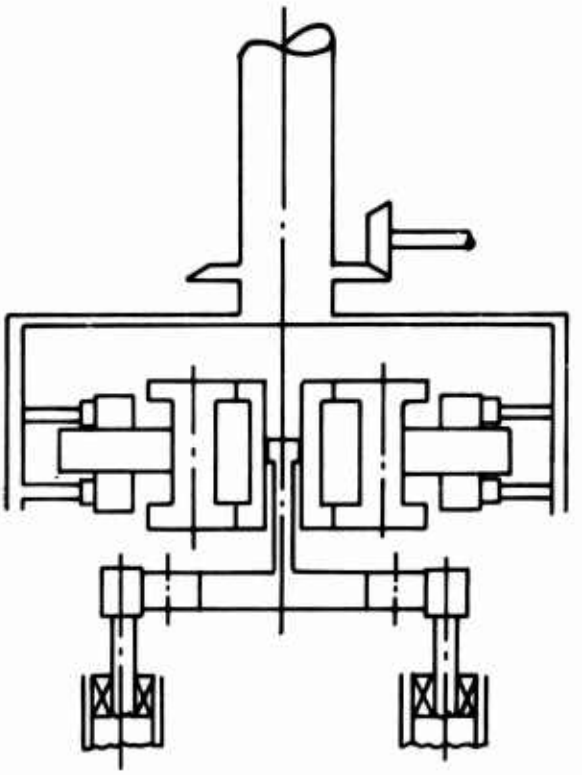

Figure 31. Roller Gear Drive Schematic.

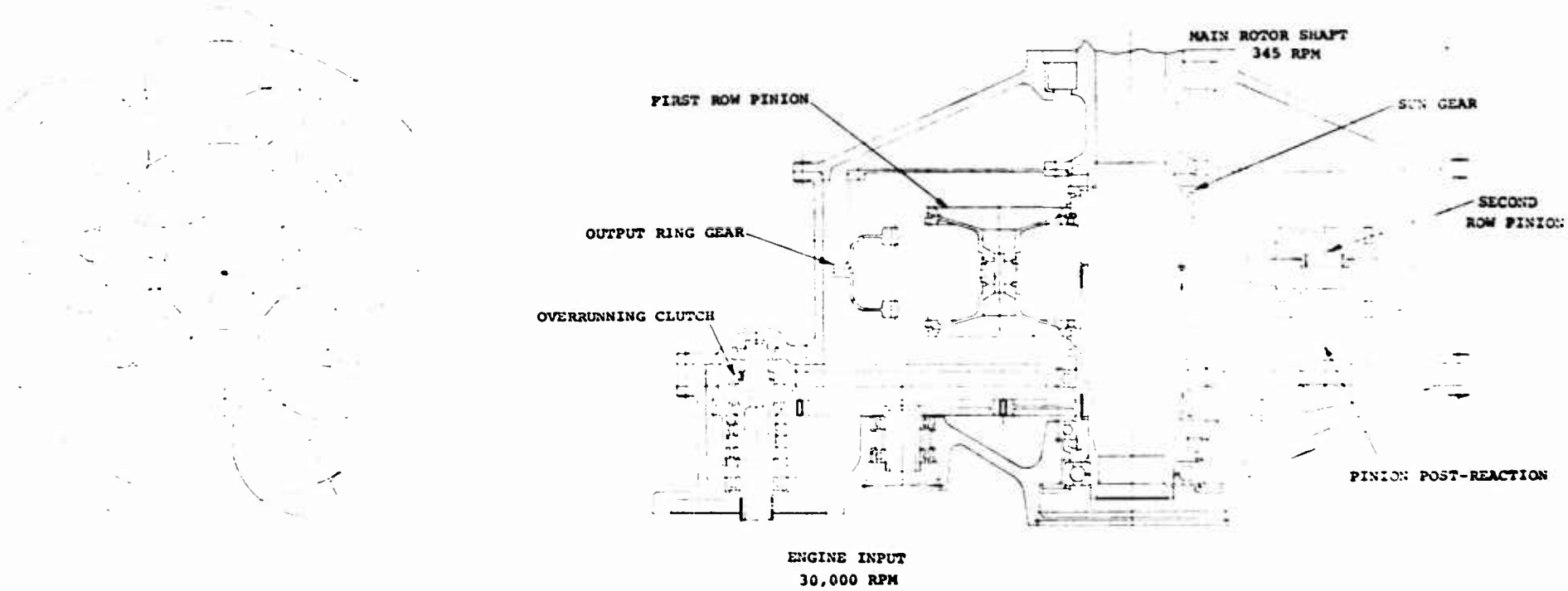

Figure 32. Roller Gear Drive Layout.

row pinion is similarly positioned by the rollers of the first-row pinion and the separating component of the ring gear. Torque is reacted through spherical bearings located in the second-row pinion. Power is thus transmitted by the gear teeth while kinematic stability is provided by the rollers.

The design eliminates planet bearings except in the last row, where they are necessary to transmit the reaction torque, and ensure parallel alignment of all elements within manufacturing tolerance.

Maroth Transmission

Another of the transmission concepts investigated is the Maroth transmission, which may be designed for extremely high reduction ratios but is suited only for low power applications. The Maroth transmission was eliminated from consideration in this study due to its lack of load-carrying capability.

The Maroth transmission consists of a stationary reaction cam, a rotating output cam, a rotating plate, and an input drive and bearings as shown in Figures 33 and 34. The reduction ratio through the gearbox is accomplished as follows: Rotating the input member drives the rotating plate through a bearing which is constrained from rotating by the reaction cam. This results in the rotating plate's being forced to wobble much the same as a rotor head swashplate. The rotating plate engages and rotates the output cam as if it is being forced to wobble. The gear reduction results from there being a slight difference in the number of teeth between the rotating output cam and the reaction cam.

A number of problem areas have been uncovered which include:

- Extremely high loads on the rotating plate bearing. The loads are such that it is difficult to achieve a realistic design utilizing a rolling element bearing and obtain a design goal for B_{10} bearing life of 3000 hours. The best design to date utilizing tapered roller bearings is extremely heavy and has a B_{10} bearing life of 250 hours.

  As alternative designs, a hybrid boost bearing and a conventional hydrodynamic bearing design were considered. In both cases the viscous losses due to the high loads resulted in a frictional loss of 63 hp. This is a 3.6 percent loss in transmission efficiency.

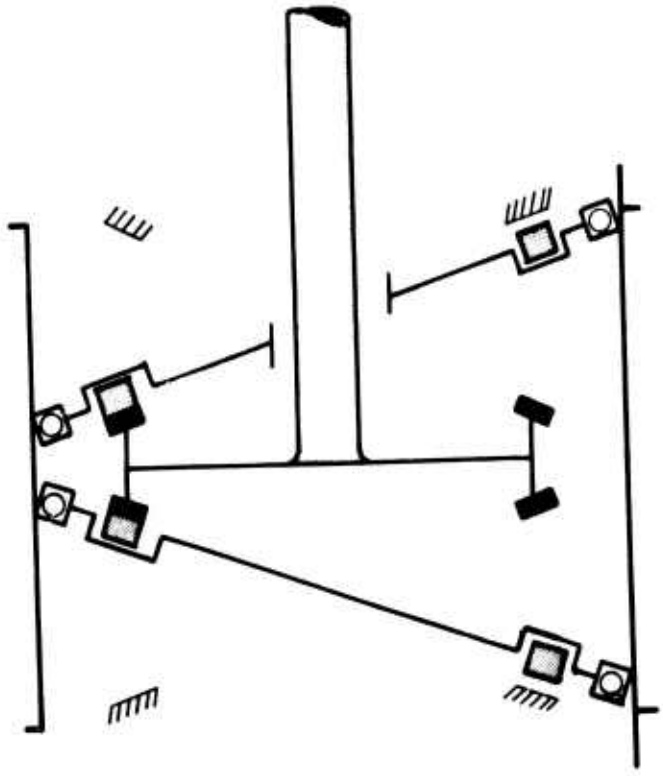

Figure 33. Maroth Transmission Schematic.

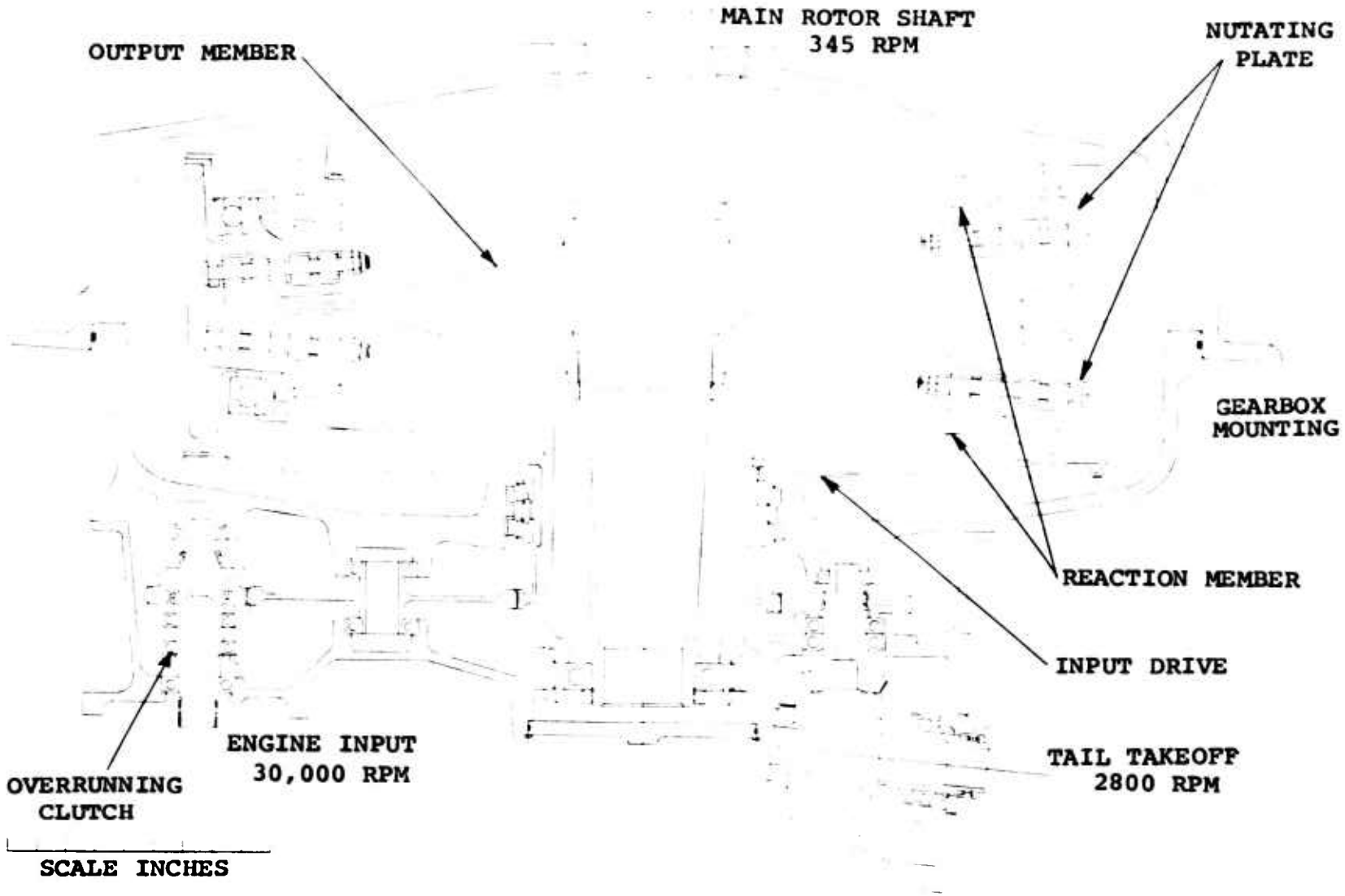

Figure 34. Maroth Transmission Layout.

- Unsymmetrical loads on output cam and reaction cam: The loads on the cam members do not balance in the horizontal plane and are not axial symmetric in the vertical plane. The loads not balancing in the horizontal plane result in a high net tangential load on the main rotor shaft. This load is also rotating relative to the main rotor shaft. The lack of axial symmetry results in the difficulty of achieving sufficient stiffness in the axial direction. The final result of this is that poor tooth form patterns under load are to be expected.

- Large number of cam follower bearings are required. Low reliability results from having a minimum of 150 rolling element bearings rotating at 8600 rpm loaded for only one-quarter of the cycle.

  As an alternative, a hydrodynamic bearing design was considered with the result that a frictional horsepower loss per bearing of .8 hp can be expected.

FAN DRIVE

The main gearbox is interconnected by shafting to the IR suppression fan to provide speed synchronization and transfer of power required during various flight regimes, including autorotation. The shafting is designed to transmit a maximum of 250 hp, accommodate deflection through two laminated flexible disc couplings at each end, permit operation up to 115 percent of 2696 rpm normal operating speed, be light in weight, and yet permit fabrication by available manufacturing technology.

For the design of the fan drive shaft, shaft diameters from 1 to 4 inches are considered as well as various support conditions, including a one-piece shaft with no center supports, a two-piece shaft with center coupling and bearing support, and a one-piece shaft with one center bearing support.

From Figure 35, fan drive shaft outside diameter of standard mill extrusions versus shaft weight, the lightest shaft weight is achieved at a 2.75-inch-diameter aluminum tube. For this geometry, adding a coupling and/or a center support will result in higher weight since, as shown in Figure 36, the minimum shaft diameter to carry the torque is 2.45 inches. This diameter with a .025-inch-thick wall has a natural frequency of 3200 rpm, which is more than 115 percent of the normal operating speed, 2696 rpm.

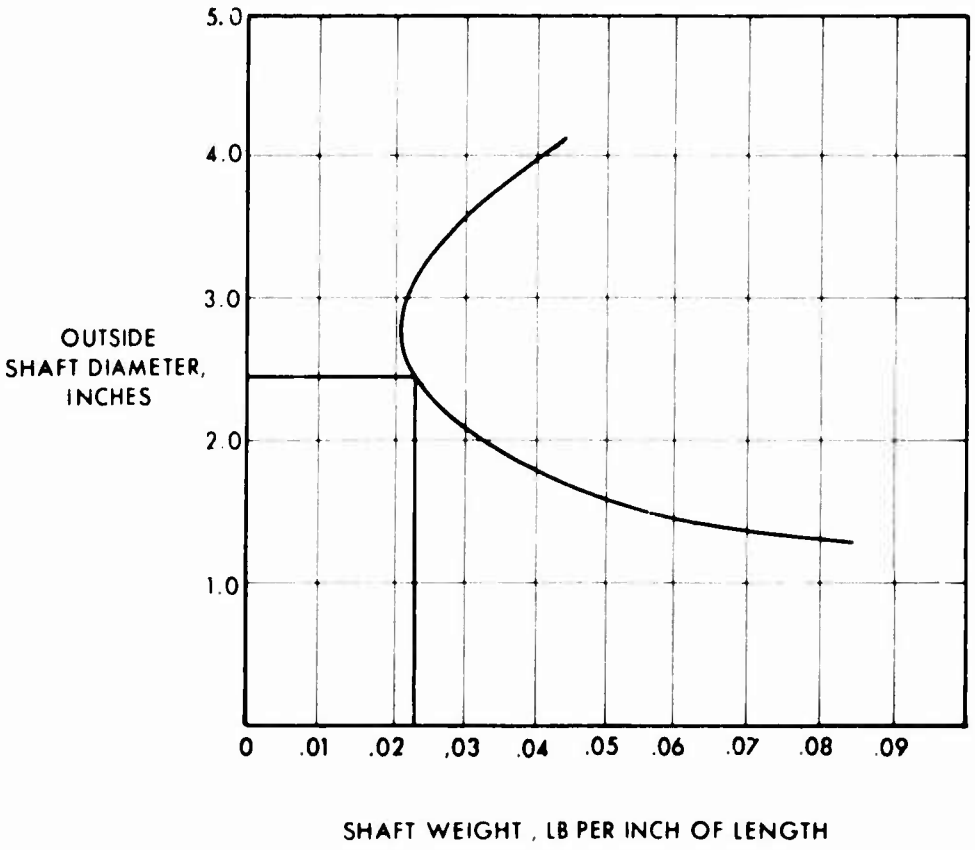

Figure 35. Fan Drive Shaft Diameter vs Weight.

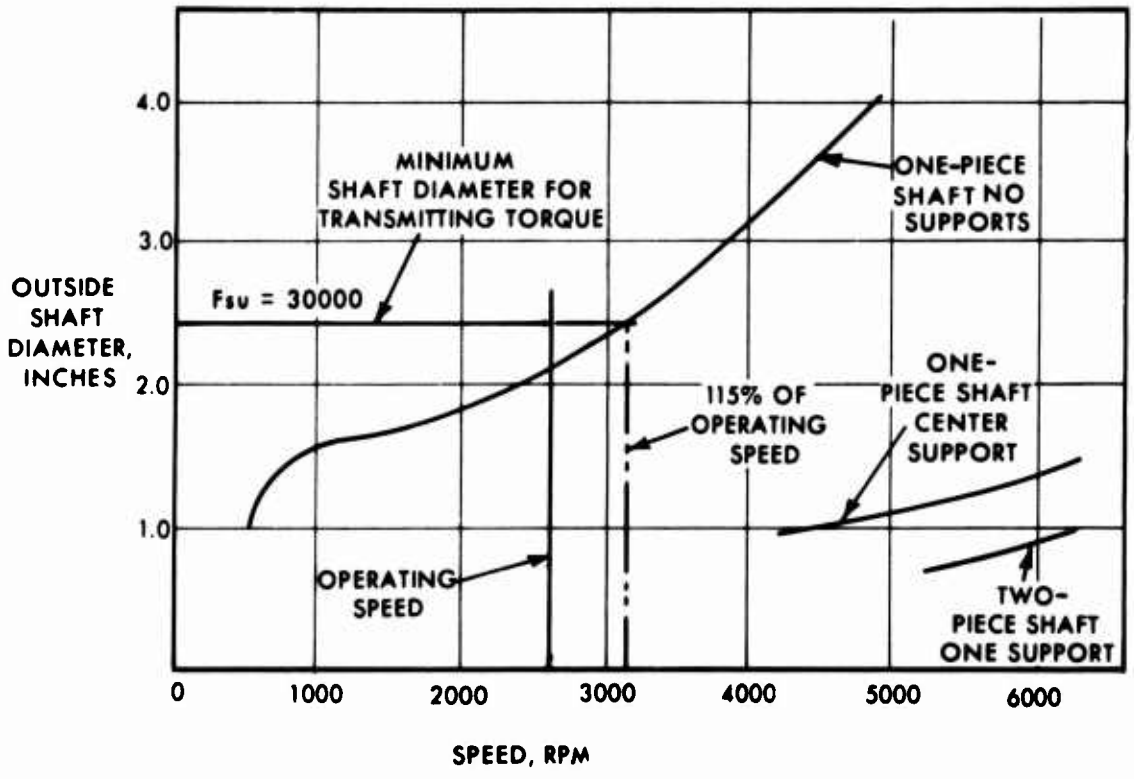

Figue 36. Fan Shaft Diameter vs Critical Speed.

The selected fan drive is a single-piece shaft design connected to the fan coupling by laminated flexible disc couplings. The shaft, which is 2.45 inches in diameter with a 0.025-inch-thick wall, is 75 inches long and made from 6061-T6 drawn aluminum alloy tubing. The shaft end fittings are of 4340 steel, which are riveted to each end of the shaft. The coupling selected is a flexible laminated disc type coupling of 3.75 inches OD by 2.75 inches ID with a disc pack thickness of .158 inch.

Axial misalignment due to thermal expansion and installation mislocation is accommodated by a grease-packed sliding spline on the gearbox mounting flange.

TRANSMISSION COOLING REQUIREMENTS

Losses in a transmission system can be estimated from a knowledge of the type of gear mesh, the design horsepower, and the power transmitted by each gear mesh. Past experience, backed by experimental confirmation, has demonstrated that a conservative estimate of tooth mesh losses, together with bearing losses, is 1/2 percent for spur gears, 1/2 percent for bevel gears, and 3/4 percent for planetary units. A further 3/4 percent of power transmitted must then be added to account for miscellaneous churning losses.

The losses in the advanced transmission are evaluated in Table 12.

TABLE 12. LOSS SOURCES AND EFFICIENCY OF TRANSMISSION

Main Rotor Drive - 894 hp Output

Gear Mesh	Loss Percent	Loss hp
1 epicyclic	0.75	6.705
1 bevel	0.50	4.47
1 spur	0.50	4.47
Churning	0.75	6.705
	Main Rotor Drive Losses	22.35

Fan Drive - 80 hp

Gear Mesh	Loss Percent	Loss hp
1 epicyclic	.75	.6
2 bevel	1.00	.8
2 spur	1.00	.8
Churning	.75	.6
	Tail Rotor Drive Losses	2.8

TABLE 12. (Continued)

Accessory Drive - 30 hp

Gear Mesh	Loss Percent	Loss hp
1 epicyclic	.75	.225
2 bevel	1.0	.30
5 spur	2.5	.75
Churning	.75	.225
	Accessory Drive Losses	1.50

Total Input Power Required

Main Rotor Drive	894	+ 22.35	=	916.35
Fan Drive	80	+ 2.8	=	82.8
Accessory Drive	30	+ 1.5	=	31.5
	1004	+ 26.65	=	1030.65

The transmission efficiency is then calculated as follows:

$$\eta = 100(1-26.65/1030.65) \quad (38)$$

$$= .974$$

Heat Generated in Transmission

The previously calculated gear tooth and bearing losses appear as heat, and the coolant supply must be adequate to remove this heat while keeping the temperature of the oil or grease within a specified limit. For oil or grease lubrication, the lubricants considered are listed in Table 13.

TABLE 13. LUBRICANTS CONSIDERED

Lubricant	Density (gm/cm^3) @77°F	Kinematic Viscosity (centistokes) @100°F	@210°F	Temp Limit
Grease (Polyol Oliphatic Ester & Flourinated Polysiloxine)	.99	42	15.3	350
Oil MIL-L-23699	.968	26.0	5.5	550

The heat generated in the transmission was calculated based on an empirical rule; however, if Buckingham's method is used for gear efficiencies and T. A. Harris's is used for bearings, the heat generated for either an oil- or a grease-lubricated transmission is the same for the gears and approximately the same for the bearings. The grease-lubricated bearings have a slightly higher frictional loss, approximately 5 percent due to viscous effects. In any event, the same heat removal requirement is used with either grease or oil lubrication. The total heat generated is given by $Q_G = 2545\ F_{hp}$. Since $F_{hp} = 26.65$ hp, the total heat generated is 67,824 BTU/hr.

The friction horsepower and generated heat are relatively low in the transmission, while the surface area of approximately 12 square feet is relatively large. Based upon operational experience with similar oil-lubricated gearboxes, the friction heat can be dissipated to the ambient air by the normal oil flow throughout the gearbox as it is circulated via an oil pump. Based on tests with the S61 grease-lubricated main, intermediate and tail gearboxes, the heat conduction for the housing presents no problem. Cooling is provided by finning the transmission housing and ducting a portion of the IR fan airflow over it. The gearbox housing stabilized temperature is calculated to be 240°F in the AIRFLOW SUBSYSTEMS section.

GREASE VS OIL LUBRICATION

The actual choice of a transmission lubricant, whether grease or oil, depends on the level of technical risk assumed. Oil lubrication has operated successfully for over twenty years. Our operating experience with grease is outlined in Table 14. The use of a grease-lubricated transmission, however, offers a number of significant advantages, including:

- simpler service and inspection due to elimination of monitoring oil level
- improved survivability - difficult to lose lubricant
- seal leakage minimized
- contamination localized by grease boundary at component mating interfaces
- no jets or screens to clog
- no mission aborts due to pump or pumping failure
- lighter system weight
- less complex

TABLE 14. SIKORSKY OPERATING EXPERIENCE WITH GREASE LUBRICATION

Aircraft Model and Location	Pitch Line Velocity Gear	Pitch Line Velocity Bearing	Bearing Type	Test Time (hr)	Speed (rpm)	Power (hp)
SH3A Intermediate Gearbox	Spiral Bevel 5700 fpm	2670 fpm	Tapered Roller	2440	3400	100-400
SH3A Tail Gearbox	Spiral Bevel 3500 fpm	2670 fpm	Tapered Roller	2440	3400	100-400
SH3A Main Gearbox Input Section	Spur 9200 fpm	6200 fpm	Ball & Roller	10	9500	300
YH60A Intermediate Gearbox	Spiral Bevel 5700 fpm	3300 fpm	Tapered Roller	150	4200	150

The problems that can be expected with a grease-lubricated transmission include

- higher localized temperatures due to lack of a copious supply of coolant
- the lack of a viable chip detector system
- lack of sufficient test experience with grease lubrication particularly in freewheel
- no experience with grease in high-speed bearings and gears at 30,000 rpm - heat removal is expected to be a severe problem.

It is believed, on balance, that the choice of grease lubrication would entail too high a technical risk to merit inclusion in this concept.

Electrostatic Cooling

The average gearbox housing surface temperature was previously estimated to be approximately 240°F; however, the localized surface gear and bearing temperatures within the gearbox can be expected to exceed 400°F. This presents no problem with a conventional oil-lubricated transmission if sufficient cooling fluid is supplied. With a grease-lubricated transmission this temperature is beyond the limit of present gear formulations, and scoring and spalling of the gear and bearing contact surfaces can be expected. One possible approach to localized cooling of gears and bearings is electrostatic cooling.

Electrostatic cooling has been described in Patent Number 3,224,497 as a way to control the energy level in matter. It is believed that cooling is enhanced by breaking down the boundary layer at the surface of matter when the body in question is subjected to a continuous electrostatic discharge from a probe. For either a gear or a bearing, the parts are charged positively while a nearby probe has a negative potential. This tends to ionize the air and results in a stream of electrons directed from the probe to the bearing and gears. The effect appears to remove the insulating boundary layer and accelerates the flow in heat from the parts.

To cite an example from the machine tool industry: with a concentrated heat source, the temperature of a cutting tool at 1000°C was reduced to 200°C by the application to an electrostatic probe of 20 KV at .5 milliamp.

The concept of electrostatic cooling can also be applied to the outside of the finned transmission housing to improve the convective heat transfer coefficient and to reduce the fan power by removing the air boundary layer.

Electrostatic cooling as applied to transmission components would represent a major state-of-the-art advancement, which should allow a reduction in gearbox peak temperature, improve the heat transfer characteristic and reduce the required cooling power.

ENGINE/GEARBOX MOUNTING ARRANGEMENTS

Engine gearbox mounting arrangements that are considered include a conventional engine gearbox mounting such as on the CH-54A or CH-53A, where one end of the engine is supported by a torque tube and the other end is supported by struts to the airframe; a close-coupled engine arrangement, wherein the engine is bolted to and supported by the transmission; and a remote coupled engine gearbox arrangement, where the power turbine is mounted as a separate module on the transmission and the engine is remotely installed and connected to the power turbine through hot gas ducting.

The close-coupled engine gearbox mounting arrangement is selected for the advanced integration technique aircraft because it offered the best combination of features, including:

- the smallest, simplest package
- an engine gearbox package that lends itself to palletization
- a design in which the drive alignment between the engine and gearbox can be accurately controlled by the tolerance built into the interface geometry
- minimized natural frequency problems between the engine/gearbox interface by virtue of the shortest distance between them
- package arrangement with aft-mounted engines eliminates interface problems with hot exhaust gases and power turbine thermal effects
- the time response of the engine control system is the same as present conventional designs.

Conventional Rear-Drive Mounted Engines

In a typical conventionally mounted rear-drive engine, the aft end of the engine is supported by a torque tube to a gimbal ring mounted on the transmission. The front end of the engine is supported through a damper strut assembly. Surrounding the torque tube is an exhaust duct which directs the exhaust gases around the transmission. Inside the torque tube is mounted the engine drive shaft, which transmits torque between the engine power turbine and transmission input bevel gear. Any misalignment, either angular or parallel, is accommodated by a flexible disc at the power turbine end and a curvic coupling at the transmission gimbal mount end. Isolation of the engine from the transmission is achieved by means of rubber bushings in the gimbal ring.

This conventional engine gearbox mounting arrangement has the following advantages:

- the angular misalignment between the engine and gearbox is easily accommodated by the gimbal mount on the torque tube
- engine inlet or exhaust duct design subjects the airflow to only a gradual change in direction
- the engine is isolated from the transmission by the rubber isolator built in as part of the gimbal ring assembly.
- good engine separation reduces probability of loss of both engines from a single hit.

The disadvantages of this design include:

- the highest weight of any of the alternative designs that were investigated
- the lowest natural frequency for the engine gearbox drive connections investigated.

Close-Coupled Engine Mounting

In a close-coupled engine mounting arrangement, the engine is bolted to and supported by the transmission. The aft end of the engine may be supported by a damper strut assembly. Torque between the engine and gearbox is transmitted by a crowned spline quill shaft. The engine air inlet is radial or axial.

Deflections of the airframe structure do not influence the engine drive shaft-to-transmission connection, and thus the angular misalignments are reduced. The crown spline has a low probability of wearing. The misalignment, both angular and parallel, is effectively controlled by a close concentricity tolerance between engine and transmission location/mounting pilot diameters.

The use of this mounting arrangement leads to the elimination of gimbal and alignment problems. Exposed drive shafts, support forgings and struts have been eliminated.

A close-coupled engine mounting arrangement may also require a damper strut assembly to control the engine support loading and create a favorable vibrational environment for the engine.

The close-coupled engine mounting arrangement has the following advantages:

- Elimination of maintenance and inspection items, including high-speed flexible disc coupling, and spline connections.
- Engine alignment is achieved by the use of a multi-function pilot machined on the forward engine face. This pilot diameter provides automatic alignment of the engine to the gearbox, reacts shear loads, and provides concentricity of the engine output shaft to the gearbox input shaft.
- The plug-in feature of the close-coupled engine mounting allows the engine to be installed or removed simply and easily, and the mechanic is concerned only with engagement of the engine and gearbox splines, positioning of the pilot into the gearbox and the torquing of the attachment nuts.
- 360-degree accessibility is available with ample clearance for quick and easy component removal.
- The engine/gearbox package will move as a unit if the drive system is isolated from the airframe.
- The close-coupled engine gearbox package lends itself to palletization.

The disadvantages of the design include:

- Subjecting the engine to a high g level environment with an isolated engine/gearbox package.

- The gearbox and engine combination would be approximately as heavy as a conventional engine gearbox combination due to the higher loads encountered by the cantilevered design.

Remote-Coupled Engine Mounting

The gas generator and power turbine in a remote-coupled installation are treated as separate modules in the installation. The power turbine module is attached directly to the main gearbox through a torque tube and shares the lubrication system with the main gearbox. For the vertical power turbine installation, a separate oil cooling system is required.

Power is transmitted between the gas generator and power turbine section through a system of interconnecting hot gas ducting.

The remote-coupled engine mounting arrangement has the following advantages:

- Design flexibility in choice of gas generator location to enable design of the air induction system to deliver air efficiently to the engine with minimum distortion and maximum total pressure recovery.

- Design flexibility in choice of location for accessibility in consideration of the engine's high maintenance section, the gas generator.

- Design flexibility in choice of engine location for center of gravity and aerodynamic cleanliness.

The disadvantages of this design include:

- Losses in remote gas coupling (pressure and temperature) are excessive compared to mechanical coupling.

- The need of a relatively long shaft between the power turbine and gearbox input to permit a duct design in which the change in airflow is gradual.

- With remote-coupled engine design the power turbine is part of the transmission, and the transmission must now be designed to handle temperature levels up to 1500°F. Present gearbox cast housing materials are unacceptable.

For the three engine mounting arrangements considered, the close-coupled engine gearbox design offered the best combination of features for use in the advanced integration techniques aircraft, including:

- The smallest, simplest package.
- A package that lends itself to palletization.
- A design in which misalignment is minimized, the tolerance being built into the interface geometry.
- A design that minimized natural frequency problems between the engine gearbox interface.

ENGINE LOCATION

No engine mounting configurations were considered where the engines were mounted crosswise to the aircraft because of difficulty in achieving satisfactory access for engine servicing. This arrangement also has the problem of ducting the exhaust duct past and turning the exhaust gas around the transmission housing.

Vertical engine mounting allows a relatively simple, lightweight transmission design by the elimination of the bevel gears in the primary rotor drive train. The basic problem with this type of package is the relatively long vertical length of the package. This leads to difficulty in ducting the exhaust gases toward the IR suppression mixing fan. The 90-degree turning duct also creates the additional problem of having hot exhaust gases directed over the engine fuel tank. This duct turning and fuel tank location problem exists with either a forward- or an aft-mounted vertical engine configuration. Vertical engines also offer the disadvantage in limiting access for engine servicing, and the problem exists of supporting an engine during engine removal.

Vertical engine mounting has the advantage of ease of removal of the total drive system since the engine/gearbox package can be removed as a unit. One additional problem that must be resolved before vertical engine mounting could be utilized is design of engine lubrication systems and bearings for vertical operation. Vertical engine mounting is considered in the transmission concepts investigated since it offers a simple lightweight drive; however, vertical engine location does not lend itself well to the aircraft exhaust gas usages.

The engine mounting configuration that offered the best features in engine exhaust ducting, engine access for servicing, ease of engine removal, and engine air inlet design is the horizontal aft-mounted engine configuration.

HIGH-SPEED INPUTS

With future helicopter engine technology resulting in engine output speeds in excess of 30,000 rpm, current technology in transmission design will be pushed beyond the state of the art.

For aircraft that have been designed within recent years, the drive train scheme is such that the first gear mesh is either a bevel gear or a spur gear. The approach, which leads to the lightest drive train weight, has been to take a relatively high reduction ratio (approximately 3.0 to 3.5 reduction ratio) on the first gear mesh and to change the shaft orientation as quickly as possible.

An example of a high-speed bevel input is the CH-53 nose gearbox bevel set. The input bevel mesh was designed for what was considered a high-speed engine operating at 19,000 rpm. A four ball bearing stack arrangement was required on the input pinion to achieve a bearing B10 life of 2000 hours. An example of a high-speed spur mesh is the S61 main gearbox input section. This design has sleeve bearings on the input bearings with a required oil flow of 8 to 10 gpm. Bearing life for this design is considered to be infinite, with bearing journal wear occurring during the start-stop cycle where the fluid is building up or collapsing. A conventional rolling element bearing design is not used in this design since it is heavier and has a B10 life of 600 to 700 hours.

Problems that can be expected with high-speed bevel gears include scoring, which is associated with high gear pitch-line velocity, and low bearing life as a result of the thrust load induced by the bevel gear. With high-speed spur gears with ordinary rolling element bearings, the basic problem is low life due to lack of bearing capacity in wide, smaller diameter gears. With hydrodynamic bearings, the most difficult problem to overcome is the power loss in the journal bearing due to viscous effects.

The basic problem with any high-speed input design is in getting bearing designs that have sufficient load-carrying capability.

The approach that will be followed in assessing high-speed inputs will be to design a high-speed (30,000 rpm) conventional design spur and bevel gear input section and to look at some of the newer concepts, including a split power and counterrotating planetary arrangement.

In the design of a typical high-speed bearing, the biggest problem is not usually the applied load except thrust from a bevel pinion, but centrifugal forces. This usually results in the bearing outer raceway fatiguing faster than the inner race. Centrifugal loading also increases the bearing operating clearances, which tends to decrease the zone of loading, leads to a greater tendency toward skidding, and results in reduced fatigue life.

For the design of high-speed bearings in a bevel gear mounting, a number of bearing arrangements were considered. Since bearing capacity is a function of diameter, cross-sectional size, and number of bearing elements, then for a given gear size, load and speed, there is a certain maximum life for a particular bearing arrangement. This analysis was part of an advanced technology VTOL drive train configuration study in which the effort was to determine if one particular bearing arrangement would offer a significant improvement in life for the bevel gear mesh. This arrangement consisted of two rollers to carry the radial load and two split inner race ball bearings which reacted only the thrust load. The rollers are located with the ball bearings between them to give the largest span for reacting the moments.

In the design of conventional spur gear inputs, the bearing design criterion is simply one of getting the smallest diameter with sufficient bearing capacity to carry the load.

One of the ways of improving bearing life in high-speed application is in reducing skidding of the rollers and balls. This skidding is usually the result of low applied radial load and high-speed operation and may be improved by the following techniques:

- Reduce both size and number of rollers in a bearing. Most turbomachinery roller bearings could have the number of rollers reduced by 50 percent and roller size by 25 percent and still have adequate life.

- Use of lightweight separator such as AISI 4340 (silver plated).

- Arrangement of race configuration to avoid restricting the flow of lubricant.

- Increasing the number of rollers under load. In most roller bearings, the maximum number of rollers under load is 20 percent of the full roller complement. By deflecting the outer race to an elliptical shape by applying two forces at 90° to the applied load, the number of rollers under load can be increased to 60 percent.

This increases the total tractive force on the roller separator complement and helps prevent skidding.

- Preloaded hollow roller to produce a load on all rollers within a bearing without the necessity of elliptical races. This ensures that the roller always has some load as it rotates around the entire bearing. This technique eliminates the problem with the two-point elliptical race preload of a solid roller skidding in the unloaded zone of the bearing.

One possible answer to the problem of skidding of high-speed roller bearings may be the use of full complement bearings without a separator. Full complement bearings have operated in turbomachinery for thousands of hours at DM values of $1 - 1.25 \times 10^6$ without signs of skidding. Skidding frequently shows up in bearings with separators at these speeds.

Another way of solving the low bearing life problem on high-speed inputs is to eliminate them from the problem. One approach is a split power transmission. In this design, a conventional planetary is used as a torque splitter, with the planetary plate output and ring gear output each carrying part of the torque. The sun gear, which is turning at the input speed of 30,000 rpm, has no bearings since it is floated and supported by the planet pinions. The planet pinion bearings are much simpler to design since each rotates slower than the sun gear (approximately one-half) and each carries only two-thirds the sun gear tangential tooth load.

AIRFLOW SUBSYSTEMS

INTRODUCTION

The primary goal of the airflow subsystems study is to utilize the IR suppressor/directional control fan as the air moving device for other air requirements, both inside and outside of the aircraft, thereby avoiding cost, weight and power penalties associated with the use of additional fans. The airflow requirements considered in this study are cockpit/cabin heating and ventilating, windshield defogging, avionics cooling, engine compartment cooling, transmission cooling, engine oil cooling, engine air particle separation and boundary layer control. In each case, the prime design criterion is to hold pressure losses upstream of the fan to the minimum compatible with the principal purpose of the fan in order to avoid the undesirable result of allowing major impact on fan design and power from systems which require relatively small airflows.

COCKPIT/CABIN HEATING AND VENTILATING

Traditionally, heating and ventilating of occupied compartments within aircraft have been accomplished by a combination of blowers, combustion heaters and bleed-air heaters. There are also a few instances of use of exhaust muffler heat exchangers. The systems investigated in this study (Table 15) are exhaust muffler heat exchangers and, for comparison, bleed-air heaters. In all cases the cockpit airflow is assumed to be returned to the suction side of the IR fan.

TABLE 15. HEAT/VENT SYSTEMS CONSIDERED

System	Air Source	Heat Source
1	Ambient	Engine Exhaust
2	Pressure Side of IR Fan	Engine Exhaust
3	Heat = Engine Bleed Air Vent = Pressure Side of IR Fan	Engine Bleed-Air

System 1 differs from system 2 only in the source of ventilation air. System 1 has the disadvantage that only two inches of water pressure is available for heating air and distributing it to the cockpit. System 2 eliminates this distribution difficulty by tapping ventilation air from the pressure side of the IR fan, heating it as required in an exhaust muffler, distributing it, and returning it to the suction side of the fan. The lobes of the exhaust daisy used to introduce engine exhaust air into the fan make provisions for the use of pressure-side air for ventilation by locating no lobes in a sector of approximately 70° centered around the six o'clock position of the fan. The adequacy of these provisions requires test verification.

System 3 eliminates the exhaust heat exchanger and replaces it with a bleed-air mixing valve. Since the bleed-air use for heating is proportional to the cockpit heat load, there is no power penalty to the aircraft, presuming the engine is T_5 limited. The fuel flow associated with the bleed-air use is approximately 20 pounds per hour at -22°F, decreasing to zero at 70°F.

There is estimated to be no weight difference between the three systems. System number 2 is believed to be more practical than system number 1. The choice between system number 2 and number 3 is not obvious, but system number 2 is selected because the use of bleed-air is contrary to the goals of this study and, therefore, a clear advantage in its favor would have to be established to justify its use.

WINDSHIELD DEFOGGING

The use of cockpit heating air for windshield defogging is not considered advantageous because it introduces larger quantities of heat into the cockpit on warm and cool days than would be required for electrical defogging (the electrical system is present in any event for anti-icing purposes and can contain a defog temperature setting).

AVIONICS COOLING

The avionics are cooled by discharging ventilation air into the avionics bays and exhausting it through the cockpit and cabin into the IR fan.

ENGINE COMPARTMENT COOLING

The engine compartment is partially cooled by exhaust gas-powered ejectors which draw cooling air through the engine compartments. Additional cooling is provided by using the IPS scavenge air as the primary airstream for additional ejector pumping. The cooling air pumped by the engine exhaust

is discharged into the IR fan together with the engine exhaust flow. To prevent excessive IR fan erosion rates, both the IPS scavenge air and the engine compartment cooling air pumped by it are discharged overboard. Additional cooling is obtained by the transmission cooling airflow, which scrubs the lower engine compartment firewalls.

TRANSMISSION COOLING

The main gearbox is air-cooled by the IR fan, which draws 22.5 lb/sec of cooling air over the finned lower portion of the gearbox housing. The adequacy of this cooling mechanism is substantiated as follows:

Assumptions

1. Maximum allowable transmission skin temperature: 240°F
2. Transmission heat rejection: 19 BTU/sec
3. Transmission radius: .8 ft
4. Effective heat transfer area: 21.7 ft^2
5. External heat transfer coefficient corresponds to that obtained with a 6-inch turbulent boundary layer.

Based on assumption number 5 above, the heat transfer coefficient which is given by

$$h_x = (.0296\ \rho V C_p)/(Re_x^{.2}\ P_r^{.667}) \tag{39}$$

can be written as

$$h_x = (.0296)(.24)W/\ [(.5W/1.2x10^{-5}A_D)^{.2}(.77)^{.667}A_D] \tag{40}$$

after substitution of values for the thermophysical properties and W/A for ρV.

Solving for h_x, we obtain

$$h_x = .00101W^{.8}A_D^{-.8} \tag{41}$$

The heat balance for the heat transfer surfaces of the gearbox is given by

$$(T_s-T_{a,in})/(T_s-T_{a,out}) = e^{-h_xA_s/WC_p} \tag{42}$$

Substituting for the air outlet temperature $T_{a,out} = T_{a,in} + Q/WC_p$ and the expression for h_x from Equation (41) into Equation (42), we obtain

$$(T_s-T_{a,in})/T_s-T_{a,in} - Q/WC_p = e^{-.001A_s/C_pW^{.2}A_D^{.8}} \tag{43}$$

After substituting 240°F for T_s, 95°F for $T_{a,in}$, 19 BTU/sec for Q, 0.24 BTU/lb for C_p, and 21.7 ft^2 for A_s, and taking logs of both sides, we obtain

$$\ln(145/(145-79.17/W) = .0913/W^{.2}A_D^{.8} \quad (44)$$

$$A_D = \left\{\ln [145/(145-79.17/W)\ ]\ \ W^{.2}/.0913\right\}^{-1.25} \quad (45)$$

Solving for the cooling flow duct area with W = 22.5 lb/sec, we obtain A_D = 2.37 ft^2 (the minimum area which will provide adequate heat transfer).

Since this flow area is greater than the 1.85 ft^2 area required to deliver this air to the fan, no additional power is expended to accelerate the transmission cooling air, and more than adequate heat transfer is available for the transmission.

ENGINE OIL COOLING

It is considered reasonable to assume that advanced technology engines of the size envisioned for this application will be capable of rejecting their oil heat load to engine fuel. The bases for this prediction are the lack of an engine-provided reducing gearbox and the fact that a specific advanced engine specification falling within the general size of this application specifies a self-contained oil cooling system.

ENGINE AIR PARTICLE SEPARATOR

It is not recommended that the engine air particle separators be integrated with the IR fan. It is not desirable to discharge the separator scavenge air through the IR fan because of the high concentration of dirt and dust particles. It is considered more practical to use a scavenge blower for this purpose and to either provide the necessary coating for the blades and vanes or classify the blower impeller as an expendable item.

BOUNDARY LAYER CONTROL

Reference 1 has shown that a typical rotor head fairing contributes approximately one-third of the parasite drag area of a helicopter. This same reference shows experimental results that prevention or reduction of flow separation at the rear of the rotor head and pylon by means of boundary layer energization can reduce aircraft parasite drag by one-third. Based on this information, it was decided to position the primary inlet for the IR fan at the rear of the rotor head area to aid in drag reduction.

To evaluate the forward flight regimes in which the fan inlet will reduce drag, the surface pressure coefficient along the pylon behind the rotor head is compared to the minimum pressure coefficient at the top of the rotor head fairing. If the flow remains attached, it will decelerate, increasing the surface pressure behind the rotor head, creating a favorable condition for drag reduction. If the flow separates, as is the case without boundary layer control, surface pressure behind the rotor head remains at a low value, contributing to aircraft drag. With the addition of the fan inlet, surface air velocity is forced by continuity to maintain a specific value at the inlet, tending to keep the flow along the rear pylon area attached. However, if the flow is too greatly accelerated, then full pressure recovery is not achieved and less favorable surface pressures are created. Thus only certain flight conditions benefit from the presence of the fan inlet.

From Reference 2, it is found that a pressure coefficient (C_p) of approximately -.5 might be expected at the top of the rotor head fairing where

$$C_p = 1-(V/V_\infty)^2 + p-p_\infty /1/2\rho_\infty V_\infty^2) \quad (46)$$

If we assume that without boundary layer control the pressure coefficient will only increase to about -.3 before separating, then the pylon region behind the rotor head will generally remain at -.3 pressure coefficient, contributing to aircraft drag. With the fan inlet, a constant velocity will be maintained at the inlet. Thus at 4000 ft, 95°F

$$V = W/\rho A = 86.2/(.0618)(7.331) = 190 \text{ ft/sec} \quad (47)$$

In terms of pressure coefficient

$$C_p = 1-(190/V_\infty)^2 \quad (48)$$

and the pressure coefficient will vary with aircraft velocity. Solving for V_∞ at a C_p = -.3, we find that

$$V_\infty = \sqrt{190^2/(1-C_p)} = 166 \text{ ft/sec} \quad (48)$$

At this forward speed, the pressure coefficient at the normal separation point will equal -.3. Because of the fan, the flow will remain attached, but provide little favorable pressure recovery. Above this speed, the pressure coefficient at the inlet will become more positive, providing a greater pressure recovery and hence greater drag reduction. This process will continue until the flow once again separates at some high speed. Since the design cruise speed of this aircraft is only 140 knots, the fan inlet will be operating in a flight regime to afford significant drag reduction.

Although an extensive fuselage pressure analysis is required to accurately compute the drag reduction, an estimate may be made in the following manner.

Figure 37 shows estimated pressure coefficients for the main rotor pylon aft of the rotor head with and without the presence of the fan inlet. At 4000 ft, 95°F, the zero-flow pressure coefficient is assumed to be -.5 at the station of the rotor head (Station 1), expanding to -.3 at a location approximately midway between the rotor head and the fan inlet (Station 2), at which point it separates and remains at -.3. With a mass flow of 86.2 lb/sec, the pressure coefficient at the inlet (Station 3) is

$$\begin{aligned} C_{p3} &= 1 - (V_3/V_\infty)^2 \\ &= 1 - (W/\rho V_\infty A)^2 \\ &= .352 \end{aligned} \qquad (50)$$

Curves are fit through these points and scaled to determine the C_p changes that result from the fan inlet airflow. The values of C_p are multiplied by the cosine of the angle that the surface pressure makes with the flight direction. The resulting value of $C_p \cos\theta$ is plotted and graphically integrated in Figure 37. This integration predicts a drag reduction of 0.61 linear foot, which is assumed to apply to an area 40 in. high on each side. The predicted drag reduction is therefore 41.1 ft^2. At 4000 ft, 95°F and 140 knots, the dynamic pressure is 53.6 psf, so the drag reduction is Drag = 53.6 x 4.1 = 219 lb. The advanced integrated airflow schematic resulting from these studies is shown in Figure 38.

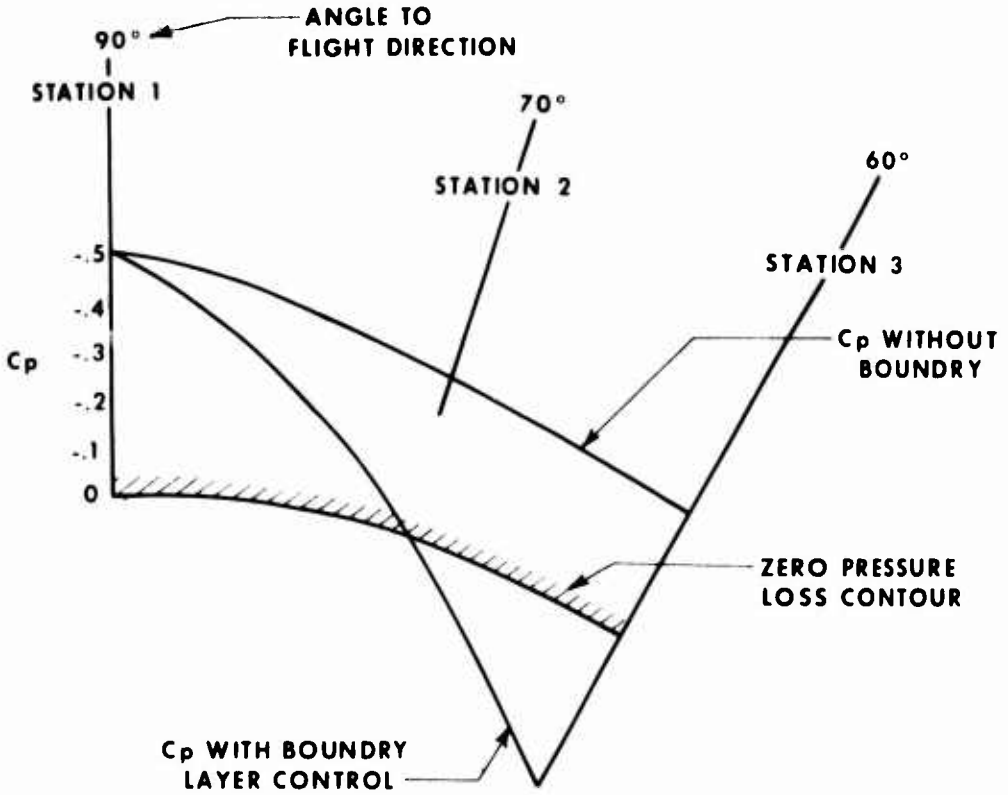

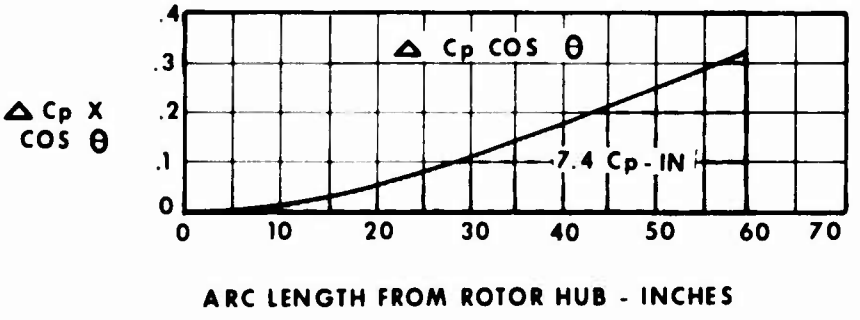

Figure 37. Effect of Fan Inlet on Rotor Pylon Drag.

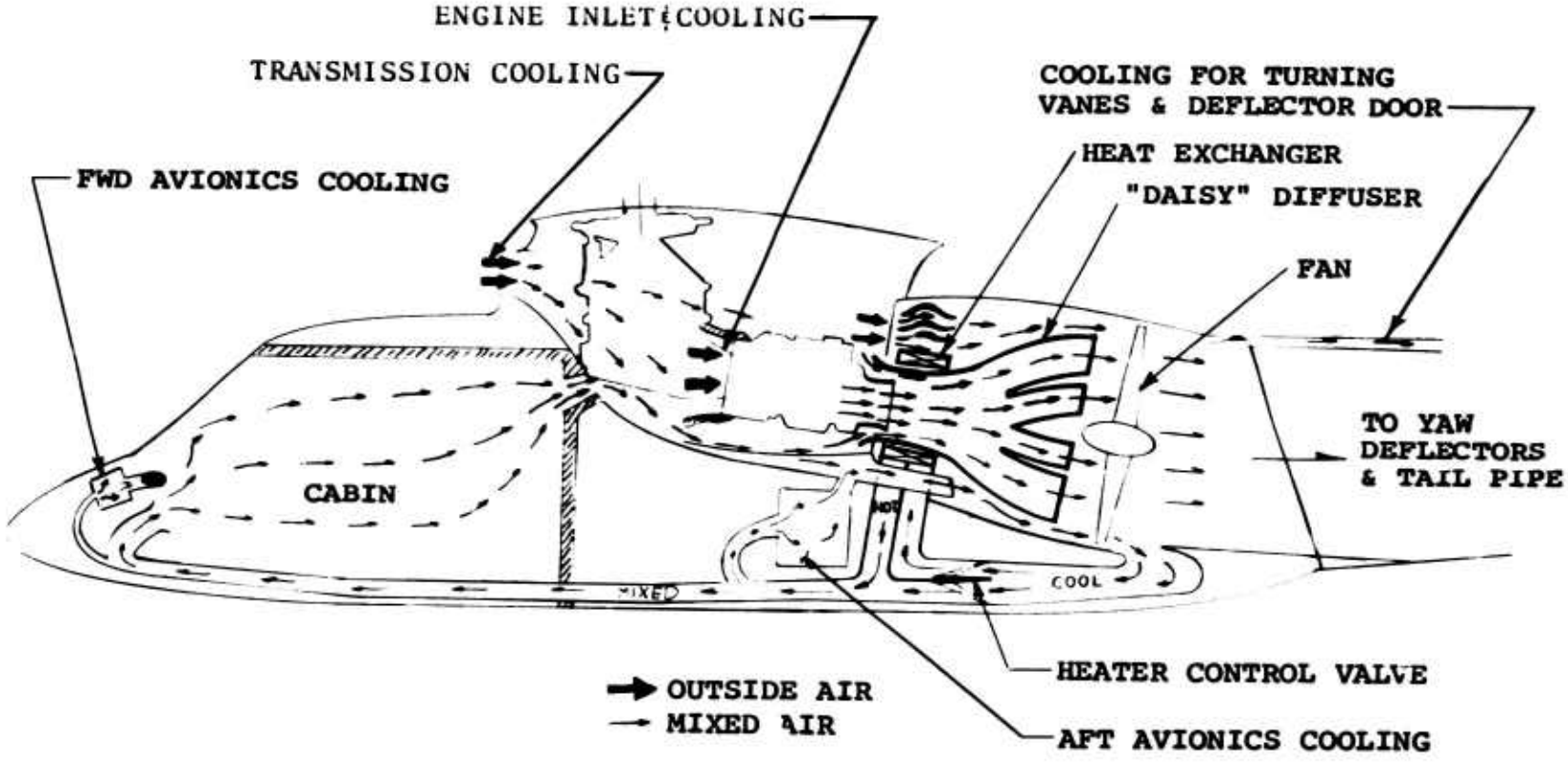

AIR FLOW SCHEMATIC
(NO SCALE)

Figure 38. Advanced Integrated Airflow Schematic.

PRELIMINARY DESIGN AND EVALUATION

INTRODUCTION

Initial integration of the advanced concepts into an advanced vehicle was performed during the period of concept development. The resulting vehicle arrangement is shown in Figure 39.

Further integration studies indicated the following areas in which the initial advanced concept could be improved:

The eight struts used to attach the fuselage to the tailcone were replaced by providing a lap joint along the lower longeron of the transition section (See Figure 40). Splice fittings provide continuity from the upper longeron of the transition section to the composite molded tailcone and absorb the bending moments at the interface between these sections. Shear capability is provided by a lap splice at the edge of the partial bulkhead and the side shear panels of the tailcone. A splice at the aft end of the shear deck to the first full frame of the tailcone also provides shear continuity for torsional loads.

Clearances for rotor flapping and ground flair angle were increased to remain consistent with the baseline vehicle. Three-view and isometric drawings of this arrangement are shown in Figures 41 and 42.

PERFORMANCE

The performance of the IR fan is shown in Table 16. The fan power in hover (210 hp) at 4000 ft, 95°F exceeds the combined power of the baseline tail rotor (95 hp) and baseline IR suppressor (90 hp) by 25 hp. This sizes the engines and transmission slightly larger than the baseline aircraft.

TABLE 16. FAN PERFORMANCE

Flight Condition	Fan Flow (lb/sec)	Pressure Rise (lb/ft^2)	Fan Eff	Fan Power (hp)
4000 ft, 95°F Hover	120	47.1	.920	210
4000 ft, 95°F, Yaw	120	57.8	.905	261
4000 ft, 95°F, Cruise	120	42.5	.925	188
SL, 59°F, Cruise	111	7.4	.57	41
SL, 59°F, Hover	111	40.9	.926	139
4000 ft, 95°F, Hover*	100	41.2	.930	155

*Without hot metal IR suppression

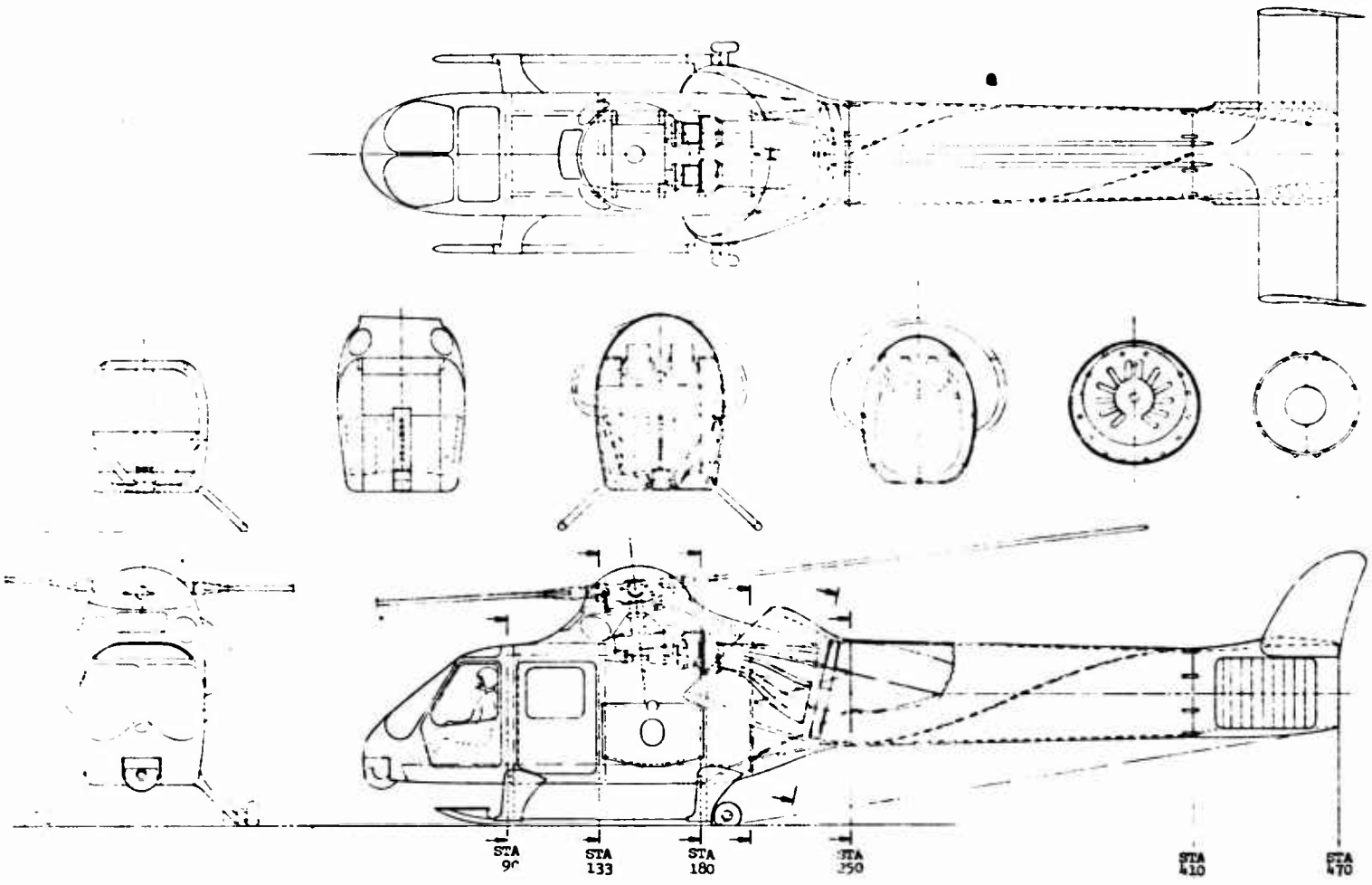

Figure 39. Preliminary Advanced Vehicle.

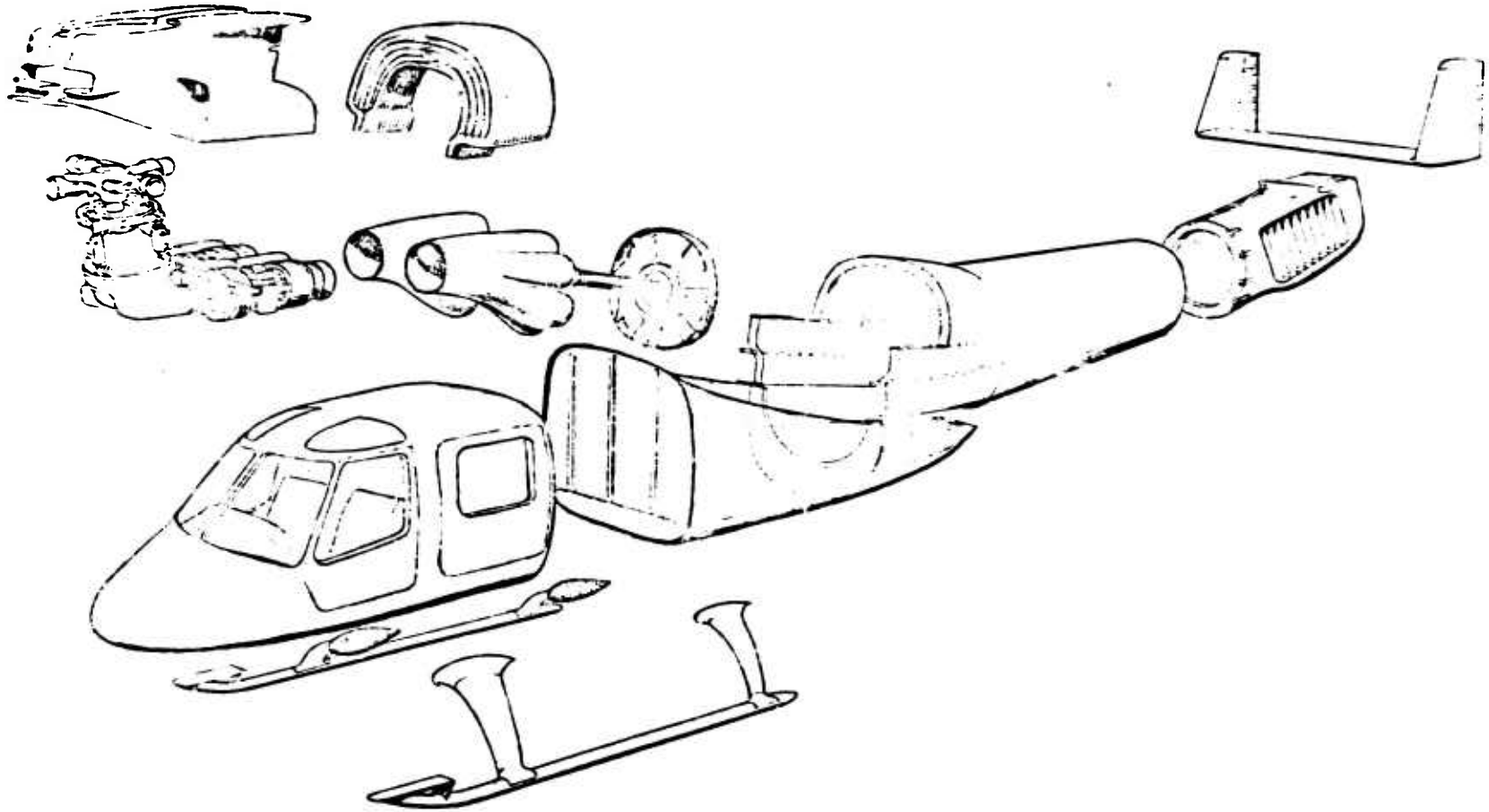

Figure 40. Advanced Aircraft Modular Construction.

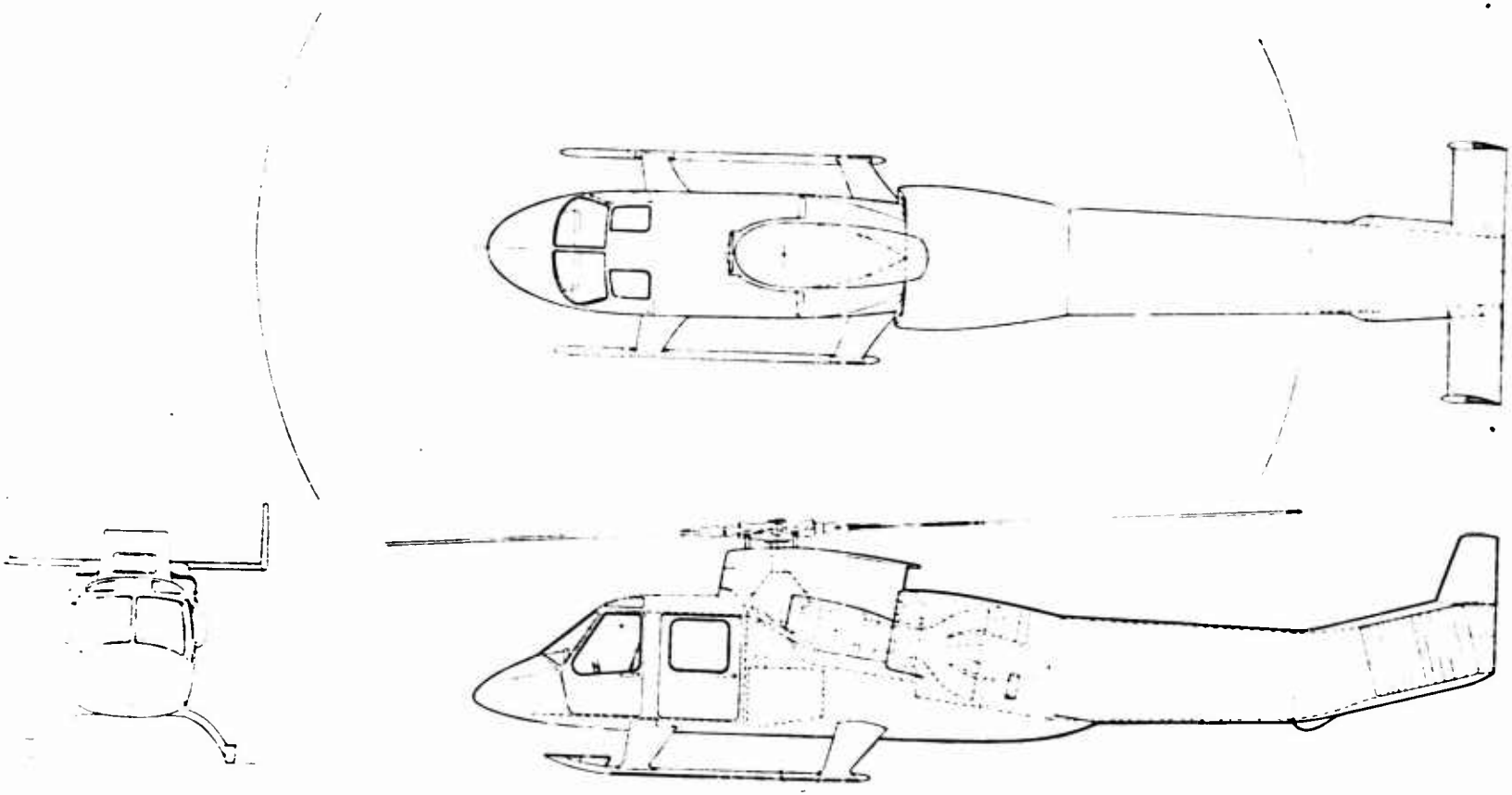

Figure 41. Advanced Vehicle Three-View Drawing.

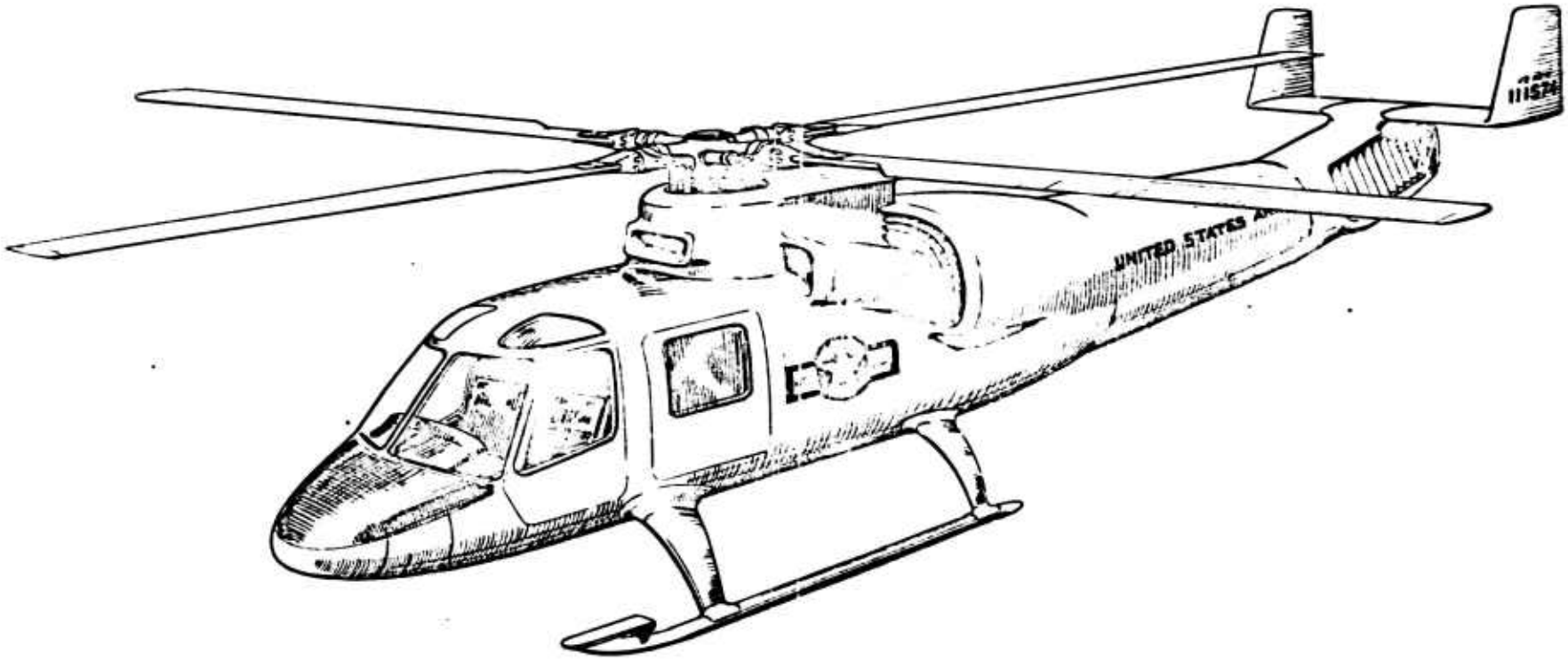

Figure 42. Advanced Vehicle Isometric.

The baseline aircraft power requirement in cruise exceeds that of the advanced by an estimated 136 hp. Thirty-one hp is attributable to the difference between 41 hp for the IR fan and the baseline cruise requirement of 27 hp for the tail rotor plus 45 hp for the IR suppressor. The remaining performance differential (105 hp) is due to drag reduction (200 lb) which results from boundary layer control on the main rotor pylon exerted by the IR fan inlet. It should be noted that similar boundary layer control could be provided on the baseline aircraft for an estimated 20 hp.

SURVIVABILITY/VULNERABILITY

Comparison of the advanced and baseline vehicles shows a significant reduction in vulnerable areas for the advanced vehicle. This reduction, which applies to both AP and HEI threats, is shown in Table 17. The following design features contribute to the vulnerable area reduction:

- No tail rotor
- No tail or intermediate gearbox
- No tail rotor drive shaft
- No drive shaft bearing support
- No transmission oil cooler
- No external oil lines

One additional design feature contributes to a very significant reduction of vulnerable areas, primarily to the HEI threat. The structural arrangement of the tailcone aft of the fan, sized to accommodate the duct, has uniformly spaced structural stringers and redundant load paths. This arrangement is survivable to the 23 mm HEI threat.

The vulnerable area reduction resulting from the elimination of the above flight-essential components is offset to some degree by the addition of the following flight-essential components and systems:

- Air and engine exhaust fan
- Fan drive shaft
- Redundant controls for directional airflow louvers.

Additional design features may be integrated into the advanced vehicle to further enhance its survivability. Extending the air duct fairing forward in the area of the engine installation will provide an increased stand-off distance for the engines against HEI threats. The addition of a ballistic barrier firewall between the engines will reduce the probability of loss of two engines. Extending the air duct fairing aft in the area of the fan will provide an increased stand-off distance for the fan against HEI threats.

TABLE 17. PROPULSION SYSTEM
VULNERABLE AREA COMPARISONS

Vulnerable Area - (Av) (Ft^2)

	12.7 mm			14.5 mm			23 mm AP			23 mm HEI		
	BL	Adv	% Imp	BL	Adv	% Imp	BL	Adv	% Imp	BL	Adv	% Imp
Engine Instl/ Main Trans	.190	.190	0	.633	.633	0	1.124	1.124	0	5.5	5.5	0
Tail Rotor Drive/Fan Drive	.025	0	100	.025	0	100	4.336	1.084	75	8.81	.7	92
Intermediate Gearbox	.083	0	100	.118	0	100	.234	0	100	.1	0	100
Tail Rotor Gearbox	.232	0	100	.338	0	100	.569	0	100	.3	0	100
Tail Rotor/ Louver Controls	.003	.002	33	.004	.003	25	.017	.014	20	.11	.01	90
Tail Rotor Head-Blades/Fan	.191	0	100	.314	.157	50	1.045	.52	50	1.5	1.5	0
Structure		0	0	0	0	0	0	0	0	8.12	2.66	67
Total Propulsion System Including Structure Changes	.724	.192	73	1.432	.793	45	7.325	2.742	63	24.44	10.37	58

Note: BL = Baseline Aircraft
Adv = Advanced Aircraft
% Imp = Percentage Improvement

REFINED DESIGN AND COMPARISONS

ADVANCED AIRCRAFT

In order to attain better aircraft balance, the IR fan contingency pressure loss allocated during the concept development phase was reallocated to increase the maximum antitorque thrust from 787 lb to 841 lb. As a result, the antitorque moment arm is reduced from 292 in. to 273 in. and the side nozzle area from 10.66 ft^2 to 9.97 ft^2.

The requirement for cooling of the side nozzles and deflector doors is analyzed in the section entitled "IR SUPPRESSION/ DIRECTIONAL CONTROL SYSTEM STUDY." The 2.5 lb/sec cooling air required and the reduction in aft nozzle size modify the fan performance given in Table 16, as shown in Table 18.

Three-view drawings and an inboard profile of this aircraft are shown in Figures 43 and 44.

TABLE 18. FAN PERFORMANCE IN REFINED AIRCRAFT

Flight Condition	Fan Flow (lb/sec)	Press Rise (psf)	Fan Eff	Fan Power (hp)
4000 ft, 95°F, Hover	122.5	48	.928	216
4000 ft, 95°F, Yaw	122.5	58.6	.902	270.5
SL, 59°F, Hover	113.5	41.5	.934	142.7
SL, 59°F, Cruise	113.5	16.4	.83	63.4

COMPARISONS

The advanced aircraft and two conventional aircraft were modeled on the HDM computer program. The conventional aircraft (one with no IR suppression and one with AAH technology level plume suppression) are constrained to the same gross weight as the advanced aircraft. Three-view drawings and inboard profiles of the two conventional aircraft are shown in Figures 45 and 46. In addition, HDM models were prepared for an advanced vehicle with a current technology transmission and a current technology vehicle with a current state-of-the-art hot metal IR suppressor. The weight breakdowns for these aircraft are shown in Table 19.

It can be seen that the advanced aircraft carries 52 lb less payload than the conventional aircraft with comparable IR suppression at the same gross weight. A conventional aircraft without IR suppression carries 426 lb more payload than the conventional aircraft with plume suppression, and 478 lb more than the advanced aircraft design. The effect

TABLE 19. COMPARATIVE WEIGHT BREAKDOWN

Group	Advanced A/C		Conventional A/C		
	Adv Trans	Conv Trans	NO IR	Plume	Hot Metal
Main Rotor Group	(678)	(678)	(655)	(655)	(655)
Tail Group	(74)	(74)	(133)	(133)	(133)
Tail Rotor	0	0	34	34	34
Horizontal Tail	37	37	40	40	40
Vertical Tail	37	37	59	59	59
Body Group	(984)	(984)	(755)	(755)	(755)
Alighting Gear	(225)	(225)	(225)	(225)	(225)
Engine Section	(105)	(105)	(140)	(140)	(140)
Propulsion Group	(1619)	(1666)	(1441)	(1783)	(1523)
Engine Instl	417	417	377	399	383
Exhaust System	212	212	25	286	90
Engine Controls	25	25	25	25	25
Starting System	19	19	16	18	17
Fuel System	214	214	207	223	215
Drive System	732	779	791	832	793
Flight Controls	(602)	(602)	(520)	(520)	(520)
Instruments	(135)	(135)	(135)	(135)	(135)
Hydraulics	(61)	(61)	(45)	(45)	(45)
Electrical	(247)	(247)	(247)	(247)	(247)
Avionics	(306)	(306)	(306)	(306)	(306)
Armament	(53)	(53)	(53)	(53)	(53)
Furnishings	(453)	(453)	(453)	(453)	(453)
Airconditioning	(30)	(30)	(30)	(30)	(30)
Anti-Ice	(18)	(18)	(18)	(18)	(18)
Load & Handling	(10)	(10)	(10)	(10)	(10)
Contingency	(57)	(57)	(52)	(56)	(54)
Weight Empty	(5657)	(5704)	(5218)	(5564)	(5302)
Useful Load	(2590)	(2543)	(3029)	(2683)	(2945)
Crew (2)	500	500	500	500	500
Fuel, Trapped	14	14	14	14	14
Fuel, Internal	1056	1056	1017	1097	1061
Oil, Trapped	6	6	6	6	6
Oil, Engine	14	14	14	14	14
Payload	1000	953	1478	1052	1350
Design Gross Weight	(8247)	(8247)	(8247)	(8247)	(8247)

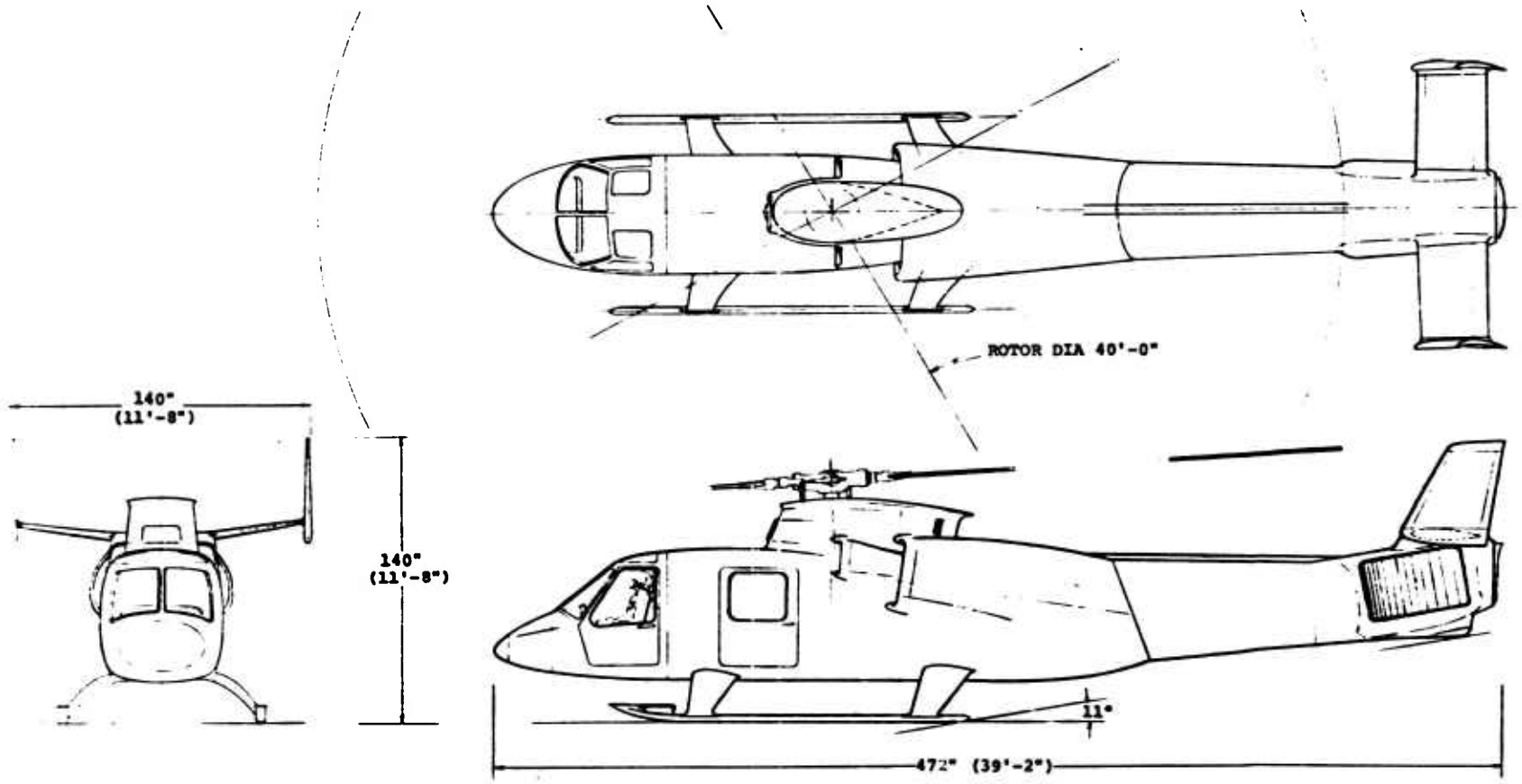

Figure 43. Refined Advanced Vehicle - Three-View Drawing.

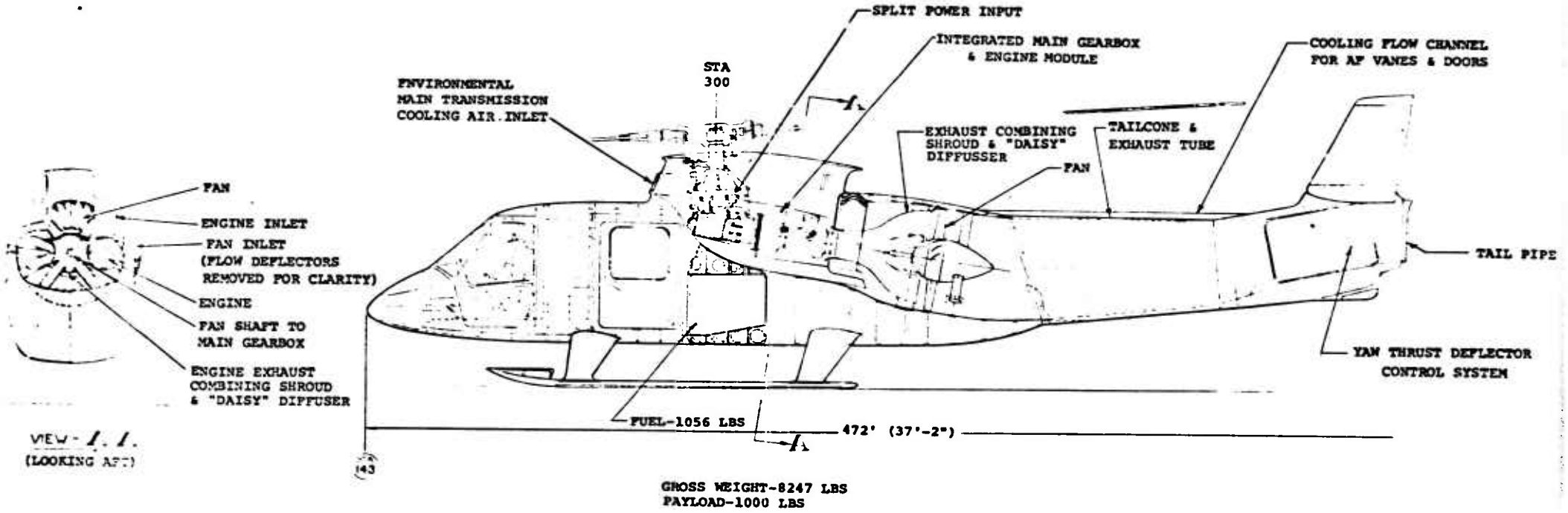

Figure 44. Refined Advanced Vehicle - Inboard Profile.

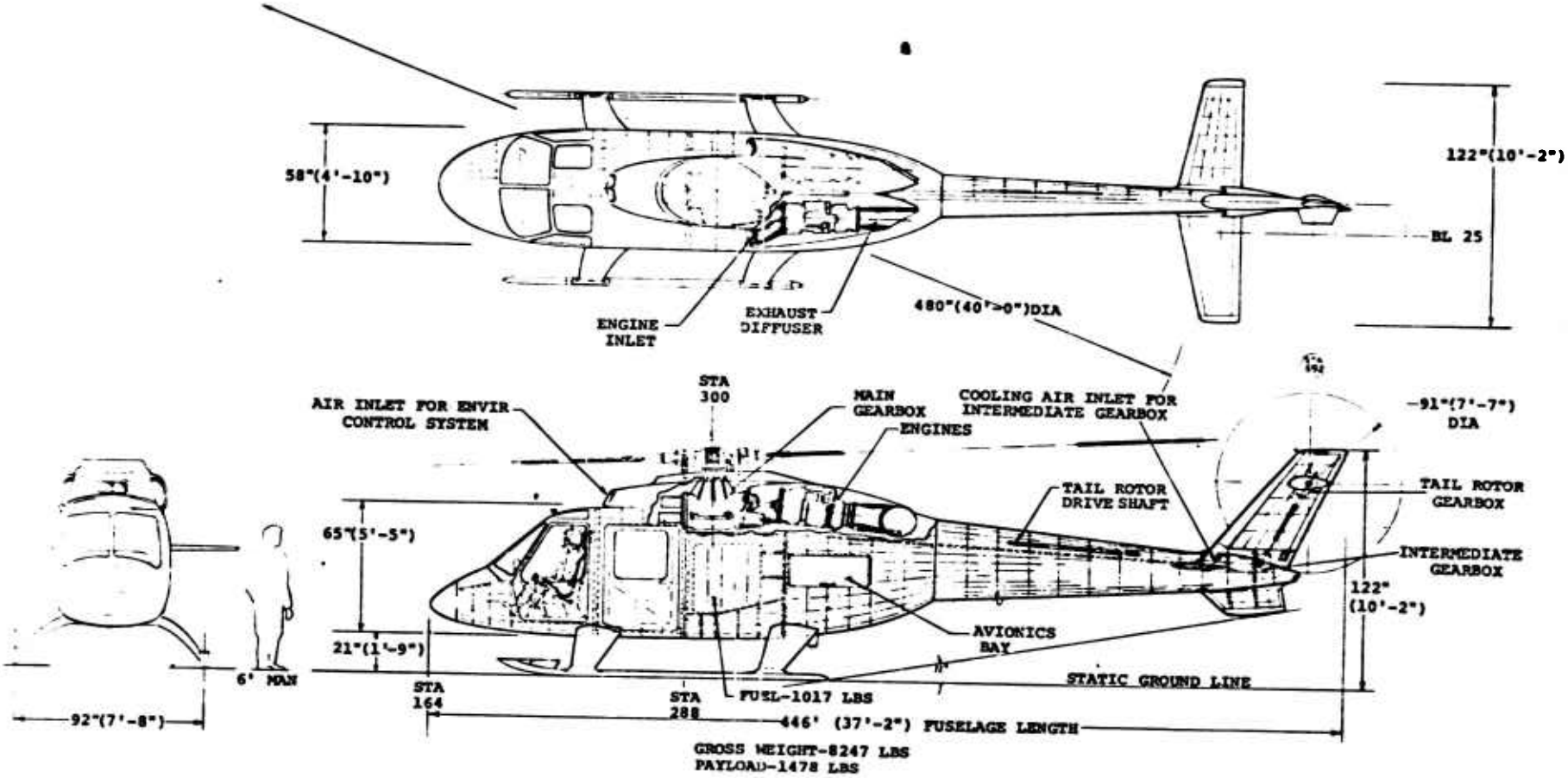

Figure 45. Three-View and Inboard Profile - Conventional Vehicle - No IR Suppression.

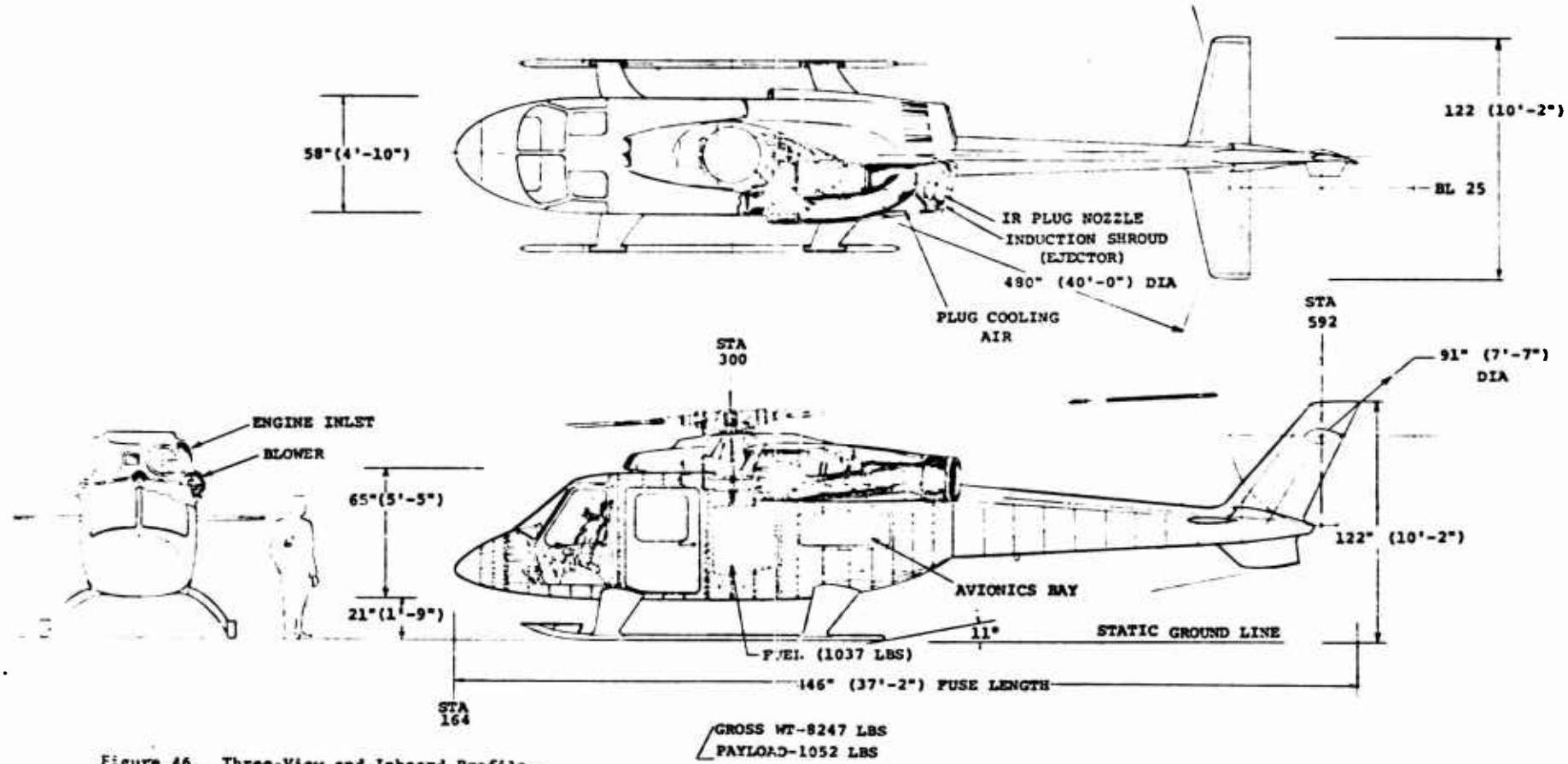

Figure 46. Three-View and Inboard Profile - Conventional Vehicle - Plume IR Suppression.

of drag reduction on the advanced aircraft is evident in the 41-lb reduction of internal fuel in the advanced aircraft by comparison with the conventional plume suppressed aircraft, even though the advanced aircraft requires more power in hover. The drag reduction is also manifested as increased range and endurance as indicated by the reserve cruise (best range) speeds in Tables 20 through 22. The mission profiles for the advanced aircraft, and the conventional aircraft with no IR suppression and with plume suppression are presented in Tables 20 through 22.

Sensitivity Analysis

The advanced aircraft loses (or gains) 1.2 lb of payload for each additional horsepower required (or eliminated) in hover. In the case of the flow outlet vanes, for example, an increase of 0.1 in loss constant represents an increase of 3.9 psf in fan pressure, which translates into 15 hp or 18 lb of payload loss.

Fleet Life-Cycle Cost Analysis

The HDM computer model was used to predict the fleet life-cycle costs for the advanced aircraft and for a conventional aircraft. For this purpose, the original baseline aircraft was chosen as the conventional aircraft because it has the same payload as the advanced aircraft. Figure 47 shows the estimated life-cycle costs of the two aircraft as a function of the number of aircraft built.

The number of conventional aircraft built is assumed to be five hundred. The number of advanced aircraft built will be five hundred less any differential in anticipated attrition. This differential consists of a differential in combat attrition due to reduced vulnerable area and a differential due to accidents involving the baseline tail rotor.

The vulnerable areas in Table 17 account only for propulsion-related vulnerability. The total vulnerable areas for the baseline aircraft were estimated by ratioing the results of a UTTAS vulnerability study proportional to the presented areas of the two vehicles. The differential in Table 17 was then subtracted to arrive at the total vulnerable area for the advanced vehicle.

The number of shots fired at the aircraft was based on a 2-1/2-year mid-intensity war scenario utilized in a UTTAS study and adjusted for the larger number of encounters anticipated for a reconnaissance aircraft by comparison with a utility transport. The resulting attrition numbers are: advanced 66, and baseline 96. In addition, the baseline

TABLE 20. MISSION PROFILE - ADVANCED AIRCRAFT

Mode	Gr Wt (lb)	Temp (°F)	Alt (ft)	Speed (kt)	Dist (mi)	Time (min)	SHP	Fuel (lb)	SFC
WU/TO	8247.	59.	0.	-	-	5.0	1543.4	59.2	0.4841
Hover	8120.	59.	0.	-	-	15.0	1022.3	134.7	0.5550
Cruise	7903.	59.	0.	140.0	93.3	40.0	769.4	298.4	0.6123
Loiter	7596.	59.	0.	70.6	70.6	60.0	534.9	351.8	0.6923
Reserve-Cruise	7296.	59.	0.	156.6	68.6	26.3	872.8	211.9	0.5834

Total Mission Fuel is 1055.9 lb
Total Mission Time is 120.0 min

TABLE 21. MISSION PROFILE - CONVENTIONAL AIRCRAFT WITH PLUME SUPPRESSION

Mode	Gr Wt (lb)	Temp (°F)	Alt (ft)	Speed (kt)	Dist (mi)	Time (min)	SHP	Fuel (lb)	SFC
WU/TO	8219.	59.	0.	-	-	5.0	1453.0	55.7	0.4841
Hover	8127.	59.	0.	-	-	15.0	967.8	127.4	0.5541
Cruise	7900.	59.	0.	140.0	93.3	40.0	918.6	327.2	0.5624
Loiter	7559.	59.	0.	64.2	64.2	60.0	546.3	350.1	0.6746
Reserve-Cruise	7268.	59.	0.	137.6	68.8	30.0	874.0	237.0	0.5708

Total Mission Fuel is 1097.4 lb
Total Mission Time is 120.0 min

TABLE 22. MISSION PROFILE - CONVENTIONAL AIRCRAFT WITH NO IR SUPPRESSION

Mode	Gr Wt (lb)	Temp (°F)	Alt (ft)	Speed (kt)	Dist (mi)	Time (min)	SHP	Fuel (lb)	SFC
WU/TO	8221.	59.	0.	-	-	5.0	1341.1	51.4	0.4841
Hover	8137.	59.	0.	-	-	15.0	886.9	116.9	0.5552
Cruise	7924.	59.	0.	140.0	93.3	40.0	874.1	308.6	0.5575
Loiter	7606.	59.	0.	64.4	64.4	60.0	504.1	323.1	0.6746
Reserve-Cruise	7338.	59.	0.	133.9	66.9	30.0	796.8	216.9	0.5730

Total Mission Fuel is 1016.9 lb
Total Mission Time is 120.0 min

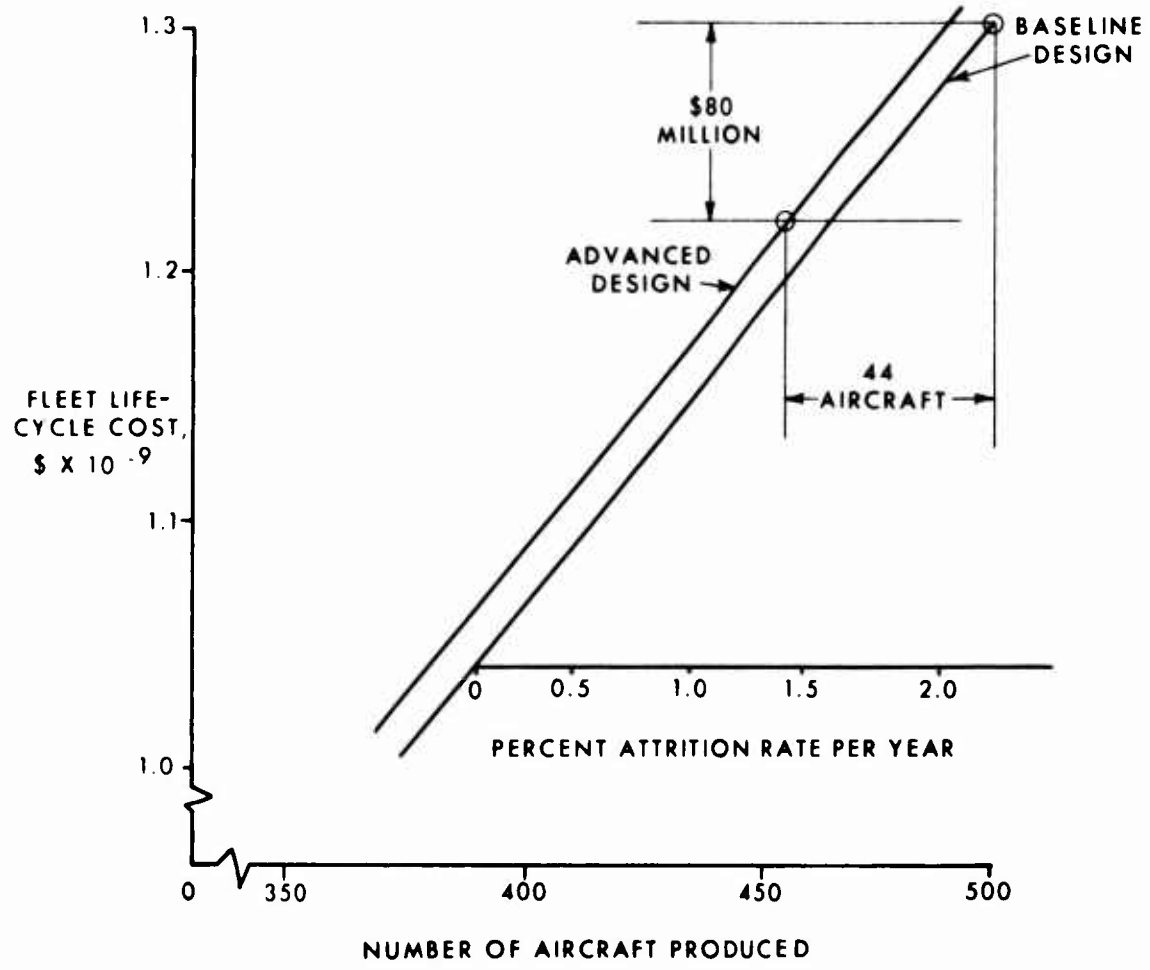

Figure 47. Life-Cycle Cost Comparison.

aircraft is expected to suffer a loss of 14 aircraft due to tail-rotor-related accidents over a ten-year period.

The advanced aircraft production is therefore estimated to be 500 - (96-66)-14 = 456. As shown in Figure 47, the anticipated differential in fleet life-cycle cost for an advanced aircraft production of 456 aircraft compared to a baseline production of 500 aircraft is $80 million, or approximately 6 percent. This savings includes an estimated reduction of 1 percent in consumed fuel resulting from pylon drag reduction.

It is also expected that there will be an additional saving based on a reduced maintenance burden. The reduction results from the replacement of the tail rotor and its drive system with the IR fan, the elimination of two IR blowers and their drives, the transmission oil cooler and its blower and the heating/ventilating system blower, and fewer repairs due to tail rotor accidents. The HDM program estimates that, for both aircraft, each 10 percent reduction in maintenance burden is worth $14 million in fleet life-cycle cost. It is estimated that the factors listed above will result in a maintenance burden reduction of 10 percent and an additional life-cycle cost saving of $14 million.

CONCLUSIONS

Total helicopter airflow and power management can result in a significant reduction in fleet life-cycle cost. As might be expected, the fan-in-tailcone configuration evaluated is a less efficient directional control device than a conventional tail rotor. However, the benefits obtained by making multiple use of the fan-in-tailcone airflow outweigh the propulsion efficiency advantage of the conventional tail rotor.

The largest multiple airflow use is that of IR plume suppression air for directional control. Therefore, most of these conclusions apply only to aircraft having a requirement for IR plume suppression in hover.

The most significant contribution to the predicted life-cycle cost saving is obtained by reduction of area vulnerable to small-arms fire, most of which results from elimination of the tail rotor. The 1 percent saving in consumed fuel, which results from rotor pylon drag reduction, could be made applicable to most helicopters with a small power expenditure for a blower. Integration of the transmission cooling with the IR fan provides both payload saving and reduction in vulnerable area.

The advanced vehicle has a reduced maintenance burden resulting from the elimination of separate IR suppression blowers and drive components, transmission cooling components, and the heating/ventilating system blower, and fewer repairs due to elimination of tail rotor accidents.

Even though this fan-in-tailcone concept appears favorable only if the IR plume suppression airflow requirement is comparable to that required for directional control, the benefits obtained from integration of the remaining airflow systems are sufficient to warrant attention on their own merit. This applies even if some different method of integration is required due to reduced or eliminated IR suppression requirements.

RECOMMENDATIONS

The following areas are believed to require further research in order to prove the feasibility of the advanced aircraft:

1. Verification of engine and ambient air mixing by a fan in a duct.

2. Investigation of noise signature effects of prefan mixing.

3. Analytical and test bed development of movable door control system.

4. Verification of a clean location downstream of a fan for tapping heating/ventilating and vane cooling air.

5. Model testing to determine the turning vane loss constant and flow distribution.

6. Analytical and/or experimental investigation of start-up transients and effects of various fan failure modes.

REFERENCES

1. Olson, J. R., Wind Tunnel Data and Analysis of Full Scale Rotor Head and Pylon Drag, p 78, SER-61027, Sikorsky Aircraft Division of United Aircraft Corporation, Stratford, Connecticut, 1958.

2. Linville, J. C., An Experimental Investigation of High-Speed Rotorcraft Drag, pp 46-55, USAAMRDL TR 71-46, Eustis Directorate, U. S. Army Air Mobility Research and Development Laboratory, Fort Eustis, Virginia, February, 1972, AD 740771.

APPENDIX A

SYSTEM STUDY SPECIFICATION

1. GENERAL CONFIGURATION

The aircraft shall be a reconnaissance-type helicopter with a capability to accommodate two passengers or, when stripped of mission equipment (paragraph 4.1), must be able to carry a payload of 1000 pounds, which may include two passengers and the mission equipment listed in paragraph 4.1.

2. PHYSICAL CHARACTERISTICS

2.1 Rotor System

Main Rotor - Single rotor. Manual blade fold if more than two blades. DL less than 10 psf.

Tail Rotor - Single, not canted.

2.2 Body Group - Two crew side-by-side. At least minimum visibility requirements of MIL-STD-850, paragraph 8. Distortion-free canopy. Fifth through ninety-fifth percentile Army aviator accommodation. Compartment suitable to accommodate two passengers; provisions for load-carrying floor to carry 1000 lb of cargo. Design limit load factors: +3.5g, -0.5g at DGW.

2.3 Landing Gear - Skids. Provisions for easy ground handling. 10 fps ROS safe limit.

2.4 Propulsion - Two turboshaft engines having front or rear drive and capable of operating in vertical or horizontal attitudes. For engine weight, performance and fuel flow, see Appendix B.
Self-starting: -25°F to 120°F.
Engine anti-ice and EAPS. Fire detection and extinguishing systems.

Fuel System - Crashworthy. 20-minute cruise supply sealed against 12.7 mm, remainder 7.62 mm. Gravity, pressure, and closed-circuit refueling.

No APU.

2.5	Flight Controls -	Dual cockpit controls. Zero single-shot vulnerability to 7.62 mm threat (same as UTTAS). Power boost by two independent hydraulic systems. Simple SAS only if required to meet UTTAS/AAH equivalent stability. No FAS.
2.6	Drive System -	No rotor brake. MGB capable of operating 30 minutes at cruise power after sustaining a single 7.62 mm hit (UTTAS threat). MGB lubrication and cooling by oil.
	MGB Rating -	1.2 times HOGE power required at 4000 ft 95°F, DGW. MGB inputs at maximum sea level standard engine rating.
2.7	Instruments -	Basic IFR instruments per AR 95-1. Minimum duplication consistent with IFR operation by either crewman.
2.8	Hydraulics -	In accordance with MIL-H-5440.
2.9	Electrical -	Two independent power sources. Secondary source to provide essential loads for 30 minutes (OTAS is not essential load).
2.10	Furnishings -	Soundproofing, insulation for crew compartment as necessary. 1 Crash Ax 1 Portable Fire Extinguisher 1 Map Case 2 Ash Trays 2 Armored Crew Seats 1 First Aid Kit Provisions for two foldable passenger seats.
2.11	Environmental Systems -	Heating and ventilation for crew compartment. No ECS. Windshield anti-ice, defog, defrost, and rain removal.

2.12 Survivability/ Vulnerability - Lower hemisphere of all flight-essential equipment: Zero vulnerable area against 7.62 mm at 100 meters, zero degrees obliquity (UTTAS threat).

Back, bottom and side protection for crew against 7.62 mm at 100 meters, zero degrees obliquity.

Crew compartment: roll-over protection.

Exits and entrances: individual for each crewmember. Two cargo compartment doors on left and right side of fuselage.

Crashworthiness: to be survivable in ninety-fifth percentile crash of TR 71-22.

Infrared - Hot metal and plume suppression in both hover and cruise.

Noise - Not to exceed 5000 ft detectability distance from forward quadrant during 150-knot approach, deceleration and HOGE, NOE short-grass terrain.

Radar Detectability - As low as practical.

Visual Detectability - As low as practical. Minimum windshield glint.

Damage Tolerance - Continue flight and make survivable landing after loss of tail rotor.

3. PERFORMANCE

3.1 Design Mission - Conditions: SLS, DGW
5 minutes NRP (WUTO)
15 minutes HOGE
40 minutes cruise at 140 knots
Reserve:
30 minutes cruise at 140 knots at end-of-mission gross weight.

Fuel capacity: fuel as above.

3.2 Performance at DGW, 4000 ft, 95°F, with EAPS and IR suppression operative and maximum daylight electrical load.

- 500 fpm VROC at zero wind and not more than 95 percent intermediate rated power (IRP)
- Vcruise at least 150 knots at not more than NRP and without life-limiting vibration, control loads, or blade stresses.

3.3 Maneuverability, 4000 ft, 95°F, at DGW.

- 1.75 g steady; achieve in 1 second from level flight at 150 knots; hold for 3 seconds steady without any loss in controllability.
- Zero g during recovery (NOE); completely controllable.
- Lateral: acceleration minimum 0.25 g to 35 knots.
- Yaw acceleration HOGE at AGW, minimum angular displacement of $220/\sqrt[3]{\text{AGW}+1000}$ degrees in 1 second.
- Safe autorotative landing (no crew injuries or aircraft damage).

3.4 Handling Qualities - generally comparable to UTTAS and AAH.

3.5 Weights - Design GW (DGW) is that required for the design mission. For the purpose of this study, the baseline aircraft DGW shall be adjusted if necessary to remain in the range of 7000 to 10,000 pounds, by selection of equipment.

Maximum alternate GW (AGW) at SL 95°F and maximum engine power or MGB rating, whichever is lower.

Unit weights:
Crew: 250 lb including armor vests
Fuel: JP-4 at 6.5 lb/gal.
Oil: 7.5 lb/gal.
Hydraulic Fluid: 7.0 lb/gal.

4. EQUIPMENT

4.1	Mission equipment -	Observer: OTAS (observer target acquisition system), Texas Instruments, with Laser. Uninstalled weight, 413.2 lb.	
		Pilot: night vision goggles, 1 lb	
4.2	Communications -	2 VHF FM radio sets	19.0 lb
		1 VHF AM radio	8.2 lb
		1 UHF AM radio	11.5 lb
		Intercom system	3.6 lb
		KY 28 secure speech unit	23.0 lb
		IFF/SIF security unit	39.6 lb
		NOE Communication HF/SSB	62.0 lb
4.3	Navigation -	1 Loran C/D	.0 lb
		Low frequency direction finder	17.4 lb
		FM homing	13.6 lb
		VOR/LOC/GS/MG	14.0 lb
		Tactical precision approach system	32.0 lb
4.4	Instrumentation -	Radar altimeter	12.0 lb
		Gyro compass	9.3 lb
		Vertical gyro	6.6 lb
4.5	Miscellaneous -	Radar warning	19.8 lb
		Crash locator beacon	13.0 lb
		Voice warning system	3.0 lb
4.6	Lights -	Anticollision	
		Position (flashing)	
		Landing/hover light	

5. RELIABILITY/MAINTAINABILITY

MTBR	1500 hours dynamic components
Fatigue Life	4500 hours
Airframe overhaul interval	4500 hours
Reliability	Mission/System/Flight Safety: .95*/.70*/ one failure per 20,800 FH *Based on 1-hr mission time.
Maintenance	Field replacement time for any major component not to exceed 3 hours elapsed time.

APPENDIX B

APPENDIX TO CONTRACT SOW

The Contractor shall base his conceptual analyses and preliminary designs upon a hypothetical aircraft and upon requirements and considerations as follows:

Baseline Aircraft

(1) Single main rotor reconnaissance, utility, or attack helicopter (not co-axial rotor).

(2) DGW of 7000 to 10,000 lb.

(3) Two turboshaft engines having front or rear drive and capable of operating in vertical and/or horizontal attitudes.

(4) 4000 foot/95°F HOGE at DGW at 95% IRP with a 500 ft/min rate-of-climb capability.

(5) Suitable armor provided for crew and critical component protection against small-arms fire and ballistic tolerance to small shell impacts (23 mm).

(6) Design Mission: 15 min hover, cruise @ 140 kt, 60 min loiter @ 70 kt, 30 min reserve @ 140 kt at sea level, standard.

(7) Payload of approximately 1000 lb

(8) Crew of two (500 lb)

Propulsion Technology Level

(1) Drive system technology consistent with state of the art as proven by component demonstration.

(2) Engine technology consistent with that depicted in Figures B1 and B2. (Weight given includes 10% increase for integral inlet separator. However, this is a design option for this program.)

(3) Aircraft rotor system, structure, and materials consistent with current design techniques as refined by 1980.

Airflows to Consider

(1) Engine inlet.

(2) Engine inlet separator scavenge.

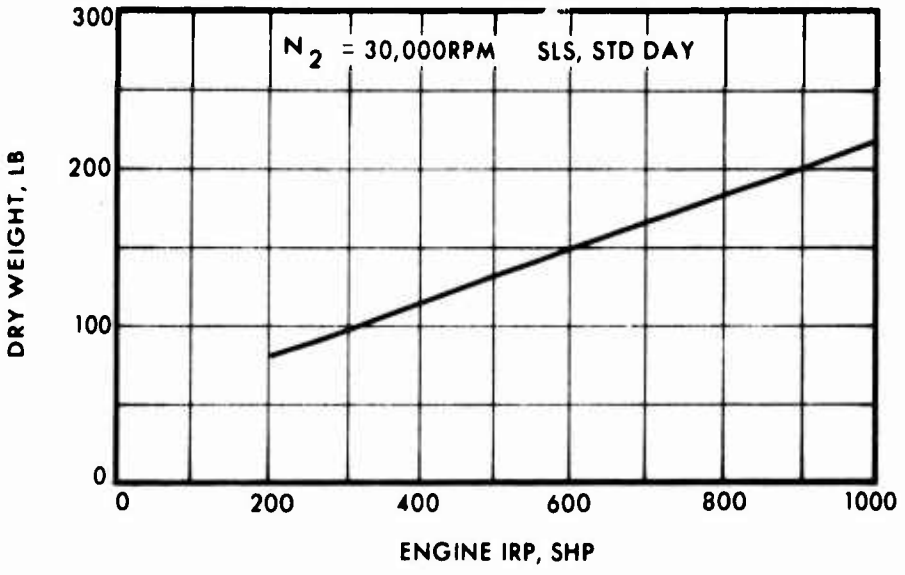

Figure B1. Advanced Technology Engine Weight.

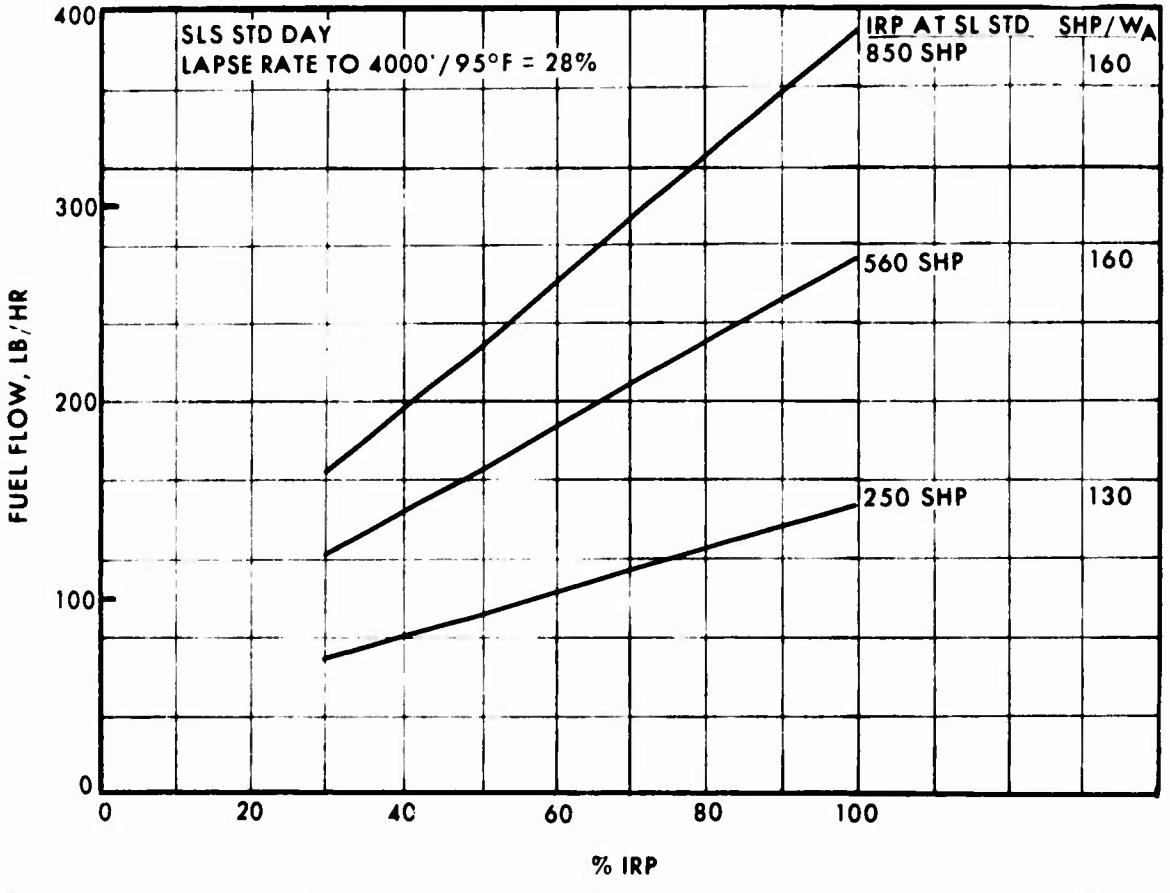

Figure B2. Typical Performance of 3 Advanced Technology Engines.

(3) Engine compartment cooling.

(4) Engine oil cooling.

(5) IR suppression (plume and hot parts).

(6) Drive train cooling.

(7) Airframe ventilation and compartment cooling (including electronic equipment).

(8) Pylon boundary layer removal for possible aircraft performance gains.

IR Suppression

(1) Plume Suppression. Maximum engine exhaust gas plume temperature shall not exceed 400°F, assuming a constant engine exhaust gas temperature of 1100°F. Only designs that can provide plume suppression over the entire flight spectrum shall be considered.

(2) Hot Parts Suppression. Design shall provide for shielding of engine turbine wheel to prevent direct viewing. The area of exposed aircraft system hot metal parts and corresponding temperatures shall not exceed the levels defined by Figure B3. This shall be accomplished in conjunction with the specified plume suppression.

General Requirements

(1) Engine compartmentalization shall conform to specification temperature and safety requirements (MIL-E-8593A and SD-24J, Vol. 2).

(2) Propulsion system component integration for efficient management of various external airflow needs in order to reduce airflow magnitude and system complexity.

(3) Goal of maximum overall propulsion system efficiency.

(4) Adequate vehicle directional control for all-engines-out autorotation.

(5) Goal of minimum power train complexity.

(6) Controls and accessory integration commensurate with best overall system performance.

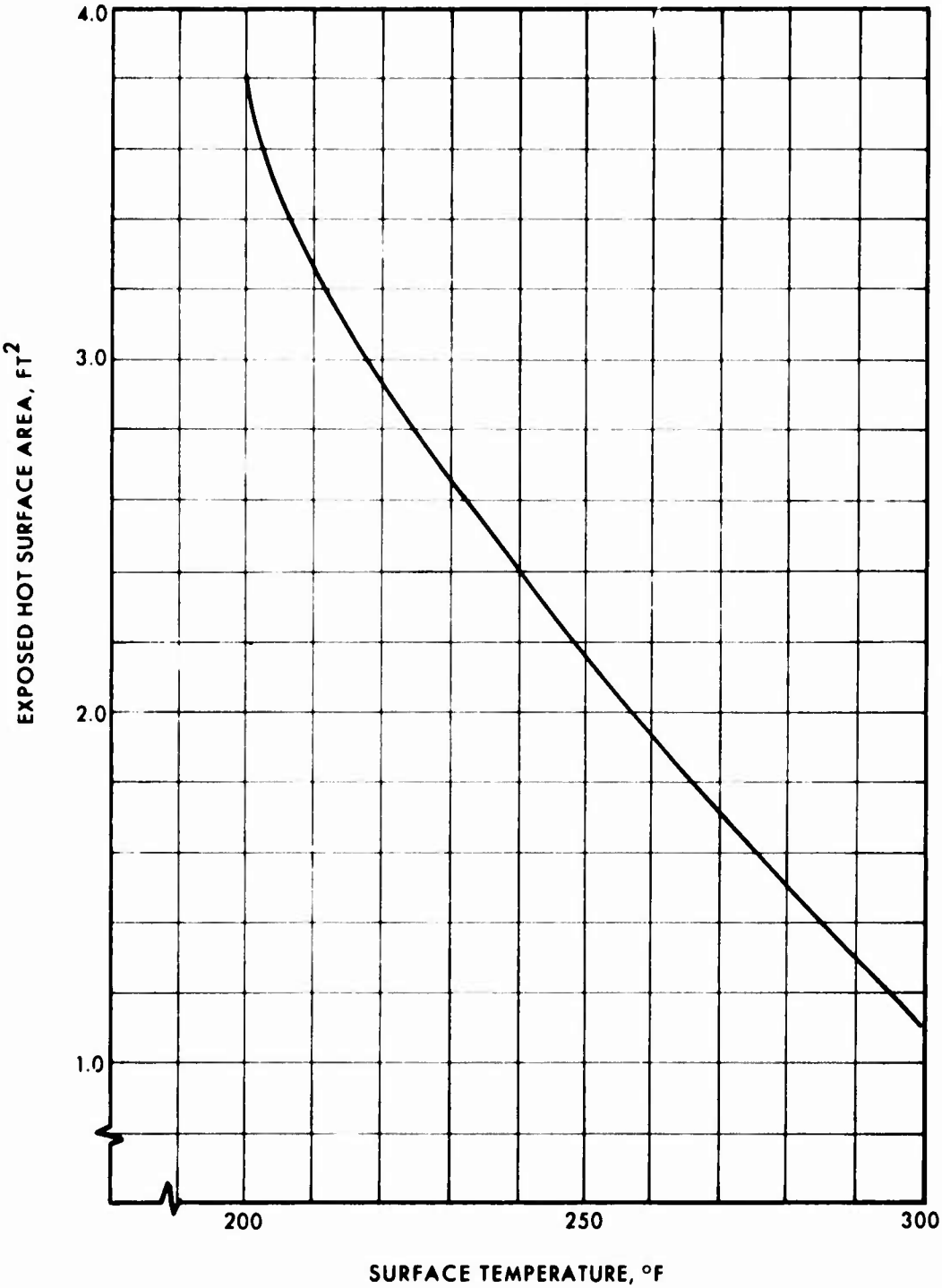

Figure B3. Hot Parts Suppression Criteria.

LIST OF SYMBOLS

A	Area - ft^2
C_p	Specific heat - BTU/lb; Pressure coefficient.
D	Diameter - ft
DR	Dilution ratio = W_a/W_e
F	Thrust - lb
f	Friction factor
g	Acceleration of gravity - ft/sec^2
h	Heat transfer coefficient BTU/ft^2-sec-°F
hp	Horsepower
J	Mechanical equivalent of heat = 778.3 ft-lb/BTU
k	Pressure loss coefficient, thermal conductivity - BTU/ft-sec
L	Length - ft
p	Pressure - lb/ft^2
P_r	Prandtl number
Q	Heat flux - BTU/sec
q	Dynamic pressure - lb/ft^2
R	Radius - ft
R_e	Reynolds number
r	Radial distance from fan axis - ft
s	Cooled arc length - ft
T	Temperature - °F
t	Gap height - ft
TAF	Total Activity Factor
T_s	Tip speed - ft/sec
U	Thermal conductance - BTU/ft^2-sec-°F

V	Velocity - ft/sec
W	Flow rate - lb/sec
Wt	Weight - lb
x	Distance - ft
η	Efficiency
Ω	Rotational velocity - rad/sec
ρ	Density - lb/ft^3
μ	Viscosity - lb/ft-hr
α	Variable grouping in Equation (29)
β	Variable grouping in Equation (29)
γ	Variable grouping in Equation (29)
σ	Solidity

SUBSCRIPTS

a	Air or ambient
B	Blade
c	Coolant
D	Duct
e	Engine exhaust
g	Gas
i	Initial
j	Jet
M	Mixture
s	Surface
w	wall
x	Local
∞	Freestream